The 1994 Arctic Ocean Section

The First Major Scientific Crossing of the Arctic Ocean

— Historic Firsts —

- First U.S. and Canadian surface ships to reach the North Pole
- First surface ship crossing of the Arctic Ocean via the North Pole
- First circumnavigation of North America and Greenland by surface ships
- Northernmost rendezvous of three surface ships from the largest Arctic nations—Russia, the U.S. and Canada—at 89°41′N, 011°24′E on August 23, 1994

— Significant Scientific Findings —

- Uncharted seamount discovered near 85°50′N, 166°00′E
- Atlantic layer of the Arctic Ocean found to be 0.5–1°C warmer than prior to 1993
- Large eddy of cold fresh shelf water found centered at 1000 m on the periphery of the Makarov Basin
- Sediment observed on the ice from the Chukchi Sea to the North Pole
- Biological productivity estimated to be ten times greater than previous estimates
- Active microbial community found, indicating that bacteria and protists are significant consumers of plant production
- Mesozooplankton biomass found to increase with latitude
- Benthic macrofauna found to be abundant, with populations higher in the Amerasia Basin than in the Eurasian Basin
- Furthest north polar bear on record captured and tagged (84°15′N)
- Demonstrated the presence of polar bears and ringed seals across the Arctic Basin
- Sources of ice-rafted detritus in seafloor cores traced, suggesting that ocean–ice circulation in the western Canada Basin was toward Fram Strait during glacial intervals, contrary to the present Beaufort Gyre
- Cloud optical properties linked to marine biogenic sulfur emissions
- Near-surface fresh water found to be derived from river runoff except in the Nansen Basin where it comes from melting ice
- Arctic Ocean determined to be a source to the atmosphere and Atlantic Ocean of some organic contaminants, rather than a sink
- Predominant sources of radionuclide contaminants in the ocean found to be from atmospheric weapons testing and European reprocessing plants

THE 1994 ARCTIC OCEAN SECTION

The First Major Scientific Crossing of the Arctic Ocean

Sponsored by

United States

National Science Foundation
Office of Naval Research
U.S. Geological Survey
U.S. Coast Guard
Defense Nuclear Agency

Canada

Department of Fisheries and Oceans
Department of Indian and Northern Affairs
Department of the Environment
Canadian Coast Guard

AOS-94 Chief Scientist: Knut Aagaard

U.S. Chief Scientist: Arthur Grantz

Canadian Chief Scientist: Eddy Carmack

Commanding Officer, CCGS *Louis S. St-Laurent*: Captain Philip O. Grandy

Commanding Officer, USCGC *Polar Sea*: Captain Lawson W. Brigham

Published by
U.S. Army Cold Regions Research and Engineering Laboratory
72 Lyme Road
Hanover, NH 03755
Special Report 96-23

Edited by Walter Tucker and David Cate
Compiled by Vicki Keating
1996

— Contents —

U.S. Preface iv
Canadian Preface v

INTRODUCTION
Introduction 1
Chronology 3
The Ships 8

SCIENCE REPORTS
Introduction 12

Ocean Circulation and Geochemistry
A CTD/Hydrographic Section across the Arctic Ocean 17
Total Carbonate and Total Alkalinity: Tracers of Shelf Waters in the Arctic Ocean 20
Transient Tracers: Chlorofluorocarbons and Carbon Tetrachloride 23
Distribution of Iron and Aluminum in the Surface Waters of the Arctic Ocean 26
Thorium Isotopes as Tracers of Scavenging and Particle Dynamics in the Arctic Ocean . 29
What Can Be Learned from Barium Distributions in the Arctic Ocean? 32

Biology and the Carbon Cycle
Cycling of Organic Carbon in the Central Arctic Ocean 34
Mesozooplankton Community Structure in the Arctic Ocean in Summer 37
Roles of Heterotrophic Bacteria and Protists in the Arctic Ocean Carbon Cycle 40
Contribution of Planktonic and Ice Algae to Dimethylsulfide Production across the Arctic Ocean in Summer 42
Transfer of Shelf-Derived Carbon to the Interior of the Arctic Ocean 45
Dimethyl Sulfide in the High Arctic 47
The Role of Biomass, Bioturbation and Remineralization in Determining the Fate of Carbon in the Arctic Ocean 51
Oxygen Consumption, Denitrification and Carbon Oxidation Rates in Near-Surface Sediments of the Arctic Ocean 53

Ecology of Marine Mammals
Upper Trophic Level Research: Polar Bears and Ringed Seals 55

Contaminants
Artificial Radionuclides in the Arctic Ocean 59
Persistent Organic Contaminants 62
Air-Water Gas Exchange of Hexachlorocyclohexanes in the Arctic 64

Volatile Halomethanes 67
C_2–C_6 Hydrocarbons 70

Cloud Radiation
Atmospheric Radiation and Climate Program 73
Aerosols 78

Sea Ice
Sea Ice Characteristics across the Arctic Ocean 81
Measurements of Ice Mechanical Properties 86

Geology and Paleoceanography
Sources of Ice-Rafted Detritus and Iceberg Tracks in the Arctic Ocean 89
Late Quaternary Paleoceanography of the Canada Basin, central Arctic Ocean 92
Elemental and Isotope Geochemistry of Sediment from the Arctic Ocean 95

Ship Technology
Real-Time Remote Sensing for Ice Navigation 97
Ship Technology Program 100
Hull–Ice Interaction Load Measurements on the CCGS *Louis S. St-Laurent* 102

COMMUNICATIONS AND DATA MANAGEMENT
Special Communications Solutions 104
Data Management 106

APPENDICES
AOS-94 Participants 108
Science Stations 114

— U.S. Preface —

"Nothing great was ever achieved without enthusiasm."
—Ralph Waldo Emerson

Enthusiasm, cooperation and the spirit of scientific exploration are terms that aptly apply to the 1994 U.S.–Canada Arctic Ocean Section. The scientific motivation for the undertaking was to substantially increase the observational base necessary for better understanding the role of the Arctic in global change. The expedition's objective was to make a series of measurements that would allow the analysis and modeling of the biological, chemical and physical systems related to the Arctic and their impact on global change, and the controlling processes in these systems.

Cooperation was necessary to bring the scientific, operational and funding mechanisms together. Over five years of planning culminated on the evening of 24 July 1994 when the CCGS *Louis S. St-Laurent* and the USCGC *Polar Sea* steamed northward from Nome, Alaska, when 70 scientists embarked with their scientific equipment on what was planned to be a 60-day expedition.

The expedition could not have happened without enthusiasm. There was scientific enthusiasm for addressing an important and timely research topic. Also there was enthusiasm within the Coast Guards of the two nations for undertaking a maritime expedition in the Arctic Ocean that was to be the first of its type for North America.

Although there were challenges and disappointments along the way, the expedition was highly successful scientifically. The data analysis, interpretation and publication will continue for several years, and the work will form the basis for new and ongoing research in the Arctic. The National Science Foundation is proud to have contributed to the project and it congratulates the men and women who worked so hard to make it a success.

R.W. Corell
Assistant Director, Geosciences
National Science Foundation
U.S.A.

— Canadian Preface —

Unfortunately, in these times of economic restraint, it is not very often that federal managers get the opportunity to support a highly relevant and focused program that is also stimulating and exciting. The Arctic Ocean Section provided such an opportunity, and the scientific planners made sure that the documentation and justification were impeccable. Now that the expedition has returned and the expectations justified, it is easy to be self-congratulatory. However, without the considerable groundwork that had been accomplished over a period of several years, nothing would have happened.

The science plan made sure that maximum use would be made of the platform availability by considering the broadest possible coverage of issues and disciplines. The legitimacy of the scientific program was ensured through clear identification of the application of the anticipated results. Even the logistics and the use of the icebreakers were folded into the science, through programs dealing with such issues as ice strength, navigation forecasts and hull stresses. Forearmed with these strong arguments for potential benefits and creative science, the fiscal obstacles proved to have been surmountable. Despite the considerable difficulties faced, almost all of the anticipated work was accomplished.

The contents of this report speak, more eloquently than I could possibly hope to describe, on the success of the mission and the considerable analysis still to be undertaken. It remains for me to dedicate my thanks to the enormous amount of less exciting, but very necessary planning that laid the foundation for the funding and approval process.

G.L. Holland
Director General
Oceans Science Directorate
Department of Fisheries and Oceans
Canada

— Introduction —

Traditionally both Canada and the United States have relied on aircraft and drifting ice camps in supporting scientific work in the Arctic Ocean. Early examples include the so-called Ski Jump project in 1951–1952 and the ice stations Alpha and Bravo in 1957. These efforts have been particularly successful in advancing process studies, obtaining certain time series measurements and exploring limited areas; they have been less successful in carrying out synoptic survey work and sophisticated geographically distributed measurements requiring heavy equipment and elaborate laboratory facilities. In the open ocean the latter are typically done from shipboard, but not until 1987, when the German research icebreaker *Polarstern* crossed the Nansen Basin of the Arctic Ocean, did a modern Western research vessel successfully operate in the Polar Basin.

Russian scientists had also primarily used aircraft and drifting stations, having pioneered these techniques beginning with Papanin's North Pole I station in 1937. While the large and powerful Russian polar icebreaker fleet, one of which first reached the North Pole in 1977, routinely operates within the Polar Basin, the vessels are generally not used as scientific platforms. Meanwhile, the voyage of the *Polarstern* in 1987 was followed in 1991 by a remarkable joint Swedish–German undertaking using the icebreakers *Oden* and *Polarstern* to cross both the Nansen and Amundsen Basins, reaching the North Pole and returning to the Atlantic via northeast Greeenland. A U.S. icebreaker, the *Polar Star*, started out with the two European vessels but had to turn back near 85°N because of mechanical difficulties.

Inspired by the planned Swedish–German undertaking, but also deeply concerned that North American scientists would be unable to participate in ship-supported work in the Arctic Ocean, Ed Carmack and I met with Canadian and U.S. Coast Guard representatives in Ottawa in the fall of 1989 to inquire about interest in making a scientific crossing of the Arctic Ocean and about whether the two Coast Guards thought such an undertaking was realistic. The immediate response was positive on both counts, and the initial target for the crossing was set as the summer of 1993. The next 58 months or so were filled with a stream of planning activities involving interested scientific parties, the ship operators and funding agencies. Two major changes were made:

- Because of the long planning time required, the expedition was moved back one year to 1994; and

- Because the yard schedule for the *Polar Sea* required her to be in Seattle on 1 October, the route was altered to return directly to the Pacific from the North Pole, rather than via the Atlantic, that is, crossing the Canada Basin twice, but with an expected net saving of time.

Thanks to the efforts of a great many caring people, the myriad pieces in this planning activity all came together, and late in the evening of the 24th of July 1994 the *Louis S. St-Laurent* and the *Polar Sea* steamed northward from Nome to start the Canada–U.S. 1994 Arctic Ocean Section.

From the beginning the scientific goal of the undertaking had been to substantially increase the observational base necessary for understanding the role of the Arctic in global change. The objective was thus to make those measurements that would best promote the analysis and modeling of the biological, chemical and physical systems related to the Arctic and global change, and the controlling processes in these systems:

- Ocean properties pertinent to understanding circulation and ice cover;
- Biological parameters essential for defining the Arctic carbon cycle;
- Geological observations necessary for understanding past climates;
- Concentration and distribution of contaminants that impact the food chain and the environment;
- Physical properties and variability of the ice cover; and
- Atmospheric and upper ocean chemistry and physics relevant to climate.

In the following chapters, we shall see how all this came out.

Knut Aagaard
Chief Scientist, AOS-94
Applied Physics Laboratory
University of Washington
Seattle, Washington, USA

— Chronology —

The CCGS *Louis S. St-Laurent* and the USCGC *Polar Sea* departed Victoria, British Columbia, together on the evening of the 17th of July 1994. The majority of the scientific party of 70 persons boarded by helicopter in Nome, Alaska, on July 24th; several scientists had sailed with the ships from Victoria to set up equipment and make preliminary measurements. We sailed through the Bering Strait on July 25th and entered the ice in the northern Chukchi Sea early in the afternoon of the following day.

During the first few days, the ships worked some distance apart, as the ice was not severe. However, from the 30th of July onward, ice coverage was typically complete, and the ships moved close together, operating in tandem for the most efficient icebreaking, taking turns leading. This greatly reduced the fuel consumption for the trailing icebreaker. The ships icebreaking in tandem averaged 3–5 knots during the northbound transit. Visibility was generally poor throughout the time spent in the ice, with fog and overcast the rule. July 31st was the only full clear day. Passive microwave satellite imagery (SSM/I) received in real time aboard the *Polar Sea* provided excellent strategic information on ice conditions for planning the northbound route and stations.

Beginning in the central Chukchi Sea, the station line ran northward east of the Russia–U.S. Convention line, but once past 200 nautical miles from Wrangell Island, our track turned northwestward across the Chukchi Abyssal Plain and onto the Arlis Plateau, which we reached on the 3rd of August at 78°N. Heavy multi-year ice limited our eastward penetration down the flank of the plateau to longitude 174°18′W. We therefore resumed the station line northward, with the intent of covering the region to the east along 78°N on the return voyage. Near 80°N we again attempted a section to the northeast, but difficult ice conditions limited our penetration in that direction to 80°13′N, 172°46′W. We therefore continued working northwestward across the Mendeleyev Ridge and into the Makarov Basin.

On Monday the 8th of August we had an overflight and data transfer by a Canadian ice reconnaissance flight carrying side-looking radar, which mapped the ice in a swath 200 km wide and extending 1100 km along our intended track northward. From this imagery it was clear that difficult ice conditions lay to the east. Detailed helicopter ice reconnaissance the next few days confirmed this, and on Sunday the 14th, near 85°N, 170°E, we decided to continue onto the Lomonosov Ridge near 150°E before turning east and running the final northward leg of the outbound voyage along 150–155°W.

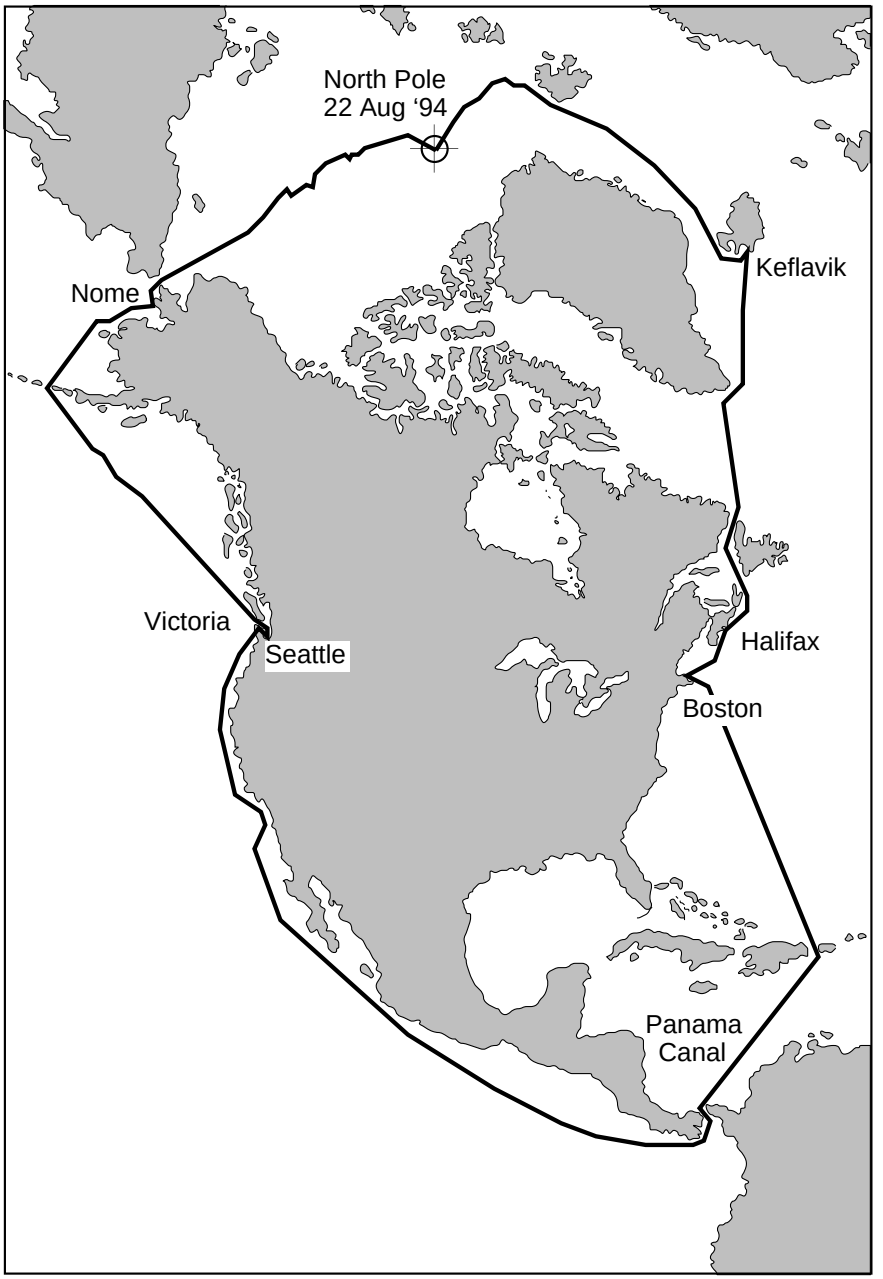

Route of the first surface circumnavigation of North America and Greenland. The *Louis S. St-Laurent* began and ended its voyage in Halifax. The *Polar Sea* began and ended in Seattle.

On the 15th of August the helicopter-borne CTD party found a new undersea mountain when the wire stopped paying out and they brought up mud from 850 m where the chart showed 3700 m. Three miles away on either side they found no bottom at 1450 m.

The next three days brought a northeast gale, snow and poor visibility, and progress was slow through the heavy ice. On the 19th we reached our station on the crest of the Lomonosov Ridge at 88°47′N, 143°E, where we planned to turn eastward. There we found the water at intermediate depth to be about

1°C warmer than we had seen at the base of the ridge, suggesting that the large gap in the ridge shown in the charts does not exist. We had also observed sediment-laden ice ("dirty ice") throughout the long northward track, from the ice edge in the Chukchi Sea to the North Pole, indicating that sediment incorporated in the ice on the shallow continental shelves is transported hundreds of kilometers across the Arctic.

Meanwhile, on the 17th we had had ice reconnaissance by a long-range Canadian aircraft, and on the 19th, while the ships remained on station on the ridge, we flew a 215-nautical-mile helicopter reconnaissance flight over the intended track. These showed very heavy ice at the location of our intended crossing point of the Lomonosov Ridge to the east, so we decided to continue northward on the section we were on and then return along an alternative route that would recross the ridge farther south. From there we would attempt to get onto the eastern flank of the Alpha Ridge to do seismic work and additional piston coring before continuing both these and our many other planned programs on the long voyage back to Alaska.

However, this was not to be, for shortly after starting northward down the steep ridge flank, early Sunday morning on the 21st of August, and about 50 nautical miles from the Pole, the *Polar Sea* lost one of its four blades on the starboard propeller. Divers also sighted some damage to the blades on the centerline and port shafts. These casualties required that the expedition take the shortest route out of the ice, which was toward Svalbard. Our intended section northward took us in that direction, and since we had already surveyed that route by helicopter and knew it to be feasible, we decided to continue on our course. That same afternoon a U.S. Coast Guard C-130 aircraft from Kodiak dropped spare parts for our satellite receiver. At 0230 Monday morning, Alaska standard time, we reached our next science station at 90°N, the first North American surface ships to do so, and the first surface ships ever to do it directly over the long unexplored route from the Pacific side of the Arctic Ocean. Our station at the Pole took 28 hours, as we fully deployed every sampling program. Not only could we compare conditions with those found three years earlier by Swedish and German investigators, but we could add a great many new measurements (for example, the concentration and distribution of a great variety of contaminants).

The last few hours before we arrived at the Pole, we had seen a large ship on the horizon. The ship, which proved to be the Russian nuclear icebreaker *Yamal*, had stopped in the ice about 20 nautical miles from the Pole to produce a children's television program. The *Yamal* planned to sail south along our intended track the next day, coincident with the shortest route out of the ice and the one that we needed to take because of the loss of one of *Polar Sea*'s propeller blades. At 0800 on the 23rd we got underway toward *Yamal*'s position, 20 nautical miles to the southeast. Before noon an extraordinary rendezvous took place as the icebreakers of the three largest Arctic nations—Russia, Canada and the United

The Russian nuclear-powered icebreaker *Yamal*, *Louis S. St-Laurent* and *Polar Sea* at an unplanned rendezvous near the North Pole.

States—commenced a historic polar gathering. More than 550 men, women and children met near the North Pole on the ice. The *Yamal*'s officers and crew hosted a barbecue on the ice, and the three ships were open for tours. This unprecedented and impromptu rendezvous near the North Pole in many ways symbolized a new era of international cooperation in the Arctic Ocean.

That evening all three ships sailed southward together toward Svalbard and made good progress, reaching south of 86°N by Thursday morning the 25th. At that point the ice conditions had improved, and we parted company with the *Yamal* to resume our scientific work, consonant with expeditiously exiting the Polar Basin. The pattern of southerly progress in somewhat lighter ice continued, and we occupied several high-quality science stations in the Eurasia Basin. On the 27th we had an airdrop of helicopter parts. The same day we received word from the U.S. Department of State that we were not permitted to continue the work southward within 200 nautical miles of Svalbard. We therefore terminated our in-ice section with a station at 83°51′N, 35°41′E. On Tuesday the 30th of August we exited the ice northwest of Svalbard, making course for Iceland. On the 31st we stopped the *St-Laurent* for a contaminant and oceanographic station in the Greenland Sea at 75°N, 6°W. This proved to provide an excellent end point for the Arctic Ocean Section, since it showed the prominent role of the Arctic Ocean outflow in changing the convective region of the Greenland Sea in recent years to a warmer and more saline state.

The *Polar Sea* disembarked most of its scientific party in Keflavik, Iceland, on the 3rd of September and then proceeded to Nova Scotia in company with the *St-Laurent*, the ships being slowed enroute by a storm with winds exceeding 60 knots. The *St-Laurent* disembarked its scientific party in Dartmouth on the 9th of September, bringing to a close a remarkable and productive

voyage. We had completed a highly successful scientific voyage literally across the top of the world, from the Pacific through Bering Strait, across Canada Basin, to the North Pole and into the Atlantic via Fram Strait.

Knut Aagaard
Chief Scientist, AOS-94

Lawson W. Brigham
Captain, U.S. Coast Guard
Commanding Officer, USCGC *Polar Sea*

Eddy Carmack
Chief Scientist, CCGS *Louis S. St-Laurent*

Philip O. Grandy
Captain, Canadian Coast Guard
Commanding Officer, CCGS *Louis S. St-Laurent*

— The Ships —

The Canadian Coast Guard Ship *Louis S. St-Laurent*, a 120-m icebreaker of 15,324-ton displacement based in Dartmouth, Nova Scotia, is the largest icebreaker in Canada. The ship has three fixed-pitch propellers. Five diesel engines supply three propulsion motors that can deliver a total of 30,000 hp to the three shafts. The *Louis S. St-Laurent* used an average of 15,000 hp on the northbound transit; occasional boosts of power to 25,000 hp were required in heavier ice conditions. The ship carried two BO 105-BS4 helicopters for ice reconnaissance and science support. Her total crew for this mission was 61, including the helicopter pilots and mechanic; the science party was 35.

The CTD/rosette, equipped with 36 ten-liter bottles, was deployed from the boat deck, starboard side. The rosette lab, a joined 16- × 20-ft container, was immediately forward of the deployment point, and the CTD lab, an 8- × 12-ft container, immediately aft. Ice work, including access to the ice, was from the foredeck, which was serviced by two cranes. Net hauls, pump deployments and box cores were done from the foredeck, starboard side. One winch serviced the net hauls and pumps, while two winches (working in tandem on deep casts) serviced the box core. Sample processing on the foredeck was done in an 8- × 12-ft container. All other laboratories were interior to the ship.

The U.S. Coast Guard Cutter *Polar Sea* is a 122-m icebreaker of 13,600-ton displacement based in Seattle, Washington, and is one of two Polar Class ships, the largest icebreakers in the U.S. The ship has three variable-pitch propellers. Each shaft can be powered by one or two diesels of 3,000 hp each (18,000 hp total in full diesel-electric mode) or by a turbine that can supply 20,000 hp in a sustained mode (60,000 hp total in an all-turbine configuration). Only the diesel-electric plant was used during the first portion of the voyage, but 50 nautical miles from the North Pole the loss of the blade on the starboard propeller necessitated the use of a gas turbine on the centerline shaft, boosting her total power to 26,000 hp. The ship carried two HH-65A helicopters for ice reconnaissance and science support. Her total crew for this mission was 142, including the aviation detachment; the science party numbered 35.

The CTD/rosette, equipped with 24 ten-liter bottles, was deployed from the main deck, port side, as were the plankton nets. The rosette lab was an enclosed, fixed, 16- × 14-ft shipboard installation located immediately forward of the deployment area. Ice work, including diving, was done from the starboard side aft, either using a platform swung from the flight deck by crane or from the main deck using the gangway. All box and piston coring was done

from the fantail, where a coring track and J-frame supported the piston coring work. Seven containers housed the science activities not accommodated within internal spaces: two on the maindeck, portside, for seismic work; two on the maindeck, starboard side, for biology, including radioisotope work; one on the 02 deck, starboard side, for ice core processing; and two on the 02 deck, port side, for radiation measurements and air and upper ocean chemistry. The latter container was adjoined by a liquid-nitrogen generating plant producing 35-40 L/day in support of a number of science programs. In addition, the port bridge wing housed a portion of the air sampling equipment. The biological productivity incubators were sited on the 01 deck, starboard side.

For expedition planning and to enhance navigation through the difficult ice conditions, an underway "ice center" was established aboard the *Louis S. St-Laurent*. Ice information was received from several sources, including real-time satellite imagery, fixed-wing aircraft reconnaissance (synthetic aperture radar and visual information), helicopter reconnaissance, shipborne radar and visual surveillance from each icebreaker. Extensive use was made of the real-time satellite images received and processed aboard the *Polar Sea*. Special sensor microwave imager (SSM/I from the Defense Meteorological Satellite Program) and advanced very high resolution radiometer (AVHRR from National Oceanic and Atmospheric Administration satellites) images were received and processed using a Terascan system. Sea ice concentration maps derived from the SSM/I data, which proved invaluable for both strategic and tactical navigation, could normally be produced and made available for interpretation less than one hour after a satellite pass. All satellite information could be passed to the ice center aboard the *Louis S. St-Laurent* using a VHF-FM ship-to-ship data link.

Effective helicopter ice reconnaissance was crucial to tactical navigation

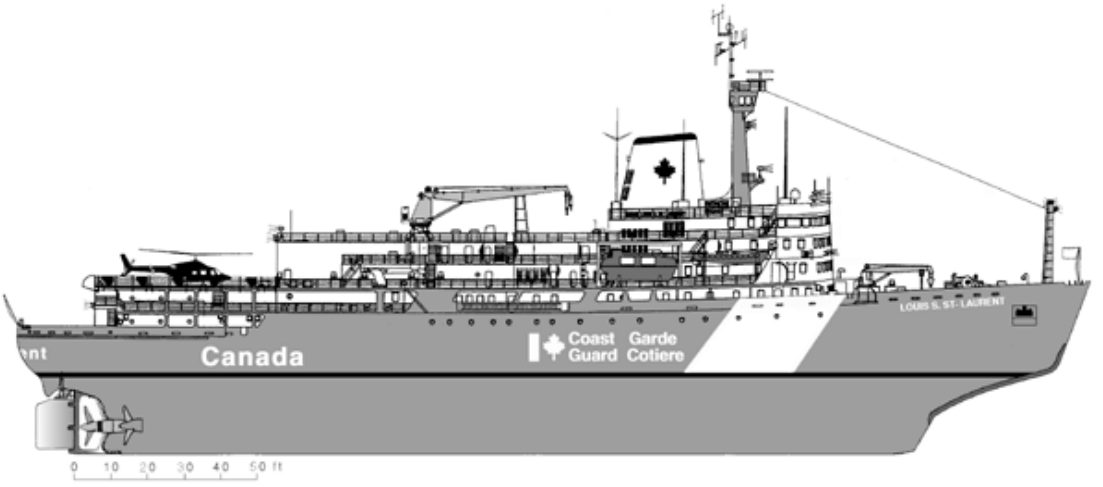

CCGS *Louis S. St-Laurent*

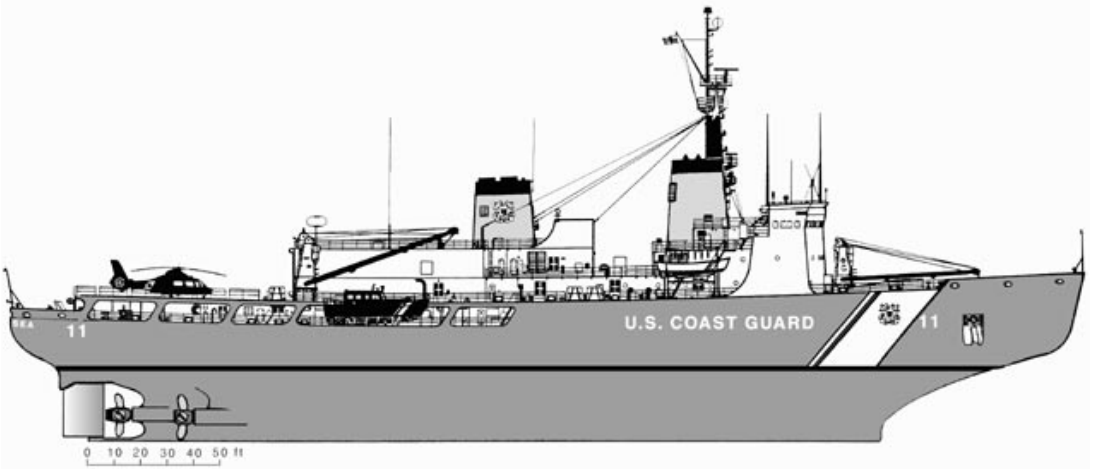

USCGC *Polar Sea*

	USCGC *Polar Sea*	CCGS *Louis S. St-Laurent*
Year built	1978	1969 (modernized 1988–1993)
Length (m)	122	120
Beam (m)	25.5	24.4
Draft (m)	9.7	9.9
Full-load displacement (tons)	13,600	15,324
Power (hp)		
Diesel-electric	18,000	30,000
Turbine	60,000	
No. of engines	6 diesel-electric 3 gas turbines	5 diesel-electric
No. of propellers	3	3
Crew	144	59

during the expedition. Global positioning system receivers aboard the helicopters provided precise coordinates of large floes, leads and other features that were plotted aboard both icebreakers. A Canadian Coast Guard helicopter with an Atmospheric Environment Service ice observer aboard flew daily ice reconnaissance flights in sectors 20–30 nautical miles ahead along the proposed expedition track. This information, coupled with radar and visual observations from both ships, greatly enhanced tactical navigation during the voyage.

Knut Aagaard
Chief Scientist, AOS-94

Lawson W. Brigham
Captain, U.S. Coast Guard
Commanding Officer, USCGC *Polar Sea*

Eddy Carmack
Chief Scientist, CCGS *Louis S. St-Laurent*

Philip O. Grandy
Captain, Canadian Coast Guard
Commanding Officer, CCGS *Louis S. St-Laurent*

— Science Reports —

Walter Tucker

In 1896 the Norwegian scientist Fridjof Nansen completed his historic drift across the Arctic Ocean in the ice-strengthened wooden ship *Fram*. Several years after his epic scientific voyage, reflecting upon the activities and achievements of Arctic scientists, Nansen predicted that the Arctic Ocean would become the best known ocean on Earth. Sadly, a century later, it is the most undersampled and least understood of the world's oceans. Canadian, U.S. and Russian scientists have conducted specific investigations from drifting ice camps and aircraft landings on the ice for many years, but the formidable ice cover of the Arctic Ocean has prevented traditional comprehensive oceanographic transects so common in other oceans of the world. Capable icebreaking vessels equipped for scientific investigations have been available for little more than a

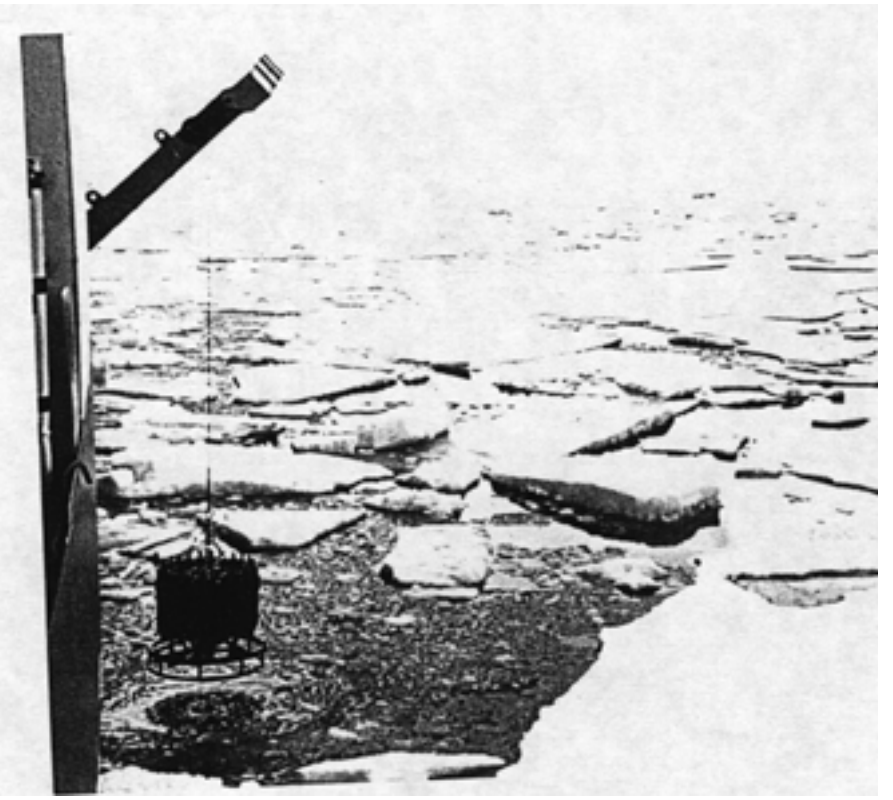

The CTD/ rosette being lowered from the *Polar Sea*.

Walter Tucker is from the U.S. Army Cold Regions Research and Engineering Laboratory in Hanover, New Hampshire, U.S.A.

Erk Reimnitz and Terry Tucker measuring the albedo of the ice surface.

decade. Yet the heavy ice conditions of the central Arctic have required that major expeditions use two ships. The expense of these scientific voyages has severely limited the number of comprehensive measurements that can be made to understand natural processes in the Arctic Ocean.

The Arctic Ocean Section was designed to fill in some of the many knowledge gaps about the Arctic Ocean. While there were several historic firsts resulting from AOS-94, most were peripheral to the purposes of the voyage—to increase our understanding of the Arctic Ocean in the context of global change and to gather baseline data on contaminants in this region.

With global climate change becoming an issue of international concern, attention has been increasingly focused on the Arctic, where all effects of global change are predicted to be amplified. It is also clear that the Arctic plays a key role in the processes that cause climate change. For instance, the ice cover of the Arctic Ocean depends on a delicate and relatively thin mixed layer that effectively insulates the ice cover from the warmer water below. Variations in the stratification may alter the heat and moisture exchanges with the atmosphere, affecting the balance of all Arctic ice masses. Predicted increases in air temperature will affect the extent of the ice cover and therfore the amount of the sun's heat absorbed

U.S. Coast Guard diver preparing to collect ice algae samples.

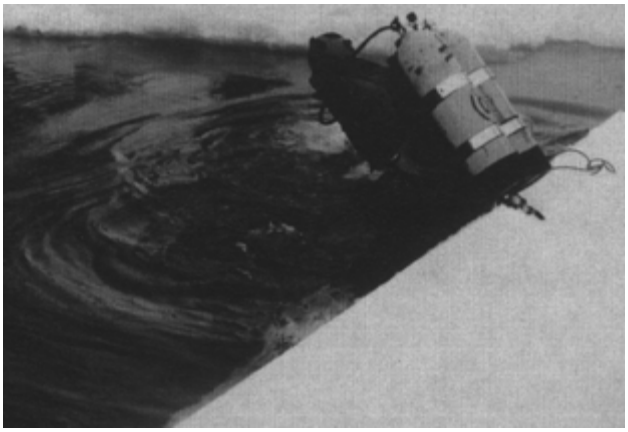

Dave Paton and Ikaksak Amagoalik collecting snow samples for contaminant studies.

or reflected back to the atmosphere. The fresh water exported from the Arctic Basin in the form of ice and river runoff into the convective gyres of the Greenland, Iceland and Laborador Seas influences the formation of North Atlantic deep water and heat transport associated with global thermohaline circulation. The ocean programs on AOS-94 were designed to investigate the ice cover, water mass structure, origins of the water masses, and ocean circulation on a major transect of the Arctic Ocean.

Global climate change and the expected increases in atmospheric carbon dioxide will have a major impact on the carbon cycle of the Arctic Ocean. Evaluating the internal cycling of carbon plus the fluxes from rivers and adjacent seas is important in understanding what the effect will be on biogeochemical cycling and the ability of the Arctic Ocean to sequester carbon dioxide. The Arctic Ocean and its marginal seas have only recently been recognized as areas of high biological productivity during the favorable solar radiation seasons. Primary productivity converts atmospheric carbon dioxide to organic carbon in the ocean, where it may then be recycled by organisms back to the atmosphere, remain dissolved in the ocean or be deposited on the sea floor as particulates. The Arctic Ocean is believed to play an important role in the global carbon cycle, but too little work has been done to quantify that role. A major goal of AOS-94 entailed examination of primary productivity levels and the organic and inorganic carbon pools of the central Arctic.

There is also major international concern that the Arctic has been polluted by a variety of contaminants, including heavy metals, organochlorines and radionuclides. Contaminants have been dumped directly into the Arctic Ocean.

Sediment trap being lowered into the water to collect samples for contaminant chemistry studies.

More important, however, is the ocean's role as a receptor for contaminants carried northward by major geochemical transport mechanisms involving the atmosphere, rivers, sediment, sea ice and currents. Little is known about sources, background levels, transport pathways and residence times of the various contaminants. Obtaining information on the levels of a variety of contaminants in the atmosphere, ice, ocean and sediments was the focus of the AOS-94 contaminants program.

AOS-94 was truly multidisciplinary. Fifty individual research programs were pursued, and the expedition indeed sampled across the entire Arctic Ocean. The word "section" implies measurements of the seafloor, ocean, ice and atmosphere—a slice from the top of the atmosphere to the bottom of the ocean. The major disciplinary efforts and their major objectives were:

Ocean Circulation and Geochemistry

Hydrographic surveys and geochemical sampling to improve our understanding of Arctic Ocean circulation and water mass structure.

Biology and the Carbon Cycle

Measurement of standing stocks and production rates of the dominant organisms and their relation to the distribution of particulate and dissolved carbon and nitrogen.

Ecology of Marine Mammals

Studies of the distribution, migration, population dynamics, genetic history and food chains of polar bears and other marine mammals.

Contaminants

Trans-Arctic sampling of atmosphere, snow, ice, water column and sea

Jim Rich in the biology van on the *Polar Sea.*

floor to detect the presence of radioactive wastes and organochlorines.

Cloud Radiation

Characterization of the aerosol and optical properties of clouds, and determination of the greenhouse effect of the Arctic Ocean by quantification of the major greenhouse gases, UV radiation and photosynthetically active radiation.

Sea Ice

Determination of ice mechanical, physical and chemical properties, sediment transport by ice, ice biota, contaminants, and albedo of the mottled summer ice surface.

Geology and Paleoceanography

Geoscience sampling to allow an interpretation of tectonic history, past climates and paleoceanography, and active transport processes in the Arctic Ocean.

Ship Technology

Determination of the utility of real-time remote sensing data for enhancement of navigation through ice and measurement of hull loads and structural response of the hull to ice loads.

Planned seismic surveys were not accomplished, so the tectonic evolution program was not successful. All other programs, however, were successful in spite of the loss of the *Polar Sea*'s propellor blade, which shortened the voyage. The following brief reports present details and preliminary results of many of the research projects.

— Ocean Circulation and Geochemistry —

A CTD/Hydrographic Section across the Arctic Ocean

James Swift

The objectives of our water column work were:

- To study the origin and circulation of the waters of the Arctic Ocean and nearby seas;
- To determine the surface-to-bottom distributions and sources of the physical and chemical characteristics;
- To study the location, origin and structure of subsurface boundary currents; and
- To contribute to studies of the response of the regimes to environmental forcing.

The water column program provided the trans-Arctic section a complete program of CTD (conductivity, temperature and depth) and "small-volume" hydrographic measurements meeting World Ocean Circulation Experiment parameter and quality recommendations.

The *Louis S. St-Laurent* is well equipped for high-latitude CTD/rosette work. On the starboard side of the vessel there is a small CTD/computer van and a large double-van rosette room. The rosette was launched through a large A-frame. The *Louis S. St-Laurent* is also outfitted with a full suite of laboratories for the analytical equipment.

The CTD/rosette being lowered from the *Louis S. St-Laurent.*

We collected water column measurements at 35 hydrographic stations along the AOS-94 route: beginning on the Chukchi shelf, then across the Chukchi Abyssal Plain and Makarov Basin, then down the Eurasian side of the Lomonosov Ridge to the North Pole. Water column work was cut short at that point because the *Polar Sea* developed mechanical problems. Both ships exited the Arctic together through Fram Strait, occupying an additional four stations en route.

The U.S./Canadian water column measurement team on the *Louis S. St-Laurent* carried out full-depth CTD profiling and 36-level rosette sampling. Water samples were collected for chlorofluorocarbons (CFCs), helium, oxygen, CO_2 system components, AMS ^{14}C, tritium, ^{18}O, nutrients, salinity, trace metals, radionuclides and organic contaminants. CTD and water sampling was carried out at 39 stations and was remarkably trouble free.

We examined sections of potential temperature, salinity and density anomalies referred to 0 and 2000 db from the CTD data for our section from the

James Swift is from the Scripps Institution of Oceanography in La Jolla, California, U.S.A.

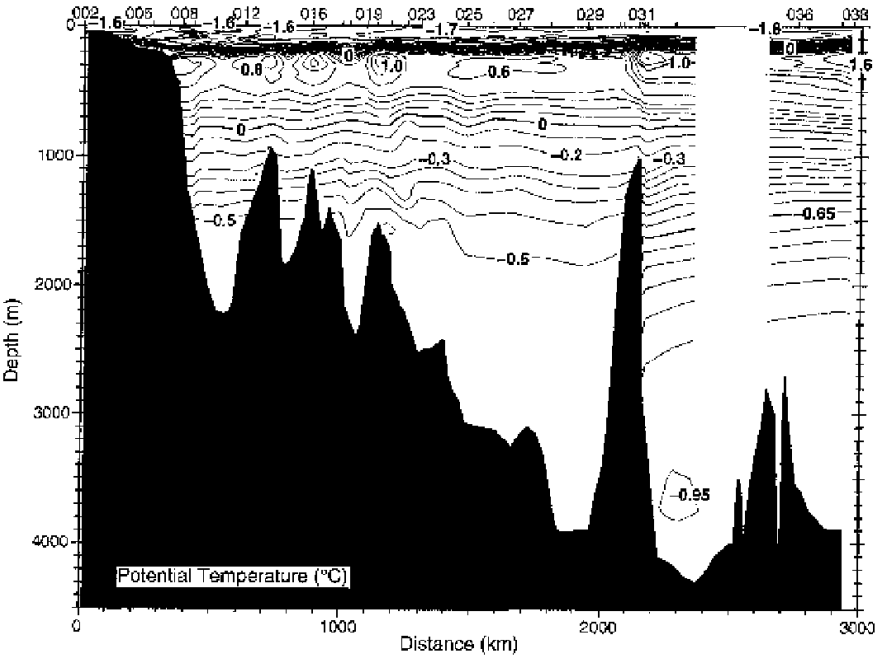

Potential temperature section from the Chukchi shelf (left) to the Eurasian flank of the Lomonosov Ridge (right). The warm cores appear at approximately 200–400 db above each primary bathymetric feature. The station numbers are across the top of the figure.

Chukchi shelf to the North Pole. We observed multiple warm cores in the Atlantic layer (depths of about 200–400 m) near 1.0°C along the Chukchi boundary and warmer than 1.5°C on the Eurasian side of the Lomonosov Ridge. Earlier data from the Makarov Basin showed no water in this layer warmer than 0.5°C. In 1993 the Institute of Oceanographic Sciences (Patricia Bay) group found water warmer than 1°C on the Makarov slope just north of the Chukchi Sea. The AOS-94 data extend this finding, showing the Atlantic layer near both the Chukchi and Lomonosov ridge boundary areas to be 0.5°C warmer than measured before 1993. In some places the insulating fresh, cold upper layer was somewhat eroded, though far from completely. One of the important issues facing us now is to place this warming in context. Such subdecadal variability is important to climate models.

We found the central Canadian sector of the Arctic Ocean to be an oceanographically active environment, not a "dead end" isolated from any active role in the global circulation by the shallow sill through the Bering Strait, the Lomonosov and other ridges, and its sheer distance from the North Atlantic Ocean. Instead, the Canadian sector is importing water, modifying it and exporting it in ways that have important effects and consequences.

For example, biological activity on the Chukchi shelf is so high in summer that phytoplankton photosynthesis can supersaturate oxygen in the surface waters there by almost 50% in places, yet the debris left behind by those organisms and their predators sinks and decays, regenerating nutrients and using up oxygen on the bottom of the shelf. These shelf-bottom waters can get rather dense, due partly to brines released from ice formation above, and then flow off the shelf, carrying regenerated nutrients and, potentially, contaminants into the central basin.

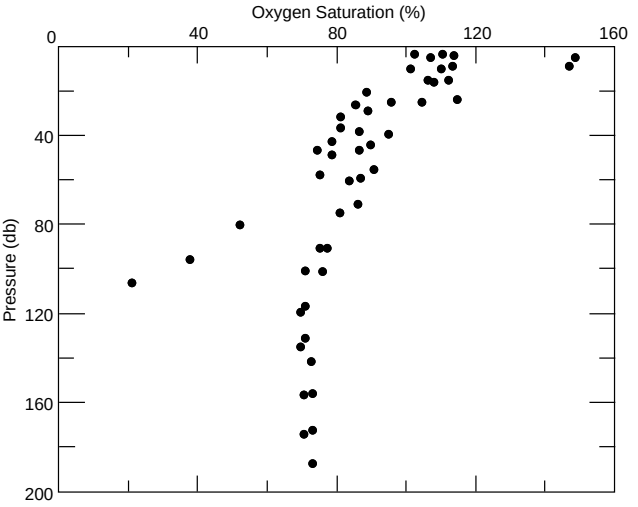

Saturation of oxygen vs. pressure for the AOS-94 stations over the Chukchi shelf (Stations 1–6).

Winter shelf waters have been thought to reach rather high densities. Although there are observations of this, establishing a direct connection to the deep waters, which seems essential to models of deep water formation in the Arctic, has been elusive. We found during AOS-94 what is perhaps an important new piece to this puzzle: At station 22, on the periphery of the Makarov Basin, we saw a bolus of water dense enough to be centered at 1000 m, with unique characteristics indicating that it could have come only from the shelf. Relatively high CFC concentrations confirmed its recent origin. This bolus has entered the Makarov Basin and now slowly freshens the deep water. This may be the first direct observation of "new" high-density shelf water actually in the deep basins.

There is a weak, deep horizontal salinity gradient across the Chukchi–Makarov sector, with higher deep salinities near the pole on the Canadian side of the Lomonosov Ridge. At station 22 in the southeastern Makarov Basin we saw deflections in the salinity isopleths due to the bolus of relatively fresh, cold, young deep water.

Isopycnals generally slope slightly down from pole to shelf across the domain covered by this section, with more significant deflections associated with each principal bathymetric feature, and circulation associated with the bolus of young deep water found at station 22. Sharp isopycnal slopes over the Lomonosov Ridge (stations 30–34) showed geostrophic adjustment to relatively strong upper-layer flow along the ridge crest. The most intense deep deflections in sigma-2 were found on the Eurasian flank of the Lomonosov Ridge and, to a lesser extent, on the southeast flank of the Makarov Basin.

On their own the AOS-94 CTD/hydrographic/tracer/contaminant data are a unique, well-placed and important data set, providing the first reference-quality section across the Chukchi Abyssal Plain and Makarov Basin and a careful, synoptic section of closely spaced stations across the Eurasian flank of the Lomonosov Ridge near the North Pole. The AOS-94 section also joins to the *Oden* 1991 section in the Makarov Basin near the Lomonosov Ridge, and these in turn can be joined to the *Polarstern* 1987 Nansen Basin section to form a nearly complete, shelf-to-shelf trans-Arctic section of high-quality surface-to-bottom multi-tracer stations.

Total Carbonate and Total Alkalinity: Tracers of Shelf Waters in the Arctic Ocean

E. Peter Jones

Modern oceanographic measurements include a suite of many tracers, each of which often has a significance in determining the origin of a particular water mass and tracing its circulation. In the Arctic Ocean, total carbonate and total alkalinity have been shown to be effective tracers of waters that have flowed into central regions from the continental shelves. In addition, these measurements are an integral part of an assessment of carbon fluxes into and within the Arctic Ocean.

Total alkalinity and total carbonate in seawater are closely related to salinity, with small deviations from a linear relationship resulting primarily from the dissolution or precipitation of calcium carbonate. In near-surface water, carbon from biological decay can also be a significant contributor to changes in total carbonate. Biological productivity can be assessed with the aid of total alkalinity and nutrient measurements, and the total carbonate and total alkalinity data will contribute to an assessment of the carbon budget of the Arctic Ocean.

Total alkalinity and total carbonate analyses are best carried out on "fresh" samples: the analyses were done onboard ship within about 20 hours after they were collected, using standard techniques (potentiometric titration and coulometry). Samples were collected at almost all oceanographic stations at almost all sampling depths, typically 36 from the surface to the bottom, using the rosette sampler. The time between stations did not allow water from every sampling depth to be analyzed, though more than 90% of them were. The quality of the data is high, reflected in replicate analyses with an average difference of just over 1 part per thousand for total alkalinity and 0.9 parts per thousand for total carbonate.

Higher total alkalinity values observed in the near-surface water at many stations during AOS-94 are attributed to dissolved calcium carbonate brought into the Arctic Ocean by runoff. This signal helps to determine the sources of fresh water by separating river runoff from sea ice meltwater, and it helps in tracing the circulation pattern of river runoff. Near-surface "excess" alkalinity, indicating the presence of river runoff, was found at all stations in the Canada

E. Peter Jones is from the Bedford Institute of Oceanography in Dartmouth, Nova Scotia, Canada.

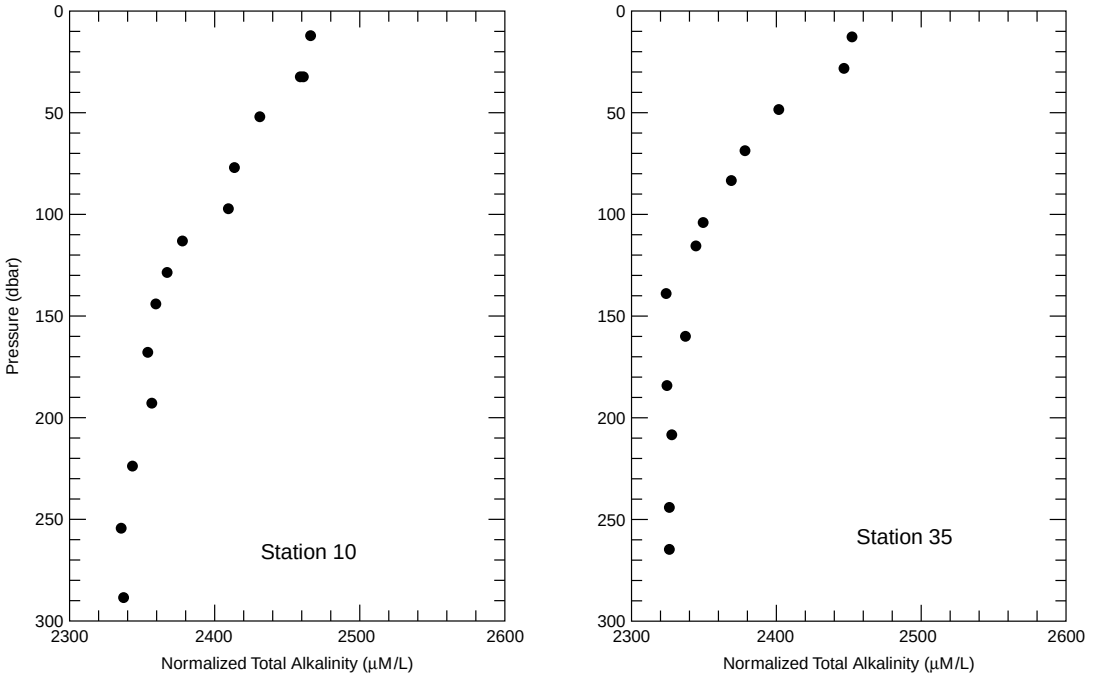

Upper profiles of total alkalinity at Stations 10 and 35 (the North Pole).

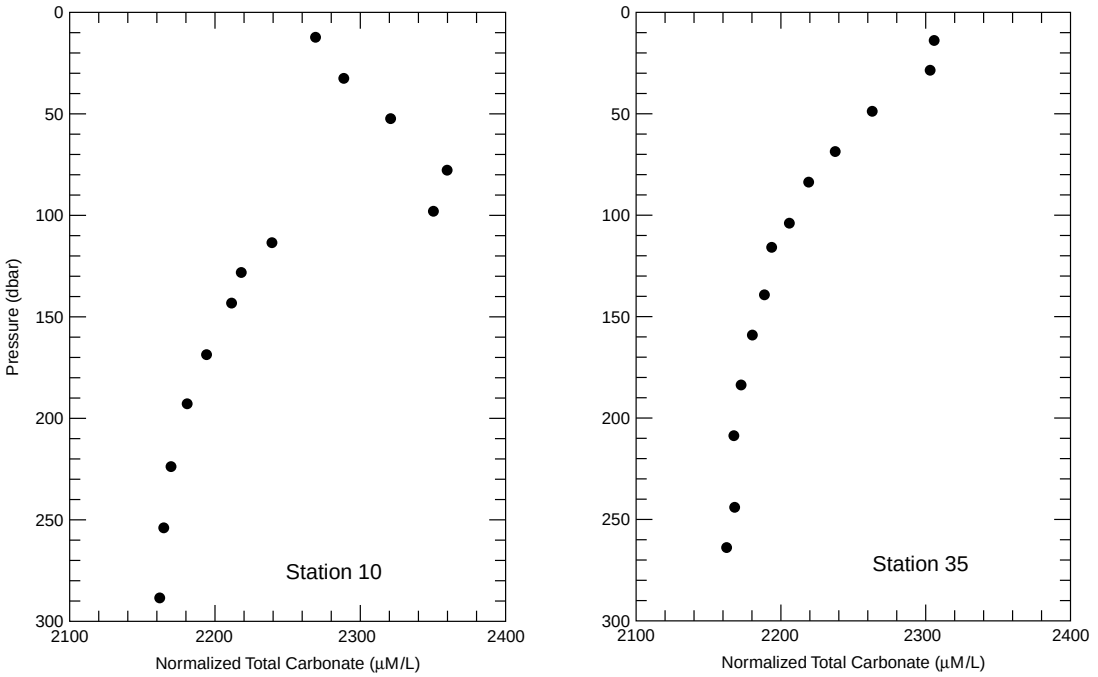

Upper profiles of total carbonate at Stations 10 and 35 (the North Pole). The maximum values in total carbonate at Station 10 correspond to maximum values in the nutrient profile and minimum values in the oxygen profile.

Basin and in the Amundsen Basin. In the Nansen Basin the "excess" total alkalinity was much reduced or not present, indicating that most of the near-surface fresh water in these regions of the AOS-94 path comes from melting sea ice.

High values of total carbonate were also observed near the surface. These correspond to the total alkalinity maximum and are consistent with dissolved calcium carbonate being brought into the Arctic Ocean by river runoff. There are also high total carbonate values in the halocline (depth about 100 m) of the Canada Basin that correspond closely with the nutrient maximum, consistent with the "excess" total carbonate being regenerated along with nutrients during the decay of biogenic matter. These high values were not present after Station 14, where the nutrient maximum also disappeared. The total carbonate in the near-surface water and in the halocline can be used to assess the amounts of carbon entering the Arctic Ocean from the Siberian tundra (river runoff) and the amount entering as a result of carbon fixation on the continental shelves.

Profiles of both total alkalinity and total carbonate show small variations in deeper water that are greater than the precision of these measurements. These structures may be interpretable in terms of the water masses present and processes such as the sequestering of anthropogenic carbon dioxide, but any definitive interpretation will have to await more detailed data analysis, not to mention inspired thought.

Transient Tracers: Chlorofluorocarbons and Carbon Tetrachloride

E. Peter Jones and Fiona A. McLaughlin

The cloud of international concern over the growing anthropogenic releases of refrigerants, aerosols and solvents and their impact on climate and the ozone layer, ironically, has had a silver lining for oceanographers. The measurement of chlorofluorocarbons (CFCs) and carbon tetrachloride (CCl_4) in seawater, from the surface to the bottom, provides a tool for tracing water masses since they were last at the sea surface with a time clock that spans most of this century. Such data give important information about the various layers within the ocean, for example: Are they rapidly flushed or isolated? Are the waters transported from other oceans or nearby shelves? These are important questions in Arctic Ocean research, as they relate directly to the transport of contaminants—such as organochlorines and radionuclides—to the Arctic food chain.

Measuring CCl_4 may also contribute to understanding the ocean's ability to absorb carbon dioxide, a critical question for those attempting to predict global warming. CCl_4 can be used as a surrogate for estimating levels of atmospheric carbon dioxide, as both compounds have been increasing in the atmosphere in a similar fashion since the turn of the century. The depth at which CCl_4 is found in the ocean thus signals the depth at which anthropogenic carbon dioxide, produced in the twentieth century, is found.

AOS-94 provided an opportunity to measure a suite of CFCs (CFC-12, CFC-11 and CFC-113) and CCl_4 on a transect crossing the Arctic Ocean. Samples were collected at almost all oceanographic stations at almost all sampling depths, typically 36 from the surface to the bottom, using the rosette sampler. The samples were analyzed using a standard purge-and-trap gas chromatograph.

Previous cruises sampled different regions in different years: the Nansen Basin in 1987, the Nansen and Amundsen Basins and the North Pole in 1991, and the southwestern Canada Basin in 1993. The latter cruise yielded information suggesting that the structure and circulation of water masses in the Arctic Ocean may be undergoing a major change. AOS-94 CFC data will allow us to determine the rate, magnitude and extent of these changes.

Although results are preliminary, certain key features are evident. CFC and

E. Peter Jones is from the Bedford Institute of Oceanography in Dartmouth, Nova Scotia, Canada. Fiona McLaughlin is from the Institute of Ocean Sciences in Sidney, British Columbia, Canada.

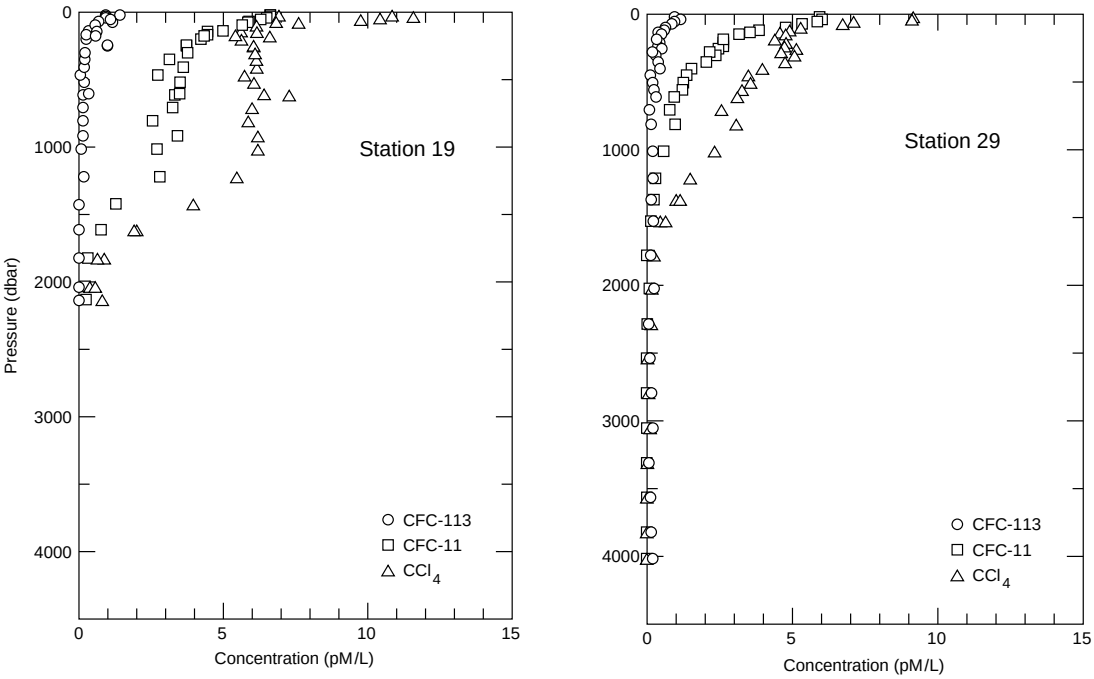

Profiles of CFC-11, CFC-113 and CCl_4 at Station 19 above the Mendeleyev Ridge and Station 29 in the central Makarov Basin.

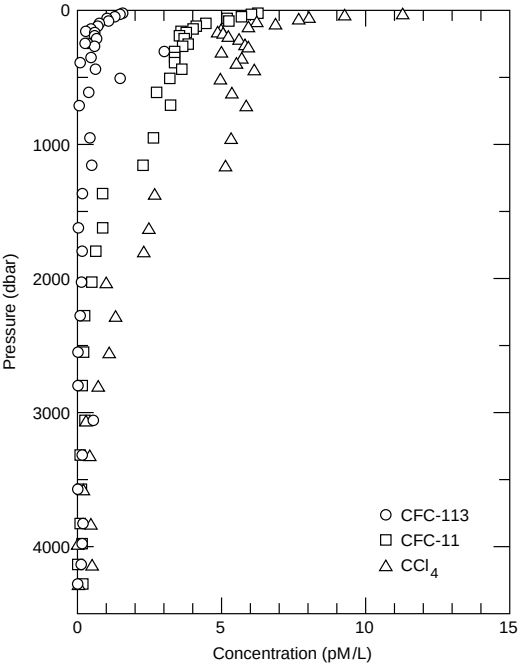

Profiles of CFC-11, CFC-113 and CCl_4 at Station 35 in the Amundsen Basin.

Frank Zemlyak and Fiona McLaughlin examining strip chart data in the chemistry lab on the *Louis S. St-Laurent*.

CCl_4 profiles obtained at Station 19 above the Mendeleyev Ridge, where boundary currents are believed strong, and at Station 29 in the central Makarov Basin, where flows are believed to be weak, show important differences in both the concentrations and the penetration depths of all the compounds. This suggests that transport mechanisms are stronger around the basin's exterior than at its interior and that bathymetry plays a major role in the circulation of the Arctic Ocean.

Furthermore, Station 35, east of the Lomonosov Ridge in the central Amundsen Basin, shows higher values of CFCs and CCl_4 in intermediate water layers compared to the central Makarov Basin. This suggests a closer connection with laterally transported incoming source waters. In the deep waters of the Makarov Basin, greater than 2000 m, concentrations of CFCs and CCl_4 are below detection limits, indicating that these waters have a residence time longer than a century. In the Amundsen Basin the penetration is deeper, with CCl_4 values above the detection limit to beyond 3000 m, signaling that these waters are less isolated than those in the Makarov Basin. A mesoscale feature is apparent from temperature and salinity measurements and is confirmed by CFC concentrations at Station 22 between 900 and 1400 m, about 20% higher than nearby stations. This eddy-like structure is evidence of a mechanism whereby waters from the Siberian Shelf are transported into the interior of the Makarov Basin.

Distribution of Iron and Aluminum in the Surface Waters of the Arctic Ocean

Chris Measures

Extremely low concentrations of dissolved iron in the surface waters of parts of the remote ocean such as the sub-Arctic Pacific are believed to play a crucial role in limiting the biological productivity of these regions, despite an abundance of the major nutrients in the surface waters. Phytoplankton require iron for various biochemical processes, including the conversion of sunlight energy and the reduction of the nutrient nitrate.

The levels at which iron becomes limiting to phytoplankton growth, and the effects of its sporadic introduction into surface waters on growth rate, species dominance and carbon export, are the subject of intense study in various oceanic regimes.

While iron is delivered to the edges of the ocean in copious quantities through fluvial run-off, little of this material escapes the intense scavenging removal of these high-productivity regions to reach the surface waters of the gyres. In the temperate and tropical oceans, iron is delivered to the surface ocean by the dissolution of eolian-transported continental dust; the regions in which iron is found to be limiting are those that receive only low inputs of this eolian material.

Mineral dust inputs to the Arctic are low, and with its annual cycle of variable ice cover, the supply of iron by this route to the surface waters is likely to be low and highly sporadic in both time and space. Little or nothing is known of the distribution of iron in the surface waters of the Arctic Ocean, because it is difficult to collect uncontaminated samples for an element that is ubiquitous in manufactured materials and because of analytical difficulties associated with determining iron at extremely low concentrations.

Recent advances have resulted in the development of analytical methodology that can be operated onboard ship and is capable of determining iron at ambient surface water concentrations. AOS-94 provided an opportunity to deploy this system to investigate the input of the eolian-transported trace metals iron and aluminum across the surface waters of the basin. Since sampling close to the ship raises questions of contamination from the ship's iron hull,

Chris Measures is from the Department of Oceanography at the University of Hawaii in Honolulu, Hawaii, U.S.A.

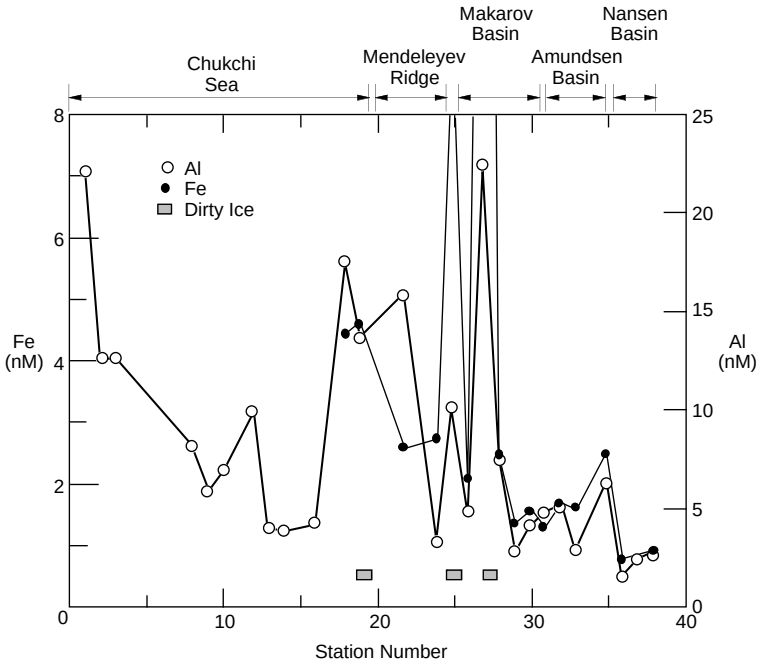

Concentrations of iron and aluminum in the surface waters vs. *Louis S. St-Laurent* station numbers.

surface samples were obtained at stations by hand-dipping bottles from the edge of ice floes located upwind of the ship.

The results indicate that concentrations of iron in the surface waters across the basin are relatively high and quite variable, with generally higher values (3.2 nM) in the western Arctic dropping to relatively low values (0.75 nM) in the Nansen Basin. Within this general trend, though, are localized regions of extremely high iron concentrations (>8 nM), particularly in the vicinity of the Mendeleyev Ridge. These highest values occur in regions where the ice floes were observed to contain significant quantities of sediment on their surface, known as "dirty ice." The suggestion that ice-rafted sediment is the source of these high iron values in the surface water is further supported by the enrichment of aluminum in the same regions.

The entrainment of sediments into ice floes during freezing at the edge of the basin and the subsequent advection and partial melting of the ice in the center of the basin represents a unique pathway for delivering reactive trace metals such as iron to the center of a basin. The partial melting of ice floes during the summer apparently is capable of delivering high levels of iron to the surface stratified waters. This delivery mechanism results in relatively high concentrations of iron, which may favor the development of the ice algae community that grows on the underside of the ice floes and is thought to make a major contribution to the primary productivity of the Arctic Ocean. Large organisms such as ice algae require higher ambient iron concentrations

than smaller organisms to meet their iron needs since their requirement scales with volume but their ability to transport scales with their surface area.

The ice rafting of sedimentary material from the edges to the center of the basin and its effect on primary production represent a unique biogeochemical pathway connecting physical, chemical and biological processes. The susceptibility of this transport route to future perturbations of Arctic climatology is unknown. However, it seems that any change that resulted in the dimunition of ice-edge freezing in winter might lead to significant changes in the nature and magnitude of primary productivity of the central Arctic.

Chris Measures in the laboratory on the *Louis S. St-Laurent*

Thorium Isotopes as Tracers of Scavenging and Particle Dynamics in the Arctic Ocean

S. Bradley Moran, Katherine M. Ellis, Richard W. Nelson and John N. Smith

The role of the Arctic Ocean in the global carbon cycle remains a key question in studies of global climate change. The Arctic Ocean and its adjacent seas are characterized by spatial and temporal extremes in the rate of biological sequestration of atmospheric CO_2, ranging from oligotrophic conditions in the central Arctic to production rates in the Bering and Chukchi Seas that are among the highest reported for any ocean. An important objective of Arctic research is to quantify the fraction of total primary production exported from Arctic surface waters to the ocean bottom in the form of sinking particulate organic carbon and associated biogenic debris. In addition, the Arctic has the largest ratio of shelf to deep waters of any oceanic region, making it a particularly good place to study the importance of shelf–basin interactions on particle dynamics and chemical transport.

As part of AOS-94, field sampling was conducted with the primary goals of:

- Using ^{234}Th as a tracer to quantify scavenging and the export flux of organic carbon by particle sinking from the upper waters and the coupling of chemical transport between the shelves and the interior Arctic Ocean; and
- Using ^{230}Th and ^{232}Th to quantify rates of particle cycling in the intermediate and deep Arctic waters.

Collection of these data within the framework of other AOS-94 field programs will contribute to the international effort to better understand the role of the Arctic Ocean in the global carbon cycle and climate change. Summarized here are preliminary ^{234}Th results of this research. Samples were also collected for determination of full-depth vertical profiles of long-lived ^{230}Th (half-life = 7.5×10^4 years) and ^{232}Th (half-life = 1.4×10^{10} years) at several locations along the cruise track. These samples are being analyzed using highly sensitive thermal ionization mass spectrometry.

S. Bradley Moran is from the Graduate School of Oceanography at the University of Rhode Island in Narragansett, Rhode Island, U.S.A. Katherine Ellis, Richard Nelson and John Smith are from the Bedford Institute of Oceanography in Dartmouth, Nova Scotia, Canada.

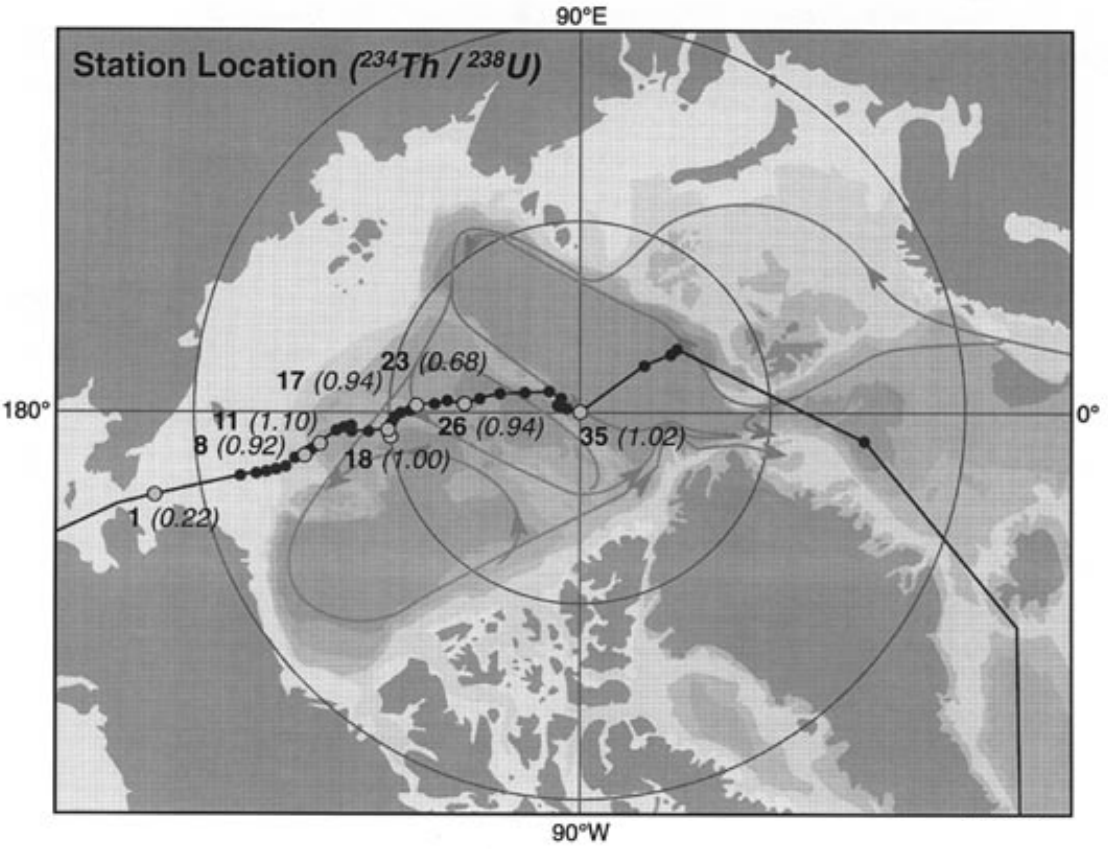

Cruise track of the CCGS *Louis S. St-Laurent* and stations occupied for vertical sampling of ^{234}Th. Shown in parentheses are ^{234}Th/^{238}U activity ratios in the surface mixed layer (0–30 m). Activity ratios less than one indicate preferential removal of ^{234}Th by particle scavenging, whereas ratios equal to one indicate ^{234}Th/^{238}U equilibrium and very low rates of particle scavenging.

During AOS-94 the naturally occurring, short-lived ^{234}Th isotope (half-life = 24.1 days) was used as a tracer to quantify scavenging and the export of sinking biogenic particulate matter and associated elements. In the surface ocean the disequilibrium between ^{234}Th and its soluble parent ^{238}U varies in response to short-term changes in particle export on a time scale of approximately 1–100 days. Because of its short half-life, it was essential to measure ^{234}Th at sea using a low-energy pure germanium detector.

The ^{234}Th/^{238}U activity ratios in the surface mixed layer (0–30 m) indicates the amount of particle scavenging along the cruise track. The low ^{234}Th/^{238}U activity ratio of 0.22 at Station 1 is consistent with removal of ^{234}Th from the water column by particle scavenging within the particle-rich Chukchi Sea. In contrast, surface waters in the interior Arctic generally show no significant ^{234}Th/^{238}U disequilibrium and hence very low rates of particle scavenging. An exception is the relatively low ^{234}Th/^{238}U activity ratio of 0.68 at Station 23, which may be due to enhanced biological productivity and associated biogenic particle scavenging of ^{234}Th at this location.

Vertical profiles of ^{234}Th, ^{238}U and silicate are another way of viewing particle scavenging. A striking observation is the subsurface deficit in total ^{234}Th evident in the Makarov Basin (Station 26). The low ^{234}Th activities may result from scavenging removal of ^{234}Th due to enhanced local biological

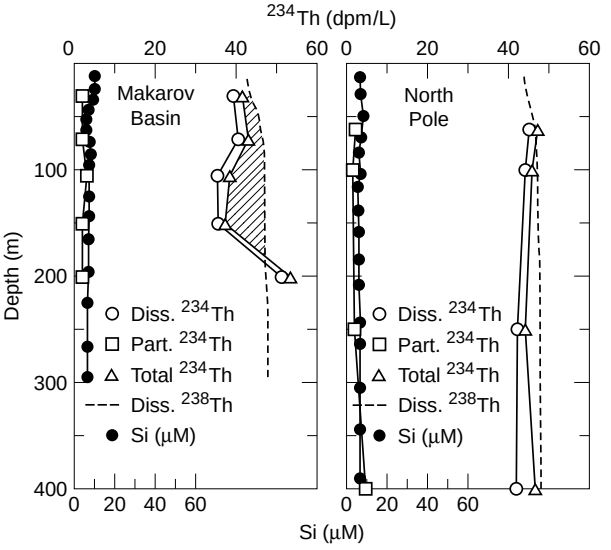

Depth profiles of ^{234}Th (dpm: disintegrations per minute) and dissolved silicate in the Makarov Basin and at the North Pole. ^{238}U activities were calculated from salinity (^{238}U = 0.069 × salinity).

productivity. On the other hand, the ^{234}Th deficit may also reflect a scavenging "history" due to ^{234}Th removal within the particle-rich shelf waters and advection into the Arctic interior. In contrast, results from the North Pole (Station 35) indicate no significant ^{234}Th/^{238}U disequilibrium and hence no appreciable scavenging of ^{234}Th.

These ^{234}Th profiles show for the first time a marked spatial variability in particle scavenging in the upper Arctic Ocean. Ongoing studies aim to determine the relative importance of ^{234}Th scavenging due to in-situ biological productivity and advective transport of shelf water containing low ^{234}Th into the central Arctic.

Finally, the ^{234}Th results are being used to quantify the sinking flux of biologically produced particulate organic carbon (POC) from the surface mixed layer (0–30 m). Preliminary estimates indicate that the export flux of POC ranges from approximately 400 mg C/m^2-day in the Chukchi Sea to 1–10 mg C/m^2-day in the Arctic interior. These particulate carbon fluxes are comparable to the limited number of carbon flux measurements obtained using sediment traps in the Arctic Ocean.

What Can Be Learned from Barium Distributions in the Arctic Ocean?

Kelly Kenison Falkner

Barium is one of several naturally occurring inorganic elements that are being studied as part of a larger project to track river- and shelf-modified water inputs to the central Arctic. In the open oceans, dissolved barium displays nutrient-type behavior, being depleted from surface waters in conjunction with biological processes and enriched at depth by regeneration. River waters tend to be enriched in dissolved barium with respect to surface seawaters, and riverine signals are further augmented in estuaries where barium adsorbed on riverine clays is desorbed as the clays encounter the more abundant cations of seawater.

AOS-94 samples have been analyzed for dissolved barium content by isotope dilution-inductively coupled plasma quadrupole mass spectrometry. Several interesting observations can be made when these results are taken in the context of previously reported barium data for the Arctic (Falkner et al. 1994) and recent results from 1993–1995 field efforts, including extensive sampling along the Russian and Siberian estuarine and shelf regions, in the Mackenzie Delta as well as the 1993 USS *Pargo* and 1995 *Cavalla* nuclear submarine missions (Falkner and Guay, unpublished data). All of these data sets have been calibrated to a common barium standard and have a precision of 3% or better.

Consistent with its higher suspended sediment loads, the Mackenzie River appears markedly enriched in barium compared to the rivers of the eastern Arctic sector. Sub-ice surface (< 25 m) barium concentrations in the central Arctic range from 35 to 70 nM and show a spatial distribution reflecting both the varying riverine inputs and the integrated surface ice motion. The highest values are concentrated in the Beaufort Gyre region, which is influenced by Mackenzie inputs. Intermediate values influenced by the Siberian rivers track the transpolar drift and are bordered toward the Fram Strait and Barents Shelf by low values characteristic of North Atlantic surface waters.

As previously observed, halocline waters that display elevated silicon contents and are believed to originate from the Bering–Chukchi regions also show pronounced barium maxima (up to 140 nM). At stations where halocline

Kelly Kenison Falkner is from the College of Oceanic and Atmospheric Sciences of Oregon State University, Corvallis, Oregon, U.S.A.

Frank Zemlyak in the *Louis S. St-Laurent* chemistry lab.

waters do not show a nutrient maximum, barium displays a halocline minimum at levels that correspond to those observed for the eastern Arctic shelf regions (30–35 nM). Underlying waters of Atlantic origin contain distinctly higher barium contents of 45–50 nM. These data demonstrate that barium has considerable promise for complementing other tracers of surface currents and halocline water formation. Full interpretation of these and other features in the barium data await complete analyses of the 1995 samples.

Reference

Falkner, K.K., R.W. MacDonald, E.C. Carmack and T. Weingartner (1994) The potential of barium as a tracer of Arctic water masses. In *The Polar Oceans and Their Role in Shaping the Global Environment: The Nansen Centennial Volume,* American Geophysical Union, Geophysical Monograph 85, p. 63–76 (O.M. Johannessen, R.D. Muench and J.E. Overland, Ed.), Washington, D.C.

— *Biology and the Carbon Cycle* —

Cycling of Organic Carbon in the Central Arctic Ocean

Patricia A. Wheeler

The central Arctic Ocean has been characterized as a region of very low biological production due to the year-round presence of ice and a short photosynthetic season. Past studies have postulated that the high concentrations of dissolved organic carbon in surface waters result from the slow growth and metabolism of bacteria at low temperatures. To determine if biological processes play a significant role in the Arctic carbon cycle, the investigators of the biology program measured nutrients, particulate and dissolved organic carbon, standing stocks of algae, micro- and mesozooplankton, and rates of primary production and bacterial production. Standing stocks and production rates are described in reports by Gosselin et al., Sherr et al., and Thibault. In this summary, I describe major patterns in the distribution of nutrients and organic carbon along the transect. Then, using biomass and rate measurements made by other investigators, I estimate the turnover time for the pool of dissolved organic carbon. The results clearly indicate that significant in-situ production and utilization of organic carbon takes place in the central Arctic Ocean and that biological processes play an important role in the Arctic carbon cycle.

Samples were collected at 16 major stations across the Arctic, starting in the Chukchi Sea, proceeding to the North Pole and exiting on the Atlantic side. Water samples were collected with a CTD/rosette, after moving ice away from the ship when necessary. Water samples from 12–24 depths in the upper 300 m were analyzed for nutrient concentrations, particulate carbon and nitrogen, and dissolved organic carbon and nitrogen. Nutrients were analyzed onboard, while the other samples were stored for later analysis in our shore-based laboratory.

In general, the major nutrients (nitrate, phosphate and silicate) were present in sufficient concentrations in surface water (0–25 m) to support the primary production of phytoplankton and ice algae. The one exception was low nitrate concentrations at stations between 76 and 80°N, 173 and 178°W. In this region, ice algae in particular may have been nitrogen-limited. Phosphate concentrations decreased from 1.0 to 0.6 μM along the transect, while silicate

Patricia Wheeler is from the College of Oceanic and Atmospheric Sciences at Oregon State University in Corvallis, Oregon, U.S.A.

concentrations decreased from 10 to 5.0 μM. These decreases may reflect the relative strength of influence of Pacific and Atlantic water masses, or they may reflect biological utilization of nutrients in water moving in the Transpolar Drift. Nitrate, however, showed the opposite pattern. Nitrate concentrations increased from 1.0 to 4.0 μM along the transect. Nitrate concentrations varied more with depth from 0 to 300 m than did phosphate and silicate concentrations. The wider range in concentrations combined with differences in diffusion and other mixing processes may account for the differences in patterns of changes in nutrients along the transect.

Pat Wheeler in the wet lab aboard the *Polar Sea*.

Particulate organic carbon (POC) ranged from 3.5 to 8.0 g/m^2 and generally decreased along the transect. Particulate organic nitrogen (PON) ranged from 0.4 to 1.3 g/m^2 and also generally decreased along the transect. The C/N ratio of particulate organic material ranged from 8 to 14 and nearly doubled along the transect. These levels of POC and PON are relatively high; this material is composed of approximately 40% living material—10% phytoplankton and 30% heterotrophs (bacteria and protists). Zooplankton standing stocks ranged from 0.2 to 2 gC/m^2, making a significant additional contribution to the total organic carbon and accounting for about 40% of the total particulate organic carbon in the central Arctic.

The largest pool of organic carbon was dissolved organic carbon (DOC), which ranged from 60 to 120 μM. DOC and zooplankton standing stocks both increased in the poleward direction, reaching maximum values around 85 to 87°N. Earlier investigators attributed the high DOC concentrations to the refractory nature of DOC from riverine inputs and presumably low rates of bacterial metabolism due to low temperatures in the central Arctic. Gosselin et al. measured significant rates of DOC excretion by phytoplankton and ice algae; these results, along with the similar spatial patterns of the distribution for zooplankton and DOC, strongly suggest the importance of biological production of DOC.

Bacterial production ranged from 17 to 53 mg C/m^2-day, comparable to rates measured in Antarctic waters. Since bacteria are the main consumers of dissolved organic carbon, bacterial production can be used to estimate the mean turnover time of DOC. Bacterial carbon utilization divided by concentrations of DOC indicated that the average turnover time for the total DOC pool is less than one year in the central Arctic. Since the mean residence time

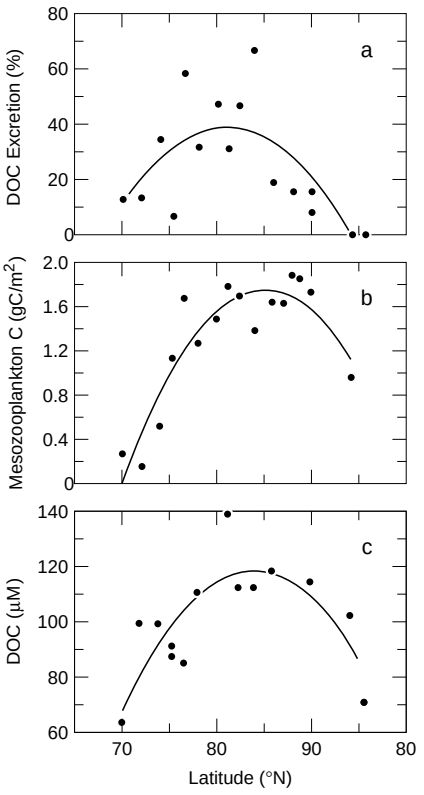

a. Percentage of the phytoplankton production released as extracellular carbon, measured by Michel Gosselin.

b. Zooplankton standing stocks for 0–100 m. Zooplankton were collected in vertical net tows (200 mm mesh, 0.75 m opening), dried onboard ship, weighed and then analyzed for carbon with a CHN analyzer. The curve is a second-order regression with r^2 = 0.834.

c. Dissolved organic carbon in the surface water. Samples were collected in duplicate and stored frozen with no preservative. The curve is a second-order regression with r^2 = 0.634.

DOC and standing stocks vs. latitude.

of surface water in the central Arctic is about 10 years, some portion of the DOC is being recycled many times.

Previous studies of the Arctic Ocean carbon cycle assumed that, since production appeared to be low in the central basins, most organic carbon was either derived from river inputs or imported from the extensive shelf regions. Our new measurements of primary production, bacterial production and zooplankton standing stocks suggest a more dynamic carbon cycle in the surface waters of the central Arctic. Higher estimates of primary production result from the activity of ice algae, which were not sampled in previous studies. Direct measurements of DOC excretion by both ice algae and phytoplankton indicate that at least a portion of the high DOC found in the central Arctic is produced in situ. Measurements of rates of bacterial production indicate a significant turnover of DOC in the central Arctic. High standing stocks of mesozooplankton are further evidence for significant cycling of organic carbon in the upper 100 m of the central Arctic. Primary production by the ice algae and the production of DOC in the central Arctic both appear to be key processes in the Arctic carbon cycle. Our results indicate that the central Arctic is not a biological desert but rather supports an active biological community that contributes to the cycling of organic carbon through dissolved and particulate pools.

Mesozooplankton Community Structure in the Arctic Ocean in Summer

Delphine Thibault

Ocean organisms range in size from tiny bacteria (0.1–1 μm) to whales (over 30 m). Mesozooplankton (200–2000 μm) represent a link between smaller organisms (<200 μm), such as phytoplankton and microzooplankton (on which they graze) and larger grazers (>200 μm), such as macrozooplankton and fish (which feed on them). By knowing their biomass, composition and metabolism, we can estimate the role of mesozooplankton in the pelagic food web and the carbon cycle.

During AOS-94, as part of the biological study, the biomass, the specific composition and the chemical composition of mesozooplankton were estimated in the upper 500 m of the Arctic Basin. Where possible, three layers were sampled at each station (0–100, 100–200 and 200–500 m). Also, the content of the gut pigments, as an indicator of grazing, was directly measured on the main species and stages in the upper layer.

The plankton net being lowered for sampling on the *Polar Sea*.

The mesozooplankton biomass in the first 100 m increased quadratically with latitude (r^2 = 0.82), showing a maximum around 87°N. A high mesozooplankton biomass (19–42 mg dry weight/m^3) was observed in the upper two layers (0–200 m), while in the deepest layer (200–500 m) the biomass was much lower, ranging from 4 to 16 mg DW/m^3. The integrated mesozooplankton standing stock varied between 0.4 and 10 g DW/m^2 and appear to be significantly higher than previously reported for the Arctic Ocean (Conover and Huntley 1991).

The mesozooplankton carbon content was nearly constant over the whole study area (around 40% of the dry weight), although it appears to be lower at the ice edge stations. Those variations might be related to modifications in the zooplanktonic population. The C/N (g/g) ratio for the

Delphine Thibault is from the Département d'océanographie of the Universite du Québec à Rimouski, Quebec, Canada.

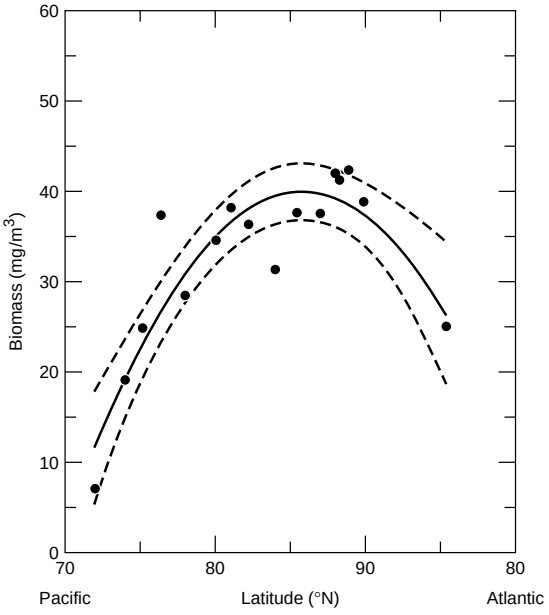

Mesozooplankton biomass in the upper 100 m along the transect. The solid line is a second-order regression, and the dashed lines show the 99% confidence interval, r^2 = 0.8158.

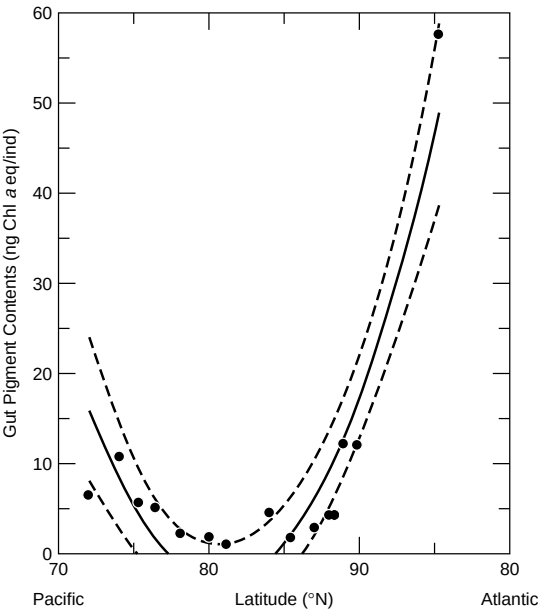

Gut pigment contents of *Calanus hyperboreus* female in the upper 100 m along the transect. The solid line is a second-order regression, and the dashed lines show the 99% confidence interval, r^2 = 0.86.

mesozooplankton population was high (6.5–8.5) compared to lower latitudes (4.5), but it stayed in the range typical at high latitudes (6.3–12.5) (Bamstedt 1986). The high lipid content (used as reserve) observed in the zooplankton may explain these high values.

The Arctic mesozooplankton taxonomic composition did not change along the transect and within the three depths. This population was mainly represented by copepods (70–90% of the total number) and specifically by three large species (*Calanus hyperboreus, C. glacialis* and *Metridia longa*) and three small genera (*Oithona, Oncea* and *Paracalanus*). However, the first group of species accounts for more than 80% of the total biomass and includes mainly late stages (C4, C5 and adult). The two species of *Calanus* are typical Arctic species. A third species of *Calanus* is present but less abundant (*C. finmarchicus*, Atlantic species). The highest concentration of this species was found at the last stations in the Nansen Basin, closest to the inflow of Atlantic water. In total, 21 species of copepod were identified. This low number is consistent with the diminution in the number of zooplankton species with latitude (there are approximately 100 species in the Mediterranean Sea). The other taxa were mainly amphipods, ostracods, pteropods, isopods, chaetognaths, siphonophores, appendicularia, medusa and euphausiacea.

The ingestion of phytoplankton by the main species of copepod was estimated by analyzing the gut pigment content. The values are expressed

in term of chlorophyll *a* equivalent (Chl *a* + pheopigments). The gut pigment content ranged from 1 to 60 ng Chl *a* eq/individual, with maximum values (>10 ng Chl *a* eq/individual) in the Chukchi Sea and the Nansen Basin. As with the biomass, those values are well described by a second-order regression. A good relationship appears between the gut pigment content and the primary production (for *Calanus hyperboreus* female, r^2 = 0.69). But the high zooplankton biomass in the first 100 m cannot be supported by the chlorophyll *a* concentration (r^2 = –0.7552). On the other hand this uncoupling, confirmed by the low gut pigment content, might be explained by the omnivorous character of the main copepods; they can feed on either phytoplankton or microzooplankton.

All these data give us new information on the role of mesozooplankton in the Arctic food web. In the Arctic Ocean the zooplankton biomass in late summer was similar to values reported for other oceans (Reid 1962, Be et al. 1971). Copepods represent 80% of the whole mesozooplanktonic population of the Arctic Ocean. The contribution of the mesozooplankton in the carbon cycle is important, accounting for approximately 40% of the total particulate organic carbon in the upper 100 m of the water column. The mesozooplankton also feed on phytoplankton but probably more on microzooplankton.

References

Bamstedt, U. (1986) Chemical composition and energy content. In *The Biological Chemistry of Marine Copepods* (E.D.S. Corner and S.C.M. O'Hara, Ed.), Oxford: Clarendon Press, p. 1–58.

Be, A.W.H., M. Forns and O.A. Roels (1971) Plankton abundance in the North Atlantic ocean. In *Fertility of the Sea*, p. 17–50.

Conover, R.J. and M. Huntley (1991) Copepods in ice-covered seas—Distribution, adaptations to seasonally limited food, metabolism, growth patterns and life cycle strategies in polar seas. *J. Mar. Syst.*, **2:** 1–41.

Reid, J.L., Jr. (1962) On circulation, phosphate–phosphorus content, and zooplankton volumes in the upper part of the Pacific ocean. *Limnology and Oceanography,* **7:** 287–306.

Roles of Heterotrophic Bacteria and Protists in the Arctic Ocean Carbon Cycle

Barry F. Sherr, Evelyn B. Sherr and David Kirchman

Our role in the AOS-94 expedition was to determine the distribution and activity of heterotrophic microbes (bacteria and phagotrophic protists) in the context of the overall food web of the upper column. Prevailing theory suggests that bacteria and heterotrophic protists have a minor role in the food webs of polar ecosystems compared to those of temperate and tropical oceanic regions, because low water temperatures inhibit microbial growth. According to this concept, the lack of heterotrophic microbial activity results in a greater fraction of plant production being available for larger consumers in polar food webs.

We determined:

- Biomass per unit volume and per square meter for bacteria and for three size classes of protists;
- Bacterial production and growth rate; and
- Rates of bacterivory.

We also investigated the hypothesis that marine bacterioplankton are metabolically suppressed by extremely low water temperature, by investigating standing stocks and turnover of labile sugars and amino acids and the response of bacterioplankton to the addition of substrates and to temperature.

The preliminary results indicate an active microbial community. Bacterial abundances were high ($0.5–1.5 \times 10^6$ cells/mL) in the upper 50 m of the water column, declining to $< 0.2 \times 10^6$ cells/mL below 100 m. Both bacterial and heterotrophic protist biomass was in the range of 0.4–1.0 g C/m^3; the total biomass of heterotrophic microbes often exceeded the phytoplankton biomass. Measured phytoplankton *production* was insufficient to support the rates of bacterial production; extracellular polysaccharides produced by bottom-ice diatoms are a probable additional source of organic substrate for pelagic bacteria.

Bacterial activity had Q_{10} values of 2–3 over a temperature range of –1°C to +15°C. The maximum growth rate was observed at a temperature of about 15°C.

Barry Sherr and Evelyn Sherr are with the College of Oceanic and Atmospheric Sciences at Oregon State University in Corvallis, Oregon, U.S.A. David Kirchman is with the Graduate College of Marine Studies, University of Delaware, Lewes, Delaware, U.S.A.

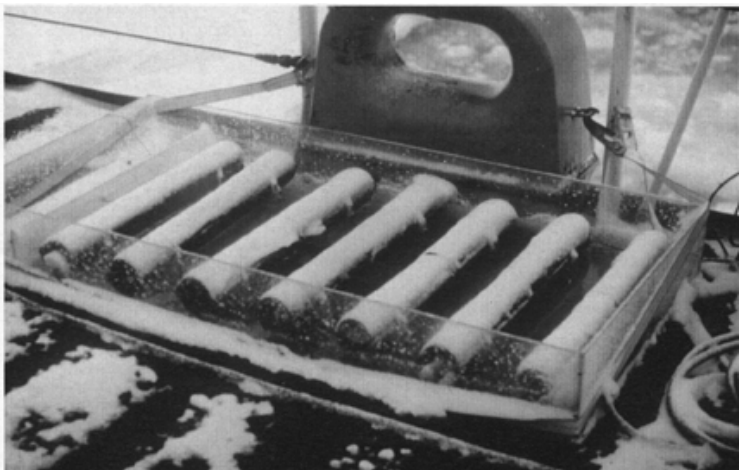

Deck incubator for productivity measurements on the *Polar Sea.*

The assemblage of heterotrophic protists was dominated by phagotrophic dinoflagellates from 6 to >50 μm in size. Ciliates were also common in most samples. There were few choanoflagellates in the water column under the ice pack, although choanoflagellates were abundant in ice-free waters of the Chukchi and Greenland Seas, as others have previously found. The smallest protists observed were 1–2 μm heterokont flagellates, which appeared to be feeding both on bacteria and on 1-μm eukaryotic phytoplankton, tentatively identified as *Micromonas pusilla*, which were present in abundances of 10^3–10^4 cells/mL in the upper 50 m. The protist biomass ranged from 0.006 to 0.1 g C/m^3 and often exceeded estimates of phytoplankton biomass determined from chlorophyll *a* concentrations. All size classes and taxonomic groups of heterotrophic protists appeared to be consuming phytoplankton cells.

Based on the data on standing stock abundance and activity of heterotrophic microbes in the central Arctic Ocean, and on biomass and production of phytoplankton and ice algae, we developed a preliminary budget of carbon fluxes through the pelagic microbial food web of the central Arctic Ocean. Integrated over the upper 50 m, stocks of bacterioplankton ranged from 0.27 to 0.70 g C/m^2, and of heterotrophic protists from 0.37 to 0.79 g C/m^2. Estimates of productivity of autotrophs and heterotrophs in the upper 50 m were comparable: 0.02–0.14 g C/m^2-day for bacteria, 0.03–0.25 g C/m^2-day for phytoplankton plus ice algae, and 0.05–0.15 g C/m^2-day for phagotrophic protists. Assuming a gross growth efficiency of 40%, heterotrophic microbes could consume on the order of 0.2–0.7 g C/m^2-day. As primary production occurring at the time of the cruise could not provide this daily amount of organic carbon, we infer that the heterotrophic community was also supported by the organic carbon present in the water as particulate material (3 g C/m^2) and as dissolved organic compounds (60 g C/m^2). This detrital organic matter may have been produced earlier in the growing season by blooms of ice algae in the central Arctic.

Our results suggest that, contrary to the initial concept of a minor role of heteorotrophic microbes in polar ecosystems, heterotrophic bacteria and phagotrophic protists are significant consumers of plant production in the food webs of the central Arctic Ocean.

Contribution of Planktonic and Ice Algae to Dimethylsulfide Production across the Arctic Ocean in Summer

Michel Gosselin, Maurice Levasseur, Nathalie Simard, Sonia Michaud, Sangeeta Sharma, Peter Brickell and Timothy Bates

Algae produce a sulfur compound that seems not only to be a key link in the global sulfur cycles but that also influences the formation of clouds and therefore the Earth's temperature. Understanding how these algae affect cloud formation in the remote oceans could be crucial to predicting how the Earth will respond to global warming. The link between marine microscopic algae and climate involves dimethylsulfide, or DMS, the gas that gives air its bracing smell. It forms from the enzymatic breakdown of a salt, dimethylsulfoniopropionate (DMSP). Marine algae produce DMSP to keep their osmotic balance with seawater, without which water would leave the cells of the algae, killing them. DMSP may also play a role as a cryoprotectant for microalgae living in very-low-temperature marine environments, such as polar waters and ice. The processes by which DMSP is released into the sea are not well understood, but most researchers think it occurs when algae die or are grazed by zooplankton. In the sea DMSP breaks down to form DMS. A fraction of this DMS, perhaps

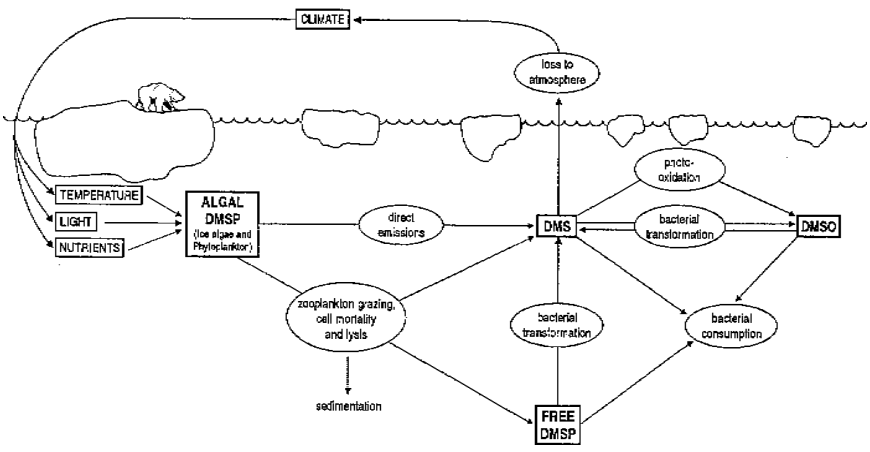

Marine biogeochemical cycle of DMS: production, transformation and utilization pathways that may ultimately influence the quantity of DMS lost to the atmosphere.

Michel Gosselin is with the Département d'océanographie of the Universite du Québec à Rimouski, Rimouski, Quebec, Canada. Maurice Levasseur, Nathalie Simard and Sonia Michaud are with the Institut Maurice-Lamontagne, Ministére des Péches et des Océans, Mont-Joli, Quebec, Canada. Sangeeta Sharma and Peter Brickell are with Atmospheric Environment Service, Downsview, Ontario, Canada. Timothy Bates is with the National Oceanic and Atmospheric Administration's Pacific Marine Environmental Laboratory, Seattle, Washington, U.S.A.

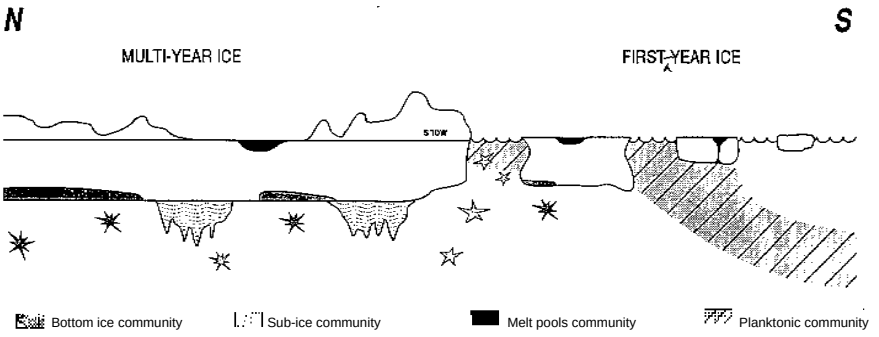

Biological communities found in sea ice and in the upper part of the water column in a North–South section of the Arctic Ocean during summer.

a tenth, then enters the atmosphere. The rest is either consumed by bacteria or broken down by sunlight to form dimethylsulfoxide (DMSO).

Algae exploit several habitats in the polar environment. In ice-free polar seas, microscopic algae are found mainly in the upper part of the water column. They are called the planktonic algae, or phytoplankton. In ice-covered seas, algae are found mainly:

- At the surface of the ice in melt pools formed by thawing surface ice, flooding or a combination of flooding and thawing;
- In the bottom 2–5 cm of the ice, where they form a brownish layer; and
- In the seawater immediately under the ice, where they form huge mats and strands up to 3 m long.

These unicellular algae that grow in and on the ice are called the sea ice algae. In the Arctic, phytoplankton and ice algae both contribute to DMS production.

The goal of our study was to determine the contribution of planktonic and sea ice microalgae to the production of DMSP and DMS in the western and central Arctic Ocean during summer. Sampling was conducted on the multi-year ice of the Arctic Ocean from 26 July to 26 August 1994, onboard the USCGC *Polar Sea*. The transect began in the continental shelf of the Chukchi Sea on the western side of the Arctic and terminated in the deep Nansen Basin on eastern side of the Arctic. Along the transect the ice thickness varied from 1 to 5 m, and ice coverage varied from 50 to 100%. Bottles specifically designed for oceanographic research were used to collect surface water samples, while melt pools were sampled by means of a bucket. An ice corer was used for collecting the bottom-ice samples. Finally, the sub-ice samples were collected by U.S. Coast Guard scuba divers, using a 2-L syringe sampler called a "slurp gun." In the laboratory, various measurements were performed on the melted ice and water samples. Chlorophyll *a* concentrations, an index of algal biomass, were determined using the fluorometric method. Particulate DMSP, dissolved DMSP and free DMS were determined by gas chromatography.

Significant DMS concentrations were measured in all the habitats studied. In surface water, DMS concentrations were highest on the continental shelf of the Chukchi Sea and rapidly decreased toward the Pole. Surface DMS concen-

trations were also relatively high in cracks (openings in the multi-year ice). These cracks, called leads, tend to be narrow (tens to hundreds of meters in width) but may extend for many kilometers. In some situations leads may reach several kilometers in width and are termed polynyas. Of the ice habitats, the highest algal biomass and DMS concentrations were found in the bottom of the ice on the eastern side of the transect. On a volume basis, the maximum DMS concentrations were three times higher in the bottom of the ice than in surface water. Significant DMS concentrations were also measured in the algal mats loosely attached to the bottom surface of the ice. These mats, composed of the centric diatom *Melosira* sp., were found mostly in the Canada Basin (from 75° to 80°N and from 86° to 88°N) and in the Makarov Basin (from 89° to 90°N). We also measured detectable levels of DMS in melt pools, which covered up to 20% of the surface of the ice. These results indicate that physical and biological processes occurring at the marginal ice zone of the Chukchi Sea favor DMS production. In the ice-covered central Arctic, although local sources of DMS exist, DMS sea-to-air fluxes are probably limited by the gas-tight ice cover. At these high latitudes, DMS produced by ice algae and phytoplankton may only reach the atmosphere through leads and other openings in the ice cover.

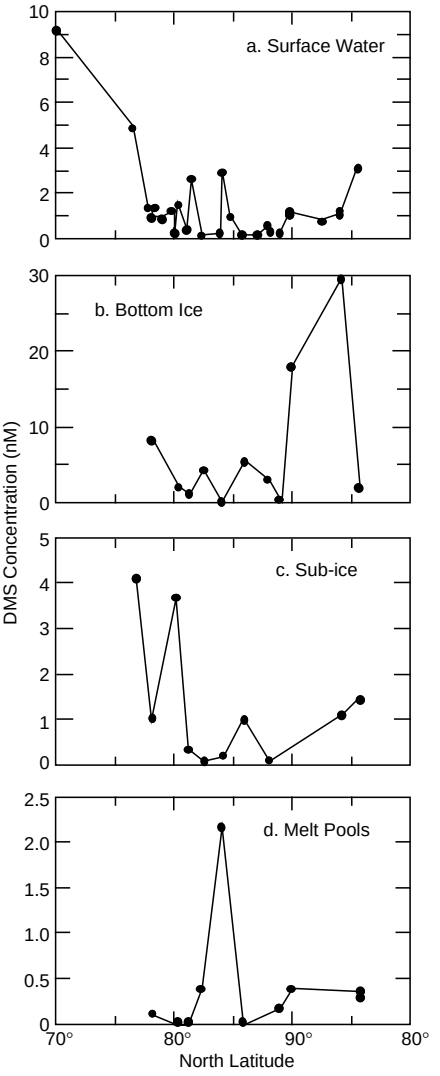

Latitudinal changes of the DMS concentration in surface water, in the bottom of the ice, at the water–ice interface and in melt pools in the Arctic Ocean in the summer of 1994.

Transfer of Shelf-Derived Carbon to the Interior of the Arctic Ocean

Raymond Sambrotto

The upper water column fluxes of carbon in the Arctic Ocean have been characterized as dominated by the lateral movement of total dissolved inorganic carbon (ΣCO_2) regenerated from productive shelves to deep water regions. At least some of this movement is associated with the production and sinking of brine during sea ice formation on the shelves. This suggests a simple carbon system in which the abundant organic matter produced on the Arctic shelves provides the source for the elevated ΣCO_2 found in the upper halocline of most of the stations thus far examined. At the same time, however, the dominance of such a horizontal flux of carbon would make the Arctic dramatically different from the carbon systems in lower-latitude basins, which are thought to be dominated by the vertical flux of organic matter.

Determining the amount of carbon that enters the Arctic is important to efforts to understand the role of the ocean as a whole as a sink for atmospheric carbon dioxide and other greenhouse gases that have increased in recent years due to human activities. The major goal of my research during AOS-94, therefore, was to evaluate the carbon flux in the interior of the Arctic Ocean quantitatively, particularly in the Canada Basin, which has been sparsely sampled.

A total of 164 bottle samples were collected from the surface 400 m of 15 stations along the AOS-94 cruise track of the *Polar Sea* and were analyzed for ΣCO_2 using a coulometric technique. Most samples were analyzed onboard, except samples from the last few stations, which were analyzed upon return to the laboratory.

The ΣCO_2 values measured during the *Polar Sea* cruise were positively correlated with salinity, and the maximum values were associated with salinities characteristic of the upper halocline (approximately 33.1 psu). Also, ΣCO_2 concentrations were correlated with those of silicate, which suggests that both signals share a common source on the surrounding shelves, which are sites of prodigious diatom production during the summer months. The organic material that is the source of the remineralized ΣCO_2, therefore, may be in large part attributable to diatoms, whose frustules provide much of the silicate as they dissolve.

Raymond Sambrotto is with the Lamont–Doherty Earth Observatory in Palisades, New York, U.S.A.

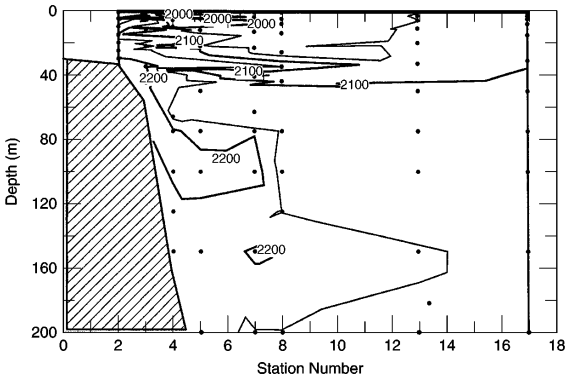

Section of ΣCO_2 (mM/kg) from the Chukchi shelf on the left to the interior of the Canada Basin on the right. The data have been normalized to a salinity of 35 psu.

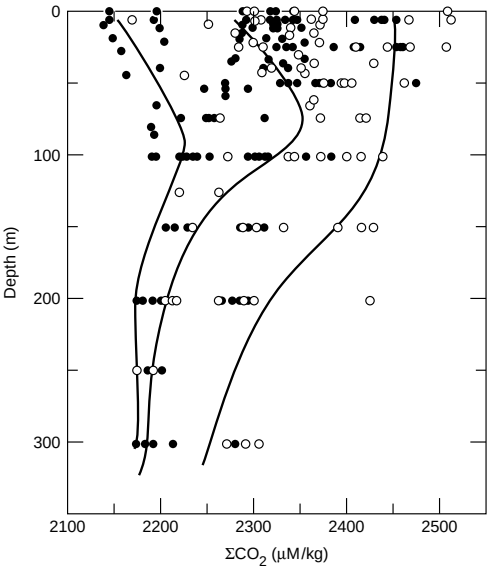

Profiles of ΣCO_2 (mM/kg) from both the AOS-94 cruise and the 1993 U.S. Navy submarine cruise. The solid lines represent the average profiles for the stations in the vicinity of the Lomonosov Ridge, Chukchi borderlands or central Canada Basin (right to left, respectively).

The ΣCO_2 maximum associated with the upper halocline is most obvious at stations near the shelf break of the Canada Basin. However, by the northern end of the Canada Basin, in the vicinity of the former T3 ice station, only silicate retains a clear maximum in the halocline and ΣCO_2 exhibits only a slight increase between 100 and 150 m. Finally, by the Nansen Basin, little evidence of any subsurface maximum in nutrient concentrations of any kind remains.

Perhaps the most significant results of my sampling thus far have been in characterizing the continuity in ΣCO_2 between the shelf and interior regions of the Canada Basin. With the effect of salinity removed, the large gradient between the shelf and oceanic regions is clear. The section reflects the continuity between shelf and slope as high-ΣCO_2 water (greater than 2200 µM/kg) detaches from the shelf edge and enters the upper halocline at approximately 100 m. This continuity presumably follows an isopycnal surface between the two regions.

Additional ΣCO_2 data are available for the Canada Basin from a U.S. Navy submarine cruise in 1993. These data suggest that a significant amount of inorganic carbon has accumulated under the ice in the central Canada Basin, where the ΣCO_2 content of the upper 300 m is at least 30 moles greater than the surrounding regions. Thus, the Canada Basin may be an important reservoir for oceanic carbon. Analysis is now focused on isolating the rate at which shelf carbon is supplied to central regions and the ultimate role of the Arctic in the global carbon budget.

Dimethyl Sulfide in the High Arctic

Sangeeta Sharma, Fred Hopper, Peter C. Brickell, Michel Gosselin, Maurice Levasseur, Natalie Simard and Timothy S. Bates

Natural and anthropogenic emissions contribute approximately equally to the total global sulfur budget. It is estimated that up to 30–50% of these natural sulfur emissions are released from the oceans. This can be the largest source of atmospheric sulfur in ocean regions far from anthropogenic sources of sulfur.

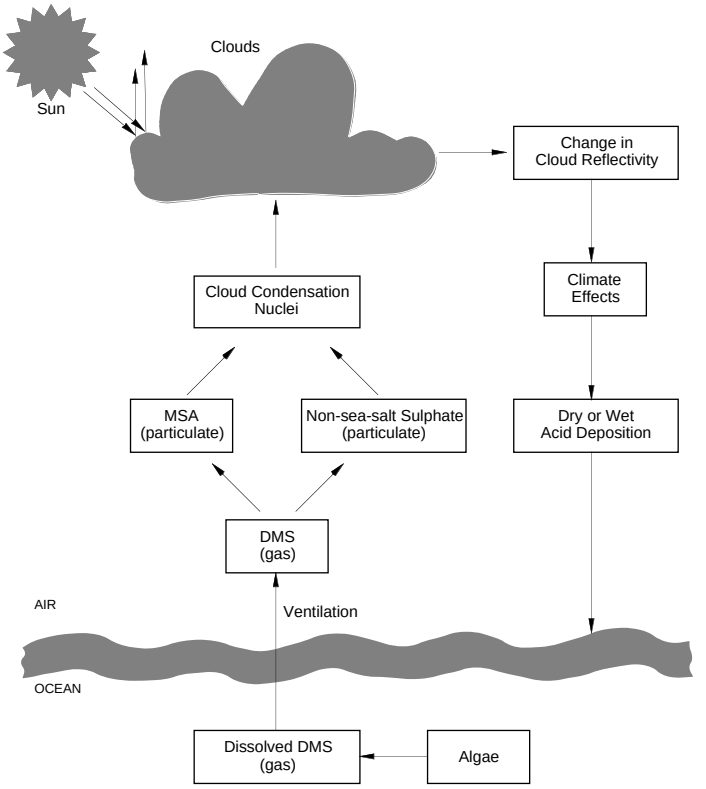

Atmospheric fate of DMS, its climate effects and biogeochemical sulfur cycling in the marine environment.

Sangeeta Sharma, Fred Hopper and Peter Brickell are with Atmospheric Environment Service, Downsview, Ontario, Canada. Michel Gosselin is with the Département d'océanographie of the Universite du Québec à Rimouski, Rimouski, Quebec, Canada. Maurice Levasseur and Nathalie Simard are with the Institut Maurice-Lamontagne, Ministére des Péches et des Océans, Mont-Joli, Quebec, Canada. Timothy Bates is with the National Oceanic and Atmospheric Administration's Pacific Marine Environmental Laboratory, Seattle, Washington, U.S.A.

Equipment used on the *Polar Sea* to analyze DMS samples. The system consists of a gas chromatograph with a sulfur chemiluminescence detector.

Dimethyl sulfide (DMS) is the dominant biogenic sulfur species produced in the oceans. It is produced by phytoplankton and is released into the atmosphere at a rate that depends on variables such as the concentration of DMS dissolved in the water phase, the wind speed and the temperature. Even small fluxes of gases from ocean waters can be globally significant when multiplied by the area covered by the oceans.

DMS is of particular interest because of its possible role in climate change. Photochemical oxidation of DMS in the atmosphere produces fine particles known as cloud condensation nuclei (CCN) upon which water vapor can condense and form cloud droplets. Changes in the regional abundance or characteristics of CCN can alter the distribution or properties of clouds, altering the radiative balance through a change in cloud albedo. It has been hypothesized that DMS is a major link in ocean–atmosphere coupling and may provide a feedback mechanism through which changes in the global climate are amplified.

Distribution of aqueous dimethyl sulfide concentrations during the AOS-94 expedition.

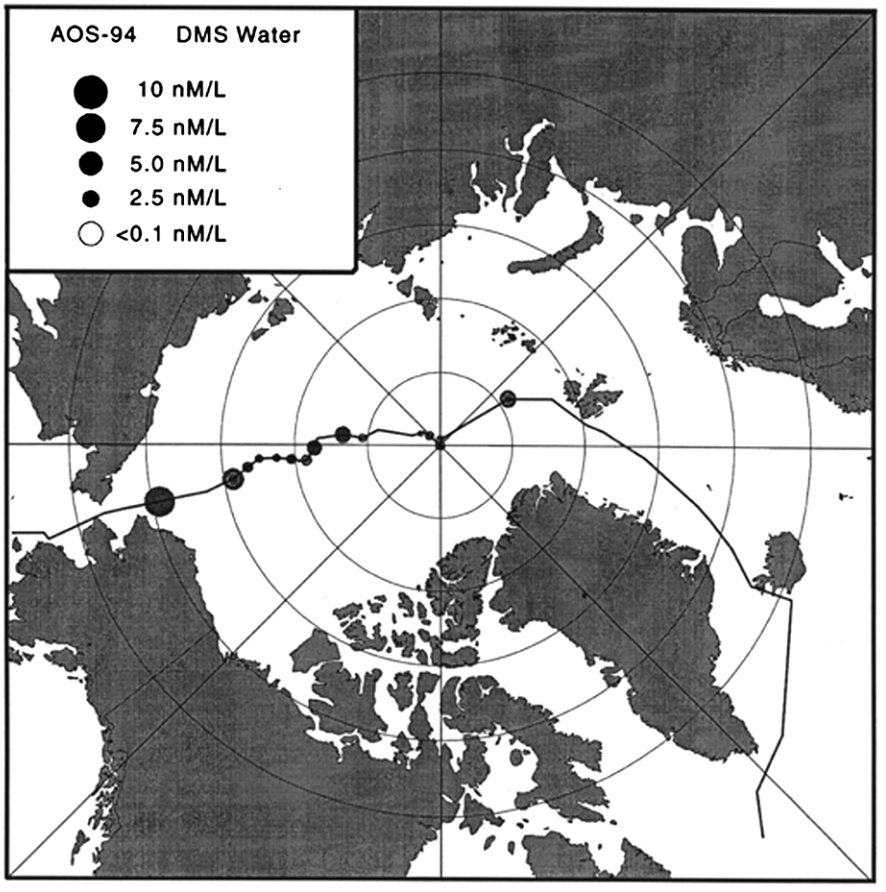

Numerous model studies have suggested that polar regions are very susceptible to changes in climate. The in-situ measurements of DMS in air and water made from the USCGC *Polar Sea* during the transect of the Arctic Ocean basin have significantly increased the data available on DMS source strengths and distribution in this sensitive region. Together with the concurrent measurements of CCN and other aerosol and chemical properties of the Arctic atmosphere, they provide a unique opportunity to investigate the possible link between DMS, CCN and clouds.

We collected water samples for DMS analysis at the science stations either with Niskin bottles at various depths or from the ship's uncontaminated seawater pumping system. DMS dissolved in water was separated by purging, preconcentrating on adsorbent cartridges and then thermally desorbing into a gas chromatograph with a sulfur chemiluminescence detector. DMS concentrations in surface seawater samples collected between 24 July and 3 September ranged from less than 0.1 to 9.1 nM/L. The concentration range was similar to that observed during the 1991 *Oden* expedition. Maximum concentrations were observed along the ice edge and minimum concentrations (below the detection limit of 0.1 nM/L) at the North Pole.

We collected atmospheric DMS samples using a portable sampler, always

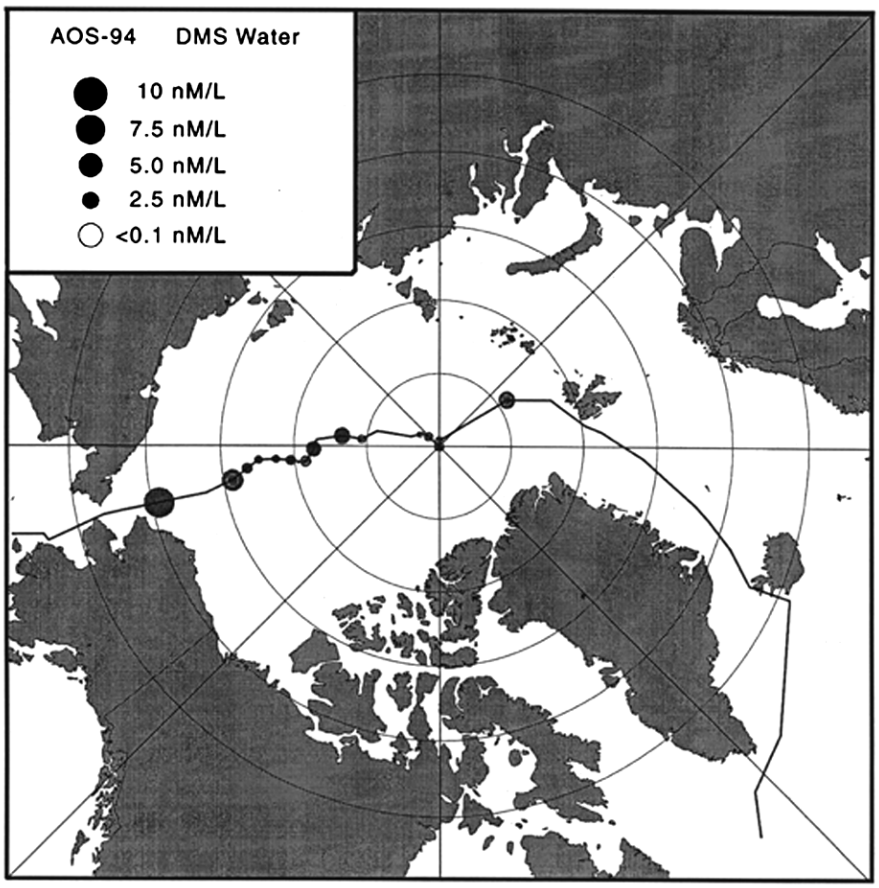

Distribution of atmospheric dimethyl sulfide concentrations during the AOS-94 expedition.

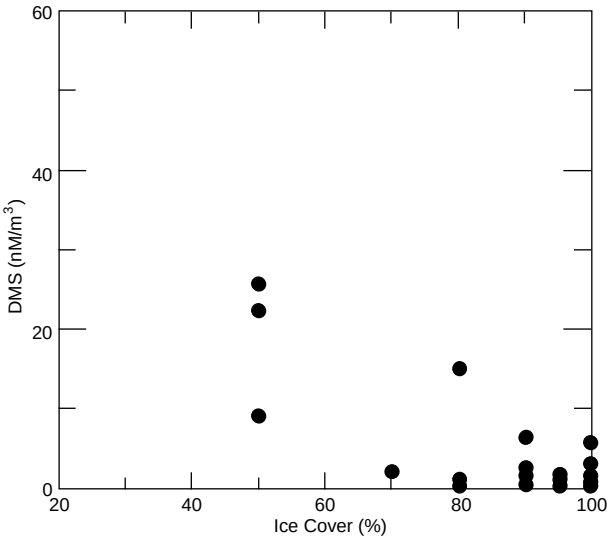

Variation of atmospheric dimethyl sulfide as a function of ice cover.

on the upwind side of the ship, away from ship stack emissions and other sources of contamination. The samples, collected on cartridges, were kept frozen until analysis (usually within 48 hours of collection). DMS was thermally desorbed from the sample cartridges by placing the cartridges in the injector of a gas chromatograph. The DMS was then transferred to the analytical column for separation and determined quantitatively by a flameless sulfur chemiluminescence detector. Samples collected from 18 July to 8 September showed atmospheric concentrations from less than 0.25 nM/m^3 (the detection limit) to 50.7 nM/m^3, with a median value of 1.95 nM/m^3.

The highest DMS concentrations were found near the ice edge at 67–70°N, in the Bering Strait and Chukchi Sea regions, and the levels decreased as a function of ice cover as the ship moved into higher latitudes. This pattern reversed as the ship exited the ice pack into the Greenland Sea, consistent with results from the *Oden* expedition. A diurnal variation was observed in open water areas, with samples collected at night having values up to four times higher than in the samples collected during the day in the lower latitudes. There was not much variation in the ambient concentration once the ship moved well into the ice pack, but most of these samples were below or just above the detection limit of the analytical system.

To identify source areas of chemical constituents in the air, we calculated Langrangian back-trajectories and applied them to the data to determine the path of air parcels reaching the sampling stations. The most frequent source area was the northwest Pacific Ocean via the Bering Strait and Chukchi Sea. Many back-trajectories showed that the air was representative of the high Arctic and had been within this region for several days. A third group of trajectories showed air originating near Greenland and Iceland.

These results are in agreement with earlier findings on the distribution of dissolved and atmospheric DMS in the eastern Arctic. Not only was the aqueous-phase DMS low in the ice-covered central Arctic Ocean, but ocean–atmosphere exchange is inhibited by the presence of the ice pack. However, the data available from this complete transect of the Arctic Ocean basin clearly demonstrate that the distribution of DMS along the ice margin and in nearby open ocean areas is asymmetric. In particular, atmospheric DMS concentrations were up to ten times higher in the Bering Strait and Chukchi Seas than in the eastern Arctic.

The Role of Biomass, Bioturbation and Remineralization in Determining the Fate of Carbon in the Arctic Ocean

Lisa M. Clough, William G. Ambrose, Jr., and J. Kirk Cochran

The goal of biological studies during AOS-94 was to understand the role of the Arctic in the global carbon cycle. In support of this goal, our research examined the fate of organic matter reaching the seafloor. Little work had been done on benthic (seafloor) carbon in the Amerasia Basin prior to this cruise, but based on work from the Eurasia Basin we surmised that a greater portion of carbon fixed by pelagic (water column) phytoplankton would reach the bottom in the entire Arctic Ocean than in other oceans. Possible explanations for a greater pelagic/benthic coupling included low zooplankton abundance and feeding rates and a temperature-supressed microbial loop. One of the major strengths of this cruise was that other researchers were addressing pelagic phytoplankton, zooplankton and microbial processes simultaneously throughout the cruise.

Our main hypothesis was that the relatively abundant and active benthic community found in the Arctic is the major factor controlling (both directly and indirectly) the fate of sedimentary carbon in polar regions. We focused on some of the possible fates of carbon reaching the benthos by examining patterns of benthic biomass (how many animals there were), particle bioturbation (how deep the animals were mixing particles in the sediment) and a variety of estimates of benthic food availabilty (how much total carbon, organic carbon, chlorophyll, phaeopigments and biologically available protein). In addition we determined a suite of rate measurements, including remineralization (how much oxygen is being used by the animals) and bioirrigation rates (how quickly the animals mix water from above the sediment into the sediment). We collected boxcores from 19 stations along the transect from the coastal waters of Alaska to the deep basins of the Barents Abyssal Plain. Because of pressure effects, remineralization experiments were only performed on cores collected from less than 2000 m deep.

Macrofaunal biomass was ten times higher than has been previously reported for the Arctic Ocean, supporting the observations made by other members of the biology group. Mixing rates of both particles and water were directly corre-

Lisa Clough is with the Department of Biology at East Carolina University in Greenville, North Carolina, U.S.A. William Ambrose is with the Department of Biology at Bates College in Lewiston, Maine, U.S.A. J. Kirk Cochran is with the State University of New York at Stony Brook, New York, U.S.A.

Lisa Clough preparing a mud sample on the *Polar Sea*.

lated with macrofaunal abundance, as were sediment remineralization rates. Given that the surface waters appeared to be capable of consuming all food being produced during the cruise, this result is surprising. It argues that the food supporting the benthos must be reaching the bottom during the early part of the summer. We will only be able to test this hypothesis by being in the Arctic during the early summer.

As a subset of our major question we hypothesized that benthic biomass and processes would decline from a maximum in the Chukchi Sea to a minimum under the permanent ice pack and then begin to increase again towards the more productive marginal ice zone north of Fram Strait. Instead, we found that macrofaunal biomass and mixing processes were typically higher in the Amerasia Basin than in the Eurasia Basin. We are developing a relationship between benthic micro- and macrofaunal biomass and the flux of particles to the bottom of the ocean for other regions of the Arctic (in collaboration with Jody Deming of the University of Washington). We hope to be able to use our AOS-94 benthic data to calculate particulate flux along the AOS-94 transect (a measurement that was not possible during the cruise).

Our analyses of sediment characteristics support the patterns discussed above. As expected, the depth of the water column above the bottom also appeared to have an effect on the simple Amerasia versus Eurasia pattern described above. Samples collected from both the Mendeleyev and Lomonosov Ridges contain more chlorophyll, phaeopigments (breakdown products of chlorophyll) and total carbon than samples collected from deeper depths, even if the deeper stations were collected nearer to the Alaskan Shelf.

When we combine and compare the estimates of water column productivity, particle flux, gradient-driven sedimentary oxygen flux and sedimentary carbon burial, we will be able to determine both the degree of pelagic/benthic coupling in the Arctic Ocean and the role that the benthic animals play in carbon cycling in the present-day Arctic. Interpreting biological modification of stratigraphic and pore-water profiles will be critical in determining the present state of carbon preservation, as well as in understanding the history of the Arctic Ocean (in conjunction with the researchers studying the geology of the Arctic Ocean Basin).

Oxygen Consumption, Denitrification and Carbon Oxidation Rates in Near-Surface Sediments of the Arctic Ocean

John P. Christensen

As part of the multidisciplinary AOS-94 expedition, boxcores and piston cores were collected at a variety of sites across the Arctic Basin. From these cores, several pore-water solutes, including oxygen, nutrients, alkalinity, pH, soluble iron and manganese, and sulfate, were measured. Sites ranged from the continental slope off the Chukchi Sea to the abyssal plains and midbasin ridges. Ten short cores were used for oxygen profiles, and seven longer cores were used for the other dissolved solutes over the entire depth of the boxcore.

Profiles of pore-water-dissolved solutes help describe the biogeochemical sequence of reactions occurring within the sediments. A slight lowering of the oxygen concentrations was found within the upper few centimeters of pore waters in all cores. In sites on the continental slope off the Chukchi Sea, pore-water nitrate profiles show lowered nitrate concentrations at depth in the sediments. This reduction in nitrate concentrations is attributable to anaerobic denitrification in the deeper strata of these sediments. These sediments also received considerable inputs of biogenic material, as indicated by the elevated levels of dissolved silicate in the pore waters. In contrast, most of the sediments throughout the central basins of the Arctic Ocean are oxygenated over

Kevin O'Toole, John Christensen, and Walt Olson standing by for a box core on the *Polar Sea.*

John Christensen is with the Bigelow Laboratory for Ocean Science in West Boothbay Harbor, Maine, U.S.A.

at least the upper 30–40 cm. No evidence is present for lowered redox conditions, which would support dramatic solubilization of iron or manganese. Silicate concentrations were elevated over bottom water contents by only 20–30 μM/L. Measurements of titration alkalinity show concentrations within the sediments to be higher than those in the bottom waters.

The oxygen gradients will be used to calculate the oxygen fluxes into the sediments. As this flux is driven by the oxidation of organic matter, rates of carbon oxidation will be calculated. The alkalinity of the pore waters was increased over bottom water concentrations due to either organic matter oxidation or dissolution of solid-phase carbonate. Fluxes of titration alkalinity out of the sediments can be compared with fluxes of oxygen to evaluate the relative importance of these two reactions. Thus, the pore-water profiles will allow us to estimate the rates of carbon oxidation and carbonate dissolution within these sediments. In conjunction with estimates of burial and productivity, the results regarding the rates of organic matter oxidation and carbonate dissolution will be useful in constructing a present-day carbon budget for the central Arctic Basin.

— *Ecology of Marine Mammals* —

Upper Trophic Level Research: Polar Bears and Ringed Seals

Malcolm Ramsay and Sean Farley

Nearshore Arctic waters are home to more than a dozen species of mammals from three orders (Cetacea, Carnivora and Pinnipedia). Prior to the AOS-94 transect, our knowledge of these mammals found in Arctic waters off the continental shelf consisted primarily of anecdotal accounts from explorers' journals and ships' logs. Logistical constraints have limited opportunities for biologists to work in the offshore pack ice, so there were few hard data, even on simple presence or absence, for species outside of a narrow band (about 200 km) from shore accessible by shore-based aircraft. The AOS-94 transect offered the first dedicated opportunity to monitor polar bears and observe other marine mammals in the permanent pack ice environment of the Arctic Ocean.

Although closely related to the terrestrial brown and black bears of North America and Asia, polar bears have adopted a marine-associated life style and are intimately associated with the sea ice of the Arctic Basin. Their southern range approximates, to a very high degree, the maximum extent of that ice in winter. They roam over the sea ice in search of their prey, primarily ringed seals, but bearded and ribbon seals as well. As carnivores, polar bears are at the top of the relatively long Arctic marine food chain and, accordingly, are nowhere abundant. Furthermore, individual bears move over very large areas each year in search of their prey.

All polar bears studied to date have been found to be members of relatively discrete, coastal subpopulations. The northern boundaries for those subpopulations on the periphery of the Arctic Ocean are poorly known. Prior to AOS-94, marine mammal researchers assumed that the central Arctic Basin was a biological desert that could not support a significant biomass of upper trophic level vertebrates. We viewed participation in the AOS-94 as a pilot project to determine whether it is feasible for vertebrate ecologists to work productively in heavy pack ice and whether polar bears and other marine mammals could be located there.

If bears were found, we wanted to determine what their affinities were with known coastal-associated populations and how the movement patterns of in-

Malcolm Ramsay is from the Department of Biology at the University of Saskatchewan in Saskatoon, Saskatchewan, Canada. Sean Farley is from the Department of Zoology at Washington State University in Pullman, Washington, U.S.A.

Mother and cub prior to capture.

dividual bears compare with those of bears found nearer to the continental shelves. To meet our goals we planned to capture as many polar bears as possible and to determine, using genetic and morphological methods, their degree of affinity with animals from known populations.

The increased use this century of environmentally persistent chlorinated hydrocarbon (CHC) compounds in industrial and agricultural practices has led to global contamination of the world's ecosystems. Although human population densities and industrial activity are low in Arctic regions, CHCs released in more southerly latitudes are advected north through a variety of physical processes and eventually reach the Arctic Ocean and its fauna. These compounds are lipid soluble and tend to become sequestered in the energy storage tissues of exposed organisms. At each successive stage in a food web, CHCs become more concentrated in the tissues of the animals, a process called bioaccumulation. Polar bears are at the top of the relatively long Arctic marine food web, so their contaminant loads are relatively high and reflect an integration of the entire marine environment. Polar bears can be considered an "early warning" species reflecting global changes in the Arctic. Consequently a second goal on the voyage was to collect tissue samples from live-caught polar bears for monitoring the extent of organochlorine contamination in the remotest parts of the Arctic marine environment.

A watch for marine mammals was conducted from the bridges of both vessels. The sea ice was scanned in a narrow band no more than a few kilometers wide along the track of the ships' path. When helicopters forayed out from the

ships, the crews watched for signs of marine mammals. During at least 25% of the observation time, fog and other atmospheric conditions limited visibility to a few hundred meters from the ships and precluded helicopter flights.

When animals were seen, their species, number and behavior were recorded. Polar bears were captured using helicopters and standard immobilization techniques. For each animal, sex was determined, uniquely numbered ear tags attached, and matching tattoos applied to the left and right upper lip for subsequent identification of recaptured individuals. Age was derived by counting annuli in the cementum of an extracted vestigial premolar tooth.

Animals were weighed using an electronic scale suspended from an aluminum tripod. Blood samples, adipose tissue biopsies from superficial depots, and milk samples were collected for subsequent contaminant assay and DNA sampling. Satellite-communicating radio collars were fitted to adult female bears to allow us to track them after capture.

We saw 12 polar bears and 15 additional sets of tracks on the expedition. Of the bears sighted, seven were captured. The remaining five were unavailable for capture because climatic conditions or extensive open water at the time made capture unsafe for both the bears and us. Those not captured included three solitary bears and a female with a yearling cub. We captured and sampled two families, one juvenile male and one juvenile female. None of the bears handled had previously been marked in any of the ongoing national polar bear studies along the periphery of the Arctic Ocean.

Both adult females were fitted with a radio transmitter that communicated with the Service Argos satellites. These radios allowed us to obtain informa-

Captured bear being prepared for weighing.

tion on location and activity patterns. Unfortunately both satellite radio transmitters failed within four months of attachment, possibly due to battery failure. Prior to the loss of radio contact, both bears moved off in a northeasterly direction, staying in regions of 90% ice cover or greater.

Tissue samples from the bears handled were assayed for organochlorines. The contaminant loads in the adipose tissue samples from the captured bears have been determined by R.J. Norstrom (Environment Canada, Ottawa). The sum of all polychlorinated biphenyls (PCBs) in the bears ranged from 1.7 to 6.6 μg/g lipid, that of the pesticide chlordane from 0.8 to 2.7 μg/g lipid, and that of the pesticide DDT from 0.1 to 0.4 μg/g lipid. These CHC contaminant loads were in the lower range of values determined for polar bears from most of the circumpolar, near-land populations. For all three measured contaminants, mean contaminant values in the adipose tissue fell within the lower 50% of mean values for the circumpolar populations of polar bears that have been sampled previously.

As with bears, more ringed seals were seen than we expected—more than 150, usually singly or in groups of fewer than three. The sighting frequency of seals remained relatively constant once we were past the continental shelf. Seals were observed on all except eight days of the transect. On five of those days, heavy fog limited visibility.

Our sampling protocol was not intended to estimate the population size for polar bears or ringed seals. We found far more bears (12), tracks of bears (15) and ringed seals (>150) along our line of transect than anticipated. Clearly there is a food resource (seals) available to polar bears in the Arctic Basin, and therefore there may be a resident population of bears. The failure of the satellite tracking program did not allow us to monitor the movements of the two adult females. The results of the DNA assays and stable-isotopic signatures from the bears are not yet completed. It is hoped they will support or belie the hypothesis that polar bears inhabiting the Arctic Ocean basin are indigenous. Estimating the size of any population of marine mammals in the deep Arctic Basin is a more difficult problem and will require a concerted effort by researchers from many countries.

Michel Gosselin and other biological oceanographers collected data during AOS-94 suggesting that a significant, if not major, portion of the food web exploited by polar bears is associated with the epontic algae, gammarid amphipods and Arctic cod of the multi-year ice floes and not with the pelagic food column. If corroborated, these findings will give considerable insight into the ecology of marine mammals. The relative importance of ice algae and amphipods compared with phytoplankton and copepods may influence the bioaccumulation of CHCs in the higher trophic levels. Certainly the feeding ecology of seals and polar bears in any region of the Arctic is poorly understood. As vertebrate ecologists, we eagerly anticipate another opportunity to study the marine mammals in such a remote and fascinating environment.

— *Contaminants* —

Artificial Radionuclides in the Arctic Ocean

Katherine Ellis, Richard Nelson, John N. Smith,
Linas Kilius and Brad Moran

Recent reports of the dumping of radioactive wastes by the former Soviet Union in the Barents and Kara Seas have caused concerns regarding levels of radioactive contaminants in the Arctic areas of North America and their impact on the environment and human health. These concerns have led to the current investigation of radionuclide levels and transport pathways in the Arctic Ocean and the ultimate fate of artificial radionuclides such as ^{137}Cs, ^{90}Sr and $^{239,240}Pu$ in the Arctic ecosystem. In addition, these isotopes can provide useful information on transit times for water movement in the Arctic Ocean by relating isotope concentrations and ratios to their source functions.

Sources of artificial radioactivity of the Arctic Ocean include:

- Fallout from atmospheric nuclear weapons tests carried out mainly in the 1950s and 1960s;
- Effluent from European reprocessing plants (including Sellafield in the U.K. and Cap le Hague in France);
- Releases during the Chernobyl accident in 1986;
- Solid and liquid radioactive waste, including spent reactor cores from nuclear submarines and ships, dumped in the Barents and Kara Seas by the former Soviet Union;
- Nuclear wastes transported down Russian rivers; and
- Nuclear wastes discharged into coastal waters associated with the present Russian nuclear fleet.

Artificial radioactivity is transported into the Arctic Ocean via several pathways. Atlantic water, carrying atmospheric fallout and effluent from Sellafield and Chernobyl, is transported into the Arctic Ocean via Fram Strait or the Barents Sea, where it may incorporate releases from Russian radioactive waste. Pacific water flowing in through Bering Strait carries atmospheric fallout from the Pacific Ocean. Surface water on the Russian continental shelves, containing Atlantic and Pacific water and river runoff, is mixed and advected into the Arctic Ocean surface layer. Dense saline plumes, produced during ice freezing

Katherine Ellis, Richard Nelson and John Smith are with the Bedford Institute of Oceanography in Dartmouth, Nova Scotia, Canada. Linas Kilius is with IsoTrace Laboratory at the University of Toronto in Toronto, Ontario, Canada. Brad Moran is with the University of Rhode Island in Narragansett, Rhode Island, U.S.A.

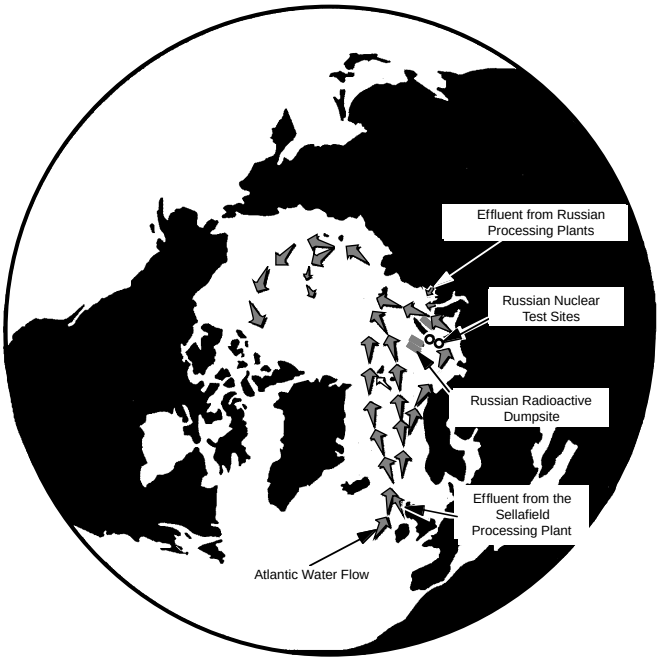

Sources of artificial radionuclides in the Arctic Ocean.

in shelf regions, are transported down into the halocline, intermediate and deep water layers of the Arctic Ocean. Particle reactive isotopes can also be transported into the interior of the Arctic Ocean through incorporation into ice and subsequent release of the ice-rafted radioactive contaminants into the water column and sediments by melting or breakup of the ice.

Until recently, studies of the transport of artificial radioactivity into the Arctic Ocean had been limited to measurements conducted from a few ice stations, such as LOREX (1979), FRAM3 (1981), CESAR (1983), AIWEX (1985) and the Canadian Ice Island (1985–1989). The use of icebreakers during AOS-94 has vastly increased the number of sampling locations in the western Arctic Ocean. Water samples were collected from many of the major areas of the Arctic Ocean, including the Chukchi Sea and the Canada, Makarov, Amundsen and Nansen Basins. Sediment cores were collected in areas of sediment accumulation along the cruise track.

The levels of artificial radionuclides in Arctic Ocean water are low and require concentration from large volumes of water in order to measure the levels by conventional counting techniques. Samples were collected either by combining several Niskin bottle samples from the rosette sampler or by using pumps to pass water through resins and absorbers that remove and concentrate specific isotopes. Cesium isotopes (^{137}Cs and ^{134}Cs) were counted on KCFC (potassium cobalt ferrocyanide) resin. Strontium, plutonium and americium isotopes (^{90}Sr, ^{239,240}Pu, ^{238}Pu and ^{241}Am) were concentrated from 60 to 100 L by precipitation, and the concentrates were returned to the laboratory for further purification and counting. Sediment cores were subsampled and analyzed at 1-cm intervals. Sediment analyses are being used to calculate sediment inventories of artificial radionuclides and to identify areas of net accumulation.

Preliminary measurements for ^{137}Cs and ^{129}I clearly show the presence of Sellafield and Chernobyl contaminants in surface and Atlantic-layer water throughout the Arctic Ocean. The main exception was surface water in the Chukchi Sea, where Pacific-origin water, containing only atmospheric fallout, flows in through the Bering Strait. The highest activities (12–15 Bq/m^3 for ^{137}Cs and 80–100 $\times$ 10^7 atoms/L for ^{129}I) were found over the Lomonosov Ridge near the North Pole, consistent with the surface circulation pattern of

the Trans Polar Drift, which carries surface water from Siberia across to Greenland. The high activities and ratios of isotopes $^{129}I/^{137}Cs$ and $^{134}Cs/^{137}Cs$ identify the source as European reprocessing plants and Chernobyl fallout and indicate that the late-1970s peak of Sellafield-labeled water has now passed over the central Arctic Ocean, approximately 15 years later. A comparison of the ^{137}Cs profile measured at the North Pole to profiles measured in 1979 and 1991 illustrates the history of the transport. In 1979 the water column contained ^{137}Cs mainly derived from atmospheric fallout, before the Chernobyl accident and before effluent from European reprocessing plants had reached the Atlantic layer of the central Arctic Ocean. A large increase in the ^{137}Cs inventory in surface waters by 1991 and 1994 was caused by the arrival of Sellafield and Chernobyl ^{137}Cs. The ^{137}Cs levels below 1000 m are not significantly different from those measured in 1979, indicating the continued maintenance of a pronounced Sellafield signal at this depth since 1979. The results from the sediment analysis indicate that the shelf slope sediments of the Chukchi Sea contain the highest inventory of artificial radionuclides, while the central Arctic areas have the lowest inventories.

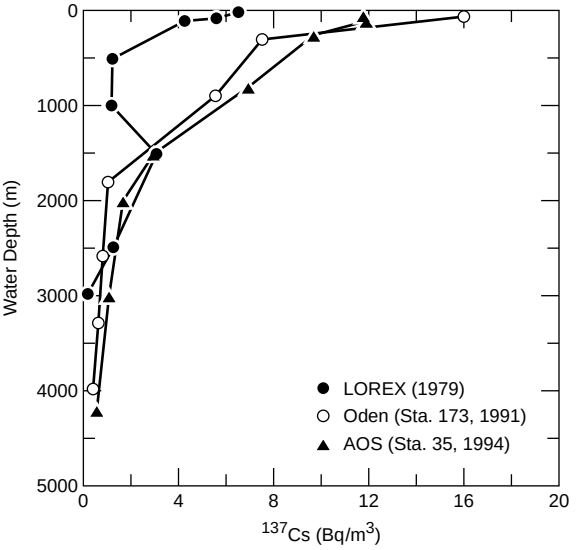

^{137}Cs profiles measured at the North Pole in 1979, in 1991 and during AOS-94.

Preliminary results provide little evidence of radioactive contamination of the Arctic Ocean from Russian sources. However, the transport pathways of potential contaminants can be delineated through studies of tracers from European reprocessing plants. Although the magnitude of the artificial radionuclide signal measured in the Arctic Ocean may be a factor of ten greater than levels due to atmospheric nuclear tests, these levels are significantly lower than levels that would constitute a radiological threat to organisms or humans along the North American coast.

Persistent Organic Contaminants

Robie Macdonald and Fiona McLaughlin

AOS-94 provided a unique opportunity to collect contaminant samples across a large, unsampled portion of the Arctic Ocean. One strength of this contaminant study is that the transect crossed all major atmospheric and ice transport routes, water bodies and three of the four main basins within the Arctic Ocean. A second strength is that samples were collected in conjunction with physical and biological data. In contrast, because of limited accessibility, previous investigations have produced a patchwork of data, collected by different groups using a variety of methods over time, generally focusing on smaller, specific regions.

Our strategy for sample collection was to examine each of the major environmental compartments; ice, water, particles, plankton, fish and sediments. Beginning with the water column, we adopted several strategies. Vertical profile samples were collected for the most water-soluble organochlorine contaminant, hexachlorocyclohexane (HCH; one form, alpha, is the pesticide Lindane), at selected stations from the Chukchi to the Greenland Seas. These samples will provide the basis for producing an HCH budget for the Arctic Ocean and may allow us to separate the contributions by source or pathway (southeast Asia versus northern Europe). Other less-soluble organochlorine contaminants, such as PCBs, require collection of larger quantities of water in order to make reliable measurements. To collect samples for these analyses, we moored submersible pumps equipped with columns and filters to obtain the 400 L or more of water required to exceed detection limits. Vertical profile samples for these less-soluble contaminants were collected at two stations; these data will augment the limited profile data collected at the Hobson's Choice Ice Island in 1986 and in the Beaufort Sea in 1992.

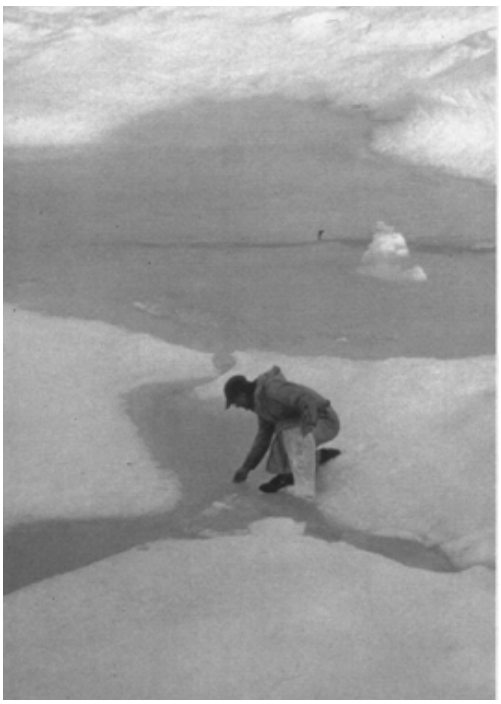

Rob MacDonald collecting Arctic cod for contaminant studies.

Robie Macdonald and Fiona McLaughlin are with the Institute of Ocean Sciences in Sidney, British Columbia, Canada.

Samples of suspended particulate material were collected in the top 30 m of the water column at many stations using a system capable of pumping and filtering large volumes of water quickly. These samples will help us to determine the fractionation of contaminants between dissolved and particulate phases, an important aspect of the process of scavenging and removal of contaminants from the euphotic zone.

Samples of zooplankton were collected using vertical net hauls in the top 100 m of the water column. These will be analyzed for organochlorine contaminants, which will determine the level of biomagnification in the lower part of the food chain. Cod, a species higher in the food chain, were collected opportunistically across the transect. By combining the zooplankton and cod data, we have a unique view of both bioaccumulation and biomagnification of organochlorines in the food chain across this section.

Sediment cores were collected at eight stations spanning the cruise track. Samples from these cores will be analyzed to provide information on particle-active contaminants, for example, lead, highly chlorinated organochlorines and PAH (polynuclear aromatic hydrocarbon). The levels of these contaminants will be examined to determine both the spatial trends across the transect and the importance of sediments as sinks for contaminants within the Arctic Ocean.

Fiona McLaughlin drawing water samples from the Niskin bottles for chemistry analysis on the *Louis S. St-Laurent*

Although many samples are already under analysis, we do not yet have any contaminant data for AOS-94. The process of analysis is complex and lengthy, involving several analytical tools, for example, high-resolution mass spectrometry and electron-capture gas chromatography. Information from the Larsen-93 cruise, which collected samples from a region that overlaps the early portion of the AOS-94 transect, suggests that we will find regional differences in contaminants produced both by delivery mechanism (transport within water masses) and by removal mechanism (biological productivity and the supply of particles). Understanding the relative importance of these mechanisms is crucial to our ability to predict the effects these compounds are likely to have on the Arctic community and the time required for a response to any environmental change, including a removal of the source.

Air-Water Gas Exchange of Hexachlorocyclohexanes in the Arctic

Liisa Jantunen and Terry Bidleman

Our objectives for the AOS-94 cruise were to measure the transfer of chlorine-containing pesticides between the atmosphere and the Arctic Ocean. The focus was on pesticides that have largely been banned in Canada and the United States but are still used in other countries. These chemicals are emitted into the atmosphere through current usage and volatilization of old residues from soils. Air currents carry them to remote areas worldwide, including the Arctic. One pesticide of special interest was hexachlorocyclohexane (HCH).

HCH is applied as a technical mixture that contains several isomers, largely α-HCH (60–70%), β-HCH (5–12%) and γ-HCH (10–15%) (Iwata et al. 1993). The active ingredient, γ-HCH, is also produced in pure form and sold as the pesticide Lindane. Both insecticides were produced during World War II and are still in large-scale use today. Canada banned technical HCH in 1971, followed by the United States in 1978. Lindane is still registered for restricted applications in these countries and is the main HCH product used in Europe (Barrie et al. 1993, Hinckley et al. 1991). Technical HCH was heavily used in Asian countries throughout the 1980s. Reports from India range from 20,000 to 47,000 tons/year (Iwata et al. 1993, Hinckley et al. 1991). It is estimated that the cumulative worldwide use since the introduction of HCH products is over 500,000 tons (Voldner and Li 1995). Because of their widespread usage and ease of transport, HCHs are the most abundant pesticides in the Arctic air and surface waters.

Air was sampled by drawing approximately 700 m^3 per day through a filter followed by a polyurethane foam cartridge. HCHs were extracted from water by passing 4–20 L through a filter followed by a C_8-bonded silica cartridge. Analysis was done in the home laboratory, using capillary gas chromatography with electron capture detection and negative ion mass spectrometry.

The accompanying figures show the results of air and water sampling for α-HCH; they also contain data collected in the Bering and Chukchi Seas in 1993 aboard the Russian R/V *Okeah* to complete the overall picture. The figures show the spatial distribution of α-HCH, from the Bering Sea to the Greenland Sea over the North Pole. Concentrations of α-HCH in water of the Bering and Chukchi Seas averaged 2.00 ± 0.48 ng/L (Jantunen and Bidleman 1995), increased in

Liisa Jantunen and Terry Bidleman are with the Atmospheric Environment Service, Downsview, Ontario, Canada.

the Arctic Ocean to 4.61 ±0.45 ng/L and decreased in the Greenland Sea to 1.52 ±0.33 ng/L. The trend of α-HCH in air was opposite to that found in the water. The concentrations were highest over the Bering and Chukchi Seas (123 ±16 pg/m^3) and the Greenland Sea (119 ±16 pg/m^3) but decreased dramatically over the Arctic Ocean (57 ±20 pg/m^3). The dip over the polar ice cap may be due to rain scavenging by fog and drizzle and inhibited revolatilization from surface water by the ice cap.

The water/air fugacity ratio can be calculated from the α-HCH concentrations in air and water and the temperature-dependent Henry's Law constant. The fugacity ratio expresses the saturation state of surface water relative to the partial pressure of the α-HCH in air. In the 1980s fugacity ratios of α-HCH were less than 1.0 in Arctic and sub-Arctic waters, indicating that the surface water was undersaturated and the net flux was air to sea. Our measurements in the Bering and Chukchi Seas (Jantunen and Bidleman 1995) and on the AOS-94 cruise show that concentrations of α-HCH in the air have decreased by three-fold since 1990. Reducing the partial pressure of α-HCH in air has raised fugacity ratios to above 1.0. Thus the surface waters are now oversaturated and volatilizing α-HCH.

Release of α-HCH from the ocean can be sensed by following the proportion of its two enantiomers in water and air. Enantiomers are mirror-image molecules that have the same physicochemical properties but that often differ in their biochemical characteristics. Right- and left-handed amino acids are familiar examples, and α-HCH is similar. The enantiomeric ratio (ER) of α-HCH is defined as (+)α-HCH /(–)α-HCH. The ER in the manufactured pesticide is 1.00 (racemic) and is not changed by abiotic reactions such as hydrolysis and photolysis. However, enzymes can and frequently do react selectively with one enantiomer, leading to ERs that differ from 1.00 (Buser and Muller 1995). We have found selective depletion of either (+) or (–) α-HCH in surface water, pre-

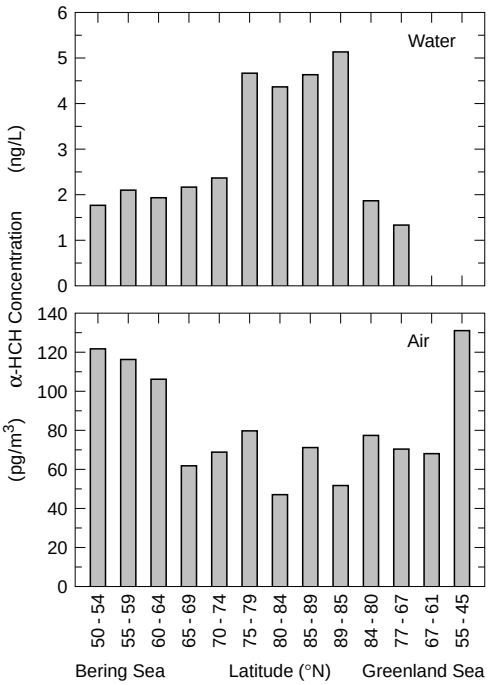

Surface water and air concentrations of α-HCH measured on BERPAC93 and AOS-94, averaged within bands of 5° latitude.

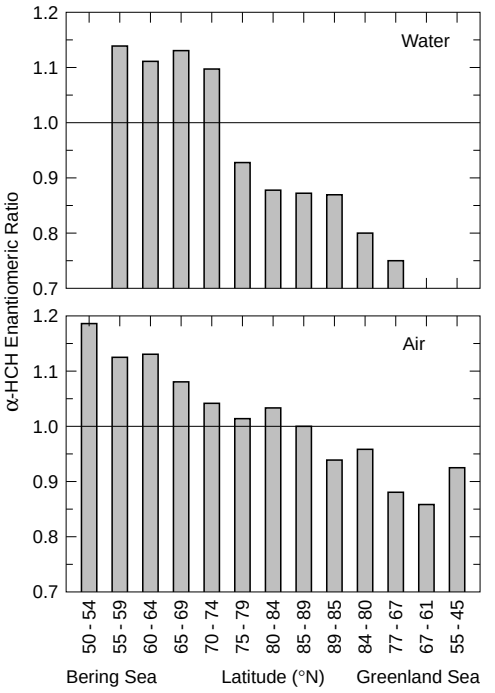

Enantiomeric ratios of α-HCH in surface water and air in the same bands of 5° latitude.

sumably the result of microbial degradation. These enantiomeric "signatures" of α-HCH are reflected in the overlying air, providing a direct indication of sea-to-air transfer.

The accompanying figures show the ERs of α-HCH in water and air with latitude. In the Bering and Chukchi Seas the ERs are greater than 1.00, indicating a degradation of (–)α-HCH relative to (+)α-HCH. Selective breakdown of (+)α-HCH in the Arctic Ocean and the Greenland Sea reverses the ERs to less than 1.00. These enantiomeric profiles are also found in air samples collected over open-water regions, indicating volatilization of α-HCH from surface water. The α-HCH in air over the ice cap was near racemic. Fugacity ratios at higher latitudes also show the potential for α-HCH to volatilize (this work and Falconer et al. 1995), but fluxes are probably inhibited by the ice cover.

Using the ER of α-HCH provides a way of distinguishing α-HCH that has been microbially processed and recycled to the atmosphere by the oceans from "fresh" α-HCH that has undergone aerial transport from source regions. Enantiomers of chiral pesticides, such as α-HCH, chlordanes and heptachlor, may also prove useful for tracing water masses with different ER signatures when employed with traditional tracers such as salinity, temperature, nutrients and dissolved oxygen.

References

Barrie, L.A., D. Gregor, B. Hargrave, R. Lake, D. Muir, R. Shearer, B. Tracey and T. Bidleman (1992) Arctic contaminants—Sources, occurrence and pathways. *Science of the Total Environment,* **122:** 1–74.

Buser, H., and M. Muller (1995) Isomer and enantioselective degradation of hexachlorocyclohexane isomers in sewage sludge under anaerobic conditions. *Environmental Science and Technology,* **29:** 664–672.

Falconer, R., T. Bidleman and D. Gregor (1995) Air–water gas exchange and evidence for metabolism of hexachlorocylohexanes in Resolute Bay, NWT. *Science of the Total Environment,* **160/161:** 65–74.

Hinckley, D., T. Bidleman and C. Rice (1991) Atmospheric organochlorine pollutants and air–sea exchange of hexachlorocylohexane in the Bering and Chukchi Seas. *Journal of Geophysical Research,* **96:** 1702–1713.

Iwata, H., S. Tanabe, N. Sakai and R. Tatsukawa (1993) Distribution of persistent organochlorines in the oceanic air and surface seawater and the role of oceans on their global transport and fate. *Environmental Science and Technology,* **27:** 1080–1098.

Jantunen, L., and T. Bidleman (1995) Reversal of the air–water–gas exchange direction of hexachlorocyclohexanes in the Bering and Chukchi Seas. *Environmental Science and Technology,* **29** (4): 1081–1089.

Voldner, E., and Y. Li (1995) Global usage of selected persistent organochlorines. *Science of the Total Environment,* 160–161, 201–206.

Volatile Halomethanes

Robert M. Moore and Charles Geen

Volatile organohalogens have an important influence on atmospheric chemistry. In particular, halogenated methanes provide a source of atmospheric chlorine and bromine radicals, which can affect ozone concentrations. There has been shown to be a strong correlation between elevated atmospheric concentrations of brominated substances and sudden tropospheric ozone depletion events, especially during the Arctic spring. There are also indications that brominated compounds play a significant role in stratospheric ozone destruction.

It is important to distinguish between natural and anthropogenic inputs of these compounds. In attempting to understand the ozone depletion events in the Arctic boundary layer, there has been considerable interest in examining the natural Arctic marine origins of volatile bromine compounds (bromoform in particular) as potentially significant sources of gaseous halogens to the atmosphere. Our research group has previously found evidence of an ice-algal source of bromoform and dibromomethane in the Arctic. Evidence also exists in northern waters for a phytoplankton source of volatile iodine compounds, which can play a role in the biogeochemical cycling of iodine and in atmospheric chemistry.

Our objective in participating in the AOS-94 cruise was to extend the database of measurements of distributions and concentrations of brominated, chlorinated and iodinated methanes in the Arctic Ocean. This would contribute to the goal of determining the natural origins of these compounds; in fact, this expedition was the culmination of a five-year, Arctic-wide study of the sources of such substances. Measurements were also made of the trace gas concentrations in seawater that had been allowed to equilibrate with the atmosphere; these are needed for calculating fluxes of the gases between the ocean and the atmosphere.

Almost 500 seawater samples were analyzed by gas chromatography during the cruise. Vertical profiles from many stations provided further general oceanographic knowledge of water column distributions of the halomethanes and generally showed the concentrations of the halocarbon gases of interest to be higher in the surface waters and to decrease with depth. However, since our

Robert Moore is with the Department of Oceanography at Dalhousie University at Halifax, Nova Scotia, Canada. Charles Geen is with Bovar-Concord Environmental in Toronto, Ontario, Canada.

Laboratory on the *Polar Sea* equipped for analysis of atmosphere and ocean contaminants. [Photo by Peter Brickell.]

interests were principally the origins and behavior of naturally produced volatile halocarbons in the upper ocean, the work focused on surface-water distributions and the results from the equilibration experiments. Initial data analysis centered on the primary compounds of interest—bromoform ($CHBr_3$), dibromomethane (CH_2Br_2) and chloroiodomethane (CH_2ClI)—but data are being processed for other compounds in our suite of analytes, including bromodichloromethane ($CHBrCl_2$), chlorodibromomethane ($CHBr_2Cl$), methyl iodide (CH_3I) and diiodomethane (CH_2I_2).

The results of the equilibration experiments indicate that the direction of flux will be from the ocean to the atmosphere, since the water is supersaturated with respect to the air. The water column is stably stratified, so there is little downward mixing. Other dissipation processes, such as hydrolysis and substitution reactions, are relatively slow, so ventilation to the atmosphere is likely to be the main short-term removal mechanism for any of these dissolved gases in the seawater.

The results of our seawater measurements during AOS-94 indicate that some of the halomethane concentrations in the upper water column at these high latitudes beneath the polar ice pack are relatively high, even during late summer and early fall. For example, bromoform concentrations at most stations are equal to or greater than any others that we have previously measured from spring to autumn in the open ocean waters or beneath the ice of several Arctic regions, including Baffin Bay, Alert, Resolute Bay, the Beaufort Sea, the Bering Sea and the Chukchi Sea. It would appear that while temporal variations may be relatively large in open ocean areas and in regions where the ice cover melts for part of the year, they may not be as great in permanently ice-covered regions.

The unexpected picture emerging from the AOS-94 expedition—that halomethane concentrations remain high beneath the polar ice cap throughout

the summer and into the fall—means it is likely that even in winter, when such substances may not be produced, large amounts would still be present in surface waters. If in fact there is a fairly constant source of halomethanes beneath the ice pack, any lead, crack, polynya or open water could provide a flux of these gases to the atmosphere at any time. In this case the question of the possible origins of the Arctic springtime atmospheric pulse of bromine then becomes one of physics and ice dynamics. That is, how often, and for how long, are open-water areas present in the Arctic during the dark winter and early spring?

Finally, in pursuing our questions of possible biological sources of these gases, it will be of interest for us to examine our halocarbon data at particular stations in collaboration with information provided by other AOS-94 colleagues. While halomethane concentrations may not be directly correlated with bulk phytoplankton biomass, they might demonstrate some correlation with the presence or species abundance of particular ice algae or phytoplankton identified by other researchers during the expedition.

C_2–C_6 Hydrocarbons

Peter C. Brickell and Jan W. Bottenheim

The aft port bridge of the *Polar Sea*, showing the triple-headed air sampling manifold leading into a rear window of the bridge superstructure.

In recent years there has been growing concern about human impact on the high Arctic regions. Light hydrocarbons (C_2–C_6) in the environment include species that are primarily anthropogenic (for example, acetylene) and those that are primarily biogenic in origin (for example, isoprene). These species are of concern in the troposphere because they play a major role in ground-level ozone formation in urban and urban-impacted regions. The study of the light hydrocarbon composition of the high Arctic troposphere can provide one more indication of human impact on the region. In addition, the study of light hydrocarbons in background environments can lead to a better understanding of photochemical reaction pathways occurring in these and other more polluted locations. The high Arctic environment is generally free of the myriad of local and regional anthropogenic hydrocarbon sources that complicate the study of hydrocarbon photochemistry in southern continental regions.

The goals of the light hydrocarbon measurement program during AOS-94 were to:

- Develop a reference light hydrocarbon database for the very high latitudes in summer;
- Compare these data with those previously taken from land-based sites in the high Arctic (for example, Barrow, Alaska; Alert, N.W.T., Canada; and the Norwegian Arctic);
- Look for evidence of unusual patterns of chemical processes in the Arctic troposphere; and
- Investigate the levels and patterns of anthropogenic light hydrocarbons at very high latitudes and compare these with the levels of other anthropogenic tracers measured during AOS-94.

Air for light hydrocarbon analysis was sampled in two ways. We collected air in electropolished stainless steel canisters using a battery-powered pump,

Peter Brickell and Jan Bottenheim are with the Atmospheric Environment Service in Downsview, Ontario, Canada.

and samples were stored for later analysis. Air was also drawn through a stainless steel sampling line mounted 22 m above the water line above the port flying bridge. The line was routed to the laboratory, where samples were preconcentrated and then immediately analyzed by in-situ gas chromatography. Canisters could also be analyzed by this system for intercomparison measurements with our laboratory in Toronto.

Because the location of the sampling line was fixed, this second method of sampling could only be used when a substantial breeze (more than 3 m/s) was blowing off the port side of the ship. This was necessary to avoid sampling emissions from the vessel itself, and it essentially limited sampling to times when the ship was stopped for science stations and when other sources of contamination (such as helicopters) were absent. Suitable conditions for sampling were determined by monitoring the real-time output of carbon monoxide and condensation nuclei counter instruments. Sampling with the portable canister system was more flexible and allowed air to be collected from any upwind location on the ship or even on the ice if conditions warranted it. In total 113 canister samples and 53 direct samples were collected; 40 of the canister samples were analyzed with the on-board gas chromatography system.

Canister data are available for the low-molecular-weight alkanes and acetylene. During AOS-94 the mean ethane concentration from 73 to 80°N was 836 ± 68 pptv on the Pacific side of the Arctic Ocean. This agrees well with the concentrations observed during the 1988 ABLE 3A aircraft study based at Barrow, Alaska. Farther north, from 81 to 87°N, ethane concentrations dropped to 726 ± 36 pptv. From 87°N through the Pole and down to 80°N on the Atlantic side of the Arctic Ocean, ethane concentrations rose slightly to 765 ±51 pptv. Propane concentrations followed a similar pattern for the three areas. Acetylene concentrations were initially 56 ± 6 pptv and rose slightly to 64–65 pptv in the high-latitude and Atlantic-side areas. The Pacific-side data agree well with those from the 1988 ABLE 3A for Alaska, and the high-latitude and Atlantic-side concentrations compare very favorably with those for the Norwegian Arctic.

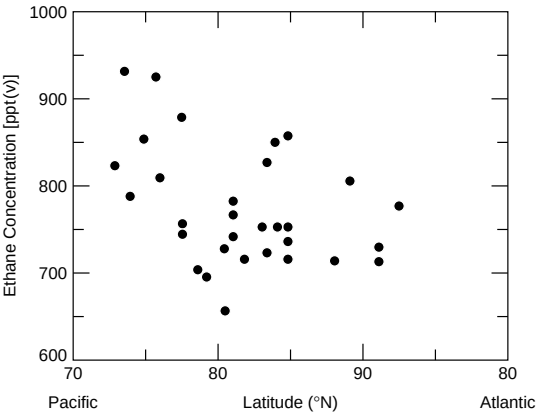

Ethane concentration vs. latitude during AOS-94.

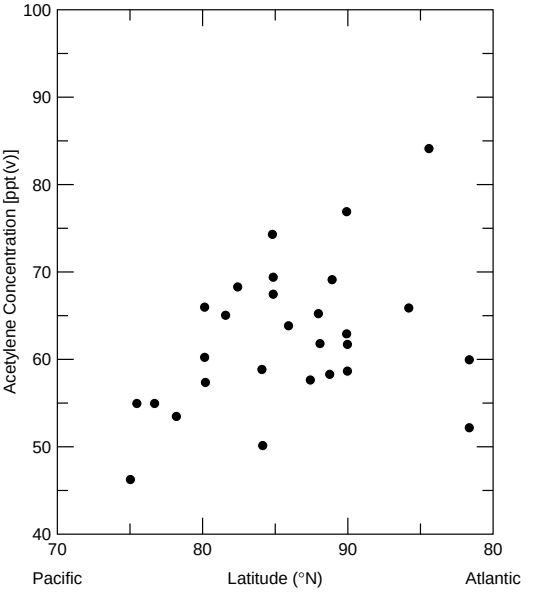

Acetylene concentration vs. latitude during AOS-94.

AOS-94 light hydrocarbon concentrations and ratios compared with those from other researchers for Alaska and the Norwegian Arctic.

	Ethane (pptv)	*Acetylene (pptv)*	*Propane (pptv)*	*Acetylene/ Ethane*	*Propane/ Ethane*
Pacific (73–80°N)	836 ± 68	56 ± 6	69 ± 12	0.061	0.084
High Latitude (80–87°N)	726 ± 36	64 ± 7	64 ± 8	0.088	0.089
Atlantic (87–90–80°N)	765 ± 51	65 ± 8	87 ± 59	0.085	0.113
Alaska*	865 ± 59	57 ± 17	53 ± 15	0.066	0.061
Norwegian Arctic†	1195 ± 27	67 ± 18	87 ± 30	0.056	0.073

* From Blake, D.R., D.F. Hurst, T.W. Smith, W.J. Whipple, T. Chen, N.J. Blake and F.S. Rowland (1992) Summertime measurements of selected nonmethane hydrocarbons in the Arctic and Subarctic during the 1988 Arctic Boundary Layer Expedition (ABLE 3A). *Journal of Geophysical Research,* **97:** 16,559–16,588.

† From Hov, O., S.A. Penkett, I.S.A. Isaksen and A. Semb (1984) Organic gases in the Norwegian Arctic. *Geophysical Research Letters,* **11:** 425–428.

Ratios of acetylene and propane to ethane concentrations were also calculated for this data set. The acetylene-to-ethane ratio for the Pacific side data is consistent with the one for Alaska, but the Atlantic-side ratio is higher than for the Norwegian Arctic. This difference is due to the lower AOS-94 ethane results for the Atlantic side. Propane-to-ethane ratios are slightly higher than those reported by other researchers for both the Pacific side and Atlantic side. The difference on the Pacific side is attributable to the somewhat higher propane concentrations, and on the Atlantic side the difference is again due to lower ethane concentrations.

The preliminary data from the light hydrocarbon canister sampling program agree well with work that has been done previously in the Alaskan and Norwegian Arctic. The lower ethane concentrations on the Atlantic side of the Arctic Ocean are probably attributable to increased distance from terrestrial sources. The ethane concentrations observed in the high-latitude portion of the transect may be useful for determining the degree of aging of the air mass encountered in this area. These light hydrocarbon concentrations will provide additional data for estimating the background tropospheric volatile organic compound levels used to input advective inflows for continental atmospheric modeling. In addition, although only data from the high Arctic regions have been presented here, we collected hydrocarbon and some additional atmospheric data throughout the entire circumnavigation of the North American continent during AOS-94. This has yielded a unique data set for assessing the nature of continental and oceanic air masses, as well as providing an extended latitudinal profile from 7 to 90°N for these atmospheric species. Finally, once the Arctic data are available from all the compounds analyzed with the in-situ gas chromatograph, it is expected that an improved understanding of background atmospheric chemical processes will have been derived from the sampling carried out on this unique expedition.

— Cloud Radiation —

Atmospheric Radiation and Climate Program

Dan Lubin and Robert H. Whritner

One of the major physical components of climate change is the way in which solar energy is redistributed in the Earth–atmosphere system. This subject also includes the simultaneous emission of thermal (infrared) energy from the Earth's surface and its partial entrapment by the atmosphere (the "greenhouse" effect). Globally well-mixed increases in carbon dioxide abundance are believed by many to be enhancing the greenhouse effect and increasing the global surface temperature field. This could have serious repercussions for Arctic Ocean climate, as the Arctic Ocean surface exists for much of the year at temperatures just below the freezing point of water. A small increase in surface temperature could potentially have a large impact on the geographic extent of Arctic sea ice, with resulting changes to the energy balance between the atmosphere and ocean.

Most of the scientific community's insight into potential "global warming" scenarios comes from large computer simulations called general circulation models (GCMs). The GCMs are quite sophisticated but often suffer from a lack of experimental input data and input physics from many remote regions throughout the world, particularly the Arctic. AOS-94 offered a unique opportunity to deploy state-of-the-art atmospheric radiation budget measurement apparatus in the high Arctic and to allow them to gather data continuously for several weeks. This was the first high-Arctic expedition to deploy these advanced optical instruments, and the large resulting data set should enable better representation of the Arctic atmosphere in the GCMs.

The California Space Institute project consisted of three major components, all deployed aboard the *Polar Sea*. The first was a battery of broad-band solar and infrared flux radiometers mounted above the pilothouse. Three Eppley Laboratory radiometers measured downwelling short-wave (0.28–2.8 μm), near-infrared (0.78–2.8 μm) and middle-infrared (4–50 μm) radiation reaching the Arctic Ocean surface. A Biospherical Instruments radiometer measured downwelling solar ultraviolet and visible radiation at 0.308, 0.320 and 0.380 μm, as well as radiation in the intervals 0.580–0.680 μm (to match a satellite radiom-

Dan Lubin is with the California Space Institute at the Scripps Institution of Oceanography in La Jolla, California, U.S.A. Robert Whritner is with the Arctic and Antarctic Research Center at the Scripps Institution of Oceanography in La Jolla, California, U.S.A.

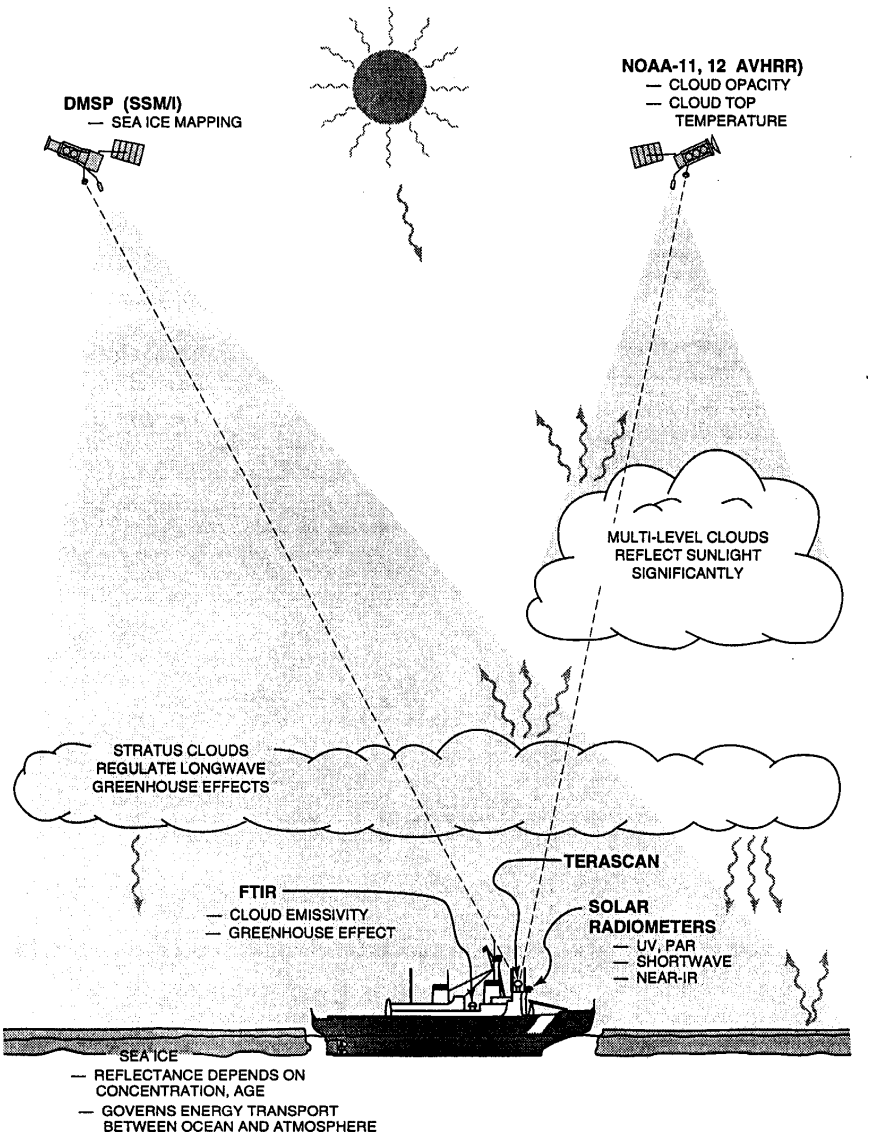

The California Space Institute experiment design during AOS-94.

eter) and 0.400–0.700 μm (total photosynthetically active radiation). These radiometers operated automatically and recorded data in one-minute averages continuously throughout the cruise.

The second component consisted of the shipboard satellite tracking facility, the TeraScan system manufactured by the SeaSpace Corporation. In addition to providing weather and ice navigation for the expedition, the satellite tracking enabled this project to measure energy reflected and emitted to space at the same time that the shipboard instruments were measuring solar and terrestrial radiation impinging on the Arctic Ocean surface. The TeraScan system was used to track NOAA polar-orbiting satellites, obtaining 1.1-km spatial resolution images from the advanced very high resolution radiometers

(AVHRR), which measure radiation at five visible and infrared wavelengths. The Defense Meteorological Satellite Program (DMSP) satellites were also tracked, giving this project access to the special sensor microwave imager (SSM/I), which was used to map sea ice along the expedition's track. Throughout the cruise, the *Polar Sea* TeraScan facility tracked between five and ten satellite overpasses per day.

The third component consisted of a Fourier transform infrared (FTIR) spectroradiometer operating in the middle infrared (5–20 μm) with a spectral resolution of 1 cm^{-1} (Lubin 1994). FTIR data collection was coordinated with the NOAA satellite overpasses, and a total of 178 sky scenes were studied with the FTIR instruments. This instrument made detailed measurements of radiation trapped by the atmosphere in the middle-infrared window (8–13 μm). Under clear skies the atmosphere is relatively transparent in this wavelength range, and a large portion of the heat given off by the ocean surface escapes to space. Under cloudy skies, this window is mostly closed, meaning that far less radiation escapes to space and the greenhouse effect is enhanced. These greenhouse enhancements due to clouds are more than an order of magnitude larger than what is expected from a doubling of carbon dioxide in the atmosphere, so understanding the role of clouds in the atmospheric energy balance is critical before we can make meaningful "global warming" predictions with GCMs.

During the summer of 1994, the atmosphere over the Arctic Ocean exhibited a great deal of complexity, much more than is now represented in the GCMs. A common occurrence was multiple-layered cloud systems. The accompanying figure is an image of terrestrial infrared radiation (10.5–11.5 μm) emitted by the Arctic ocean–atmosphere system to space, expressed in units of equivalent brightness temperature. At the time of this satellite overpass (4 August) the *Polar Sea* was at 78°N, roughly in the center of the image, where there were three distinct temperature ranges in the cloud fields corresponding to three distinct ranges in cloud top height. When the atmosphere

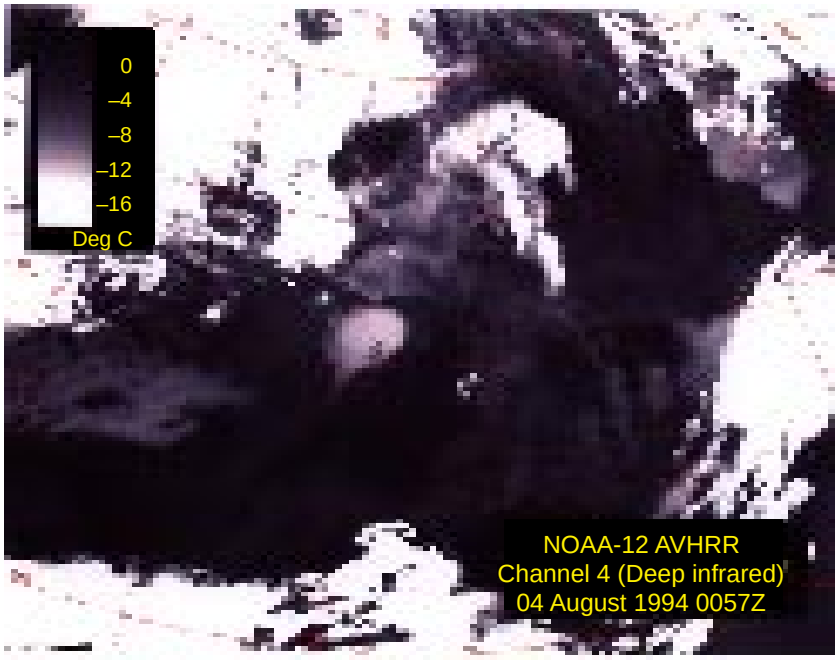

AVHRR image obtained from the shipboard TeraScan system on 4 August 1994 during AOS-94. Brighter shading refers to lower cloud top temperatures.

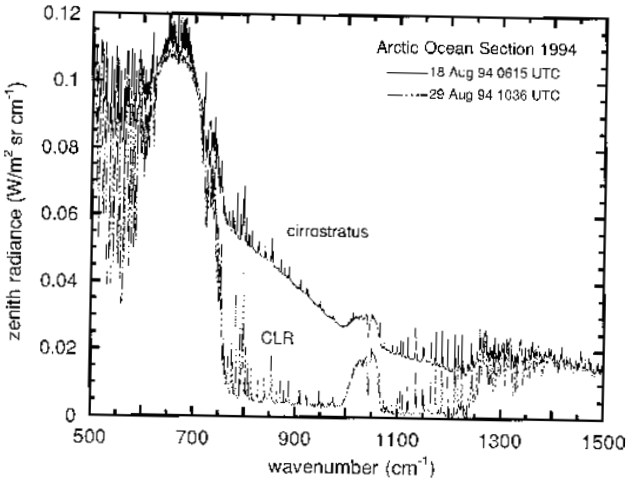

Atmospheric emission spectra measured by the CalSpace FTIR under conditions of low atmospheric opacity.

contains a large amount of liquid or ice water, as is the case with these multiple-layered cloud systems, a large portion of the sun's energy is reflected back to space or absorbed by the atmosphere before reaching the surface.

Two examples of atmospheric emission spectra from the CalSpace FTIR instrument are shown in the figure to the left, under low atmospheric opacity. Here the instrument is measuring terrestrial energy trapped by the atmosphere and emitted straight back down toward the ship. The middle infrared window exists between 800 and 1300 cm^{-1} on this plot. The dotted curve, obtained under clear skies, shows that there is very little energy being trapped and re-emitted by the atmosphere in the window, meaning that most is escaping to space. For wave numbers shorter than 800 and longer than 1300 cm^{-1}, the atmosphere is largely opaque, and most of the energy emitted by the Earth's surface at these wave numbers is always trapped by carbon dioxide and water vapor. The upper (solid) curve was obtained under a high ice cloud, and we can see that in the window this cloud results in nearly an order of magnitude more energy at the ocean surface.

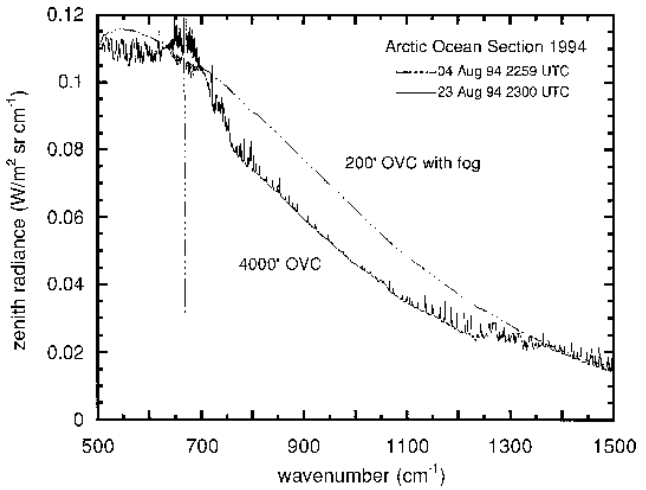

Atmospheric emission spectra measured by the CalSpace FTIR under conditions of high atmospheric opacity.

The figure to the left shows two FTIR emission spectra obtained under overcast skies (the most frequent sky condition during AOS-94). The upper (dotted) curve was obtained on 4 August, the same day as the AVHRR and solar radiometer data discussed above. At the time of this measurement there was so much liquid water in the atmosphere that the atmosphere radiated energy to the surface almost like a perfect blackbody, as signified by the smoothness of this curve. In this situation, when we have a combination of high cloud layers appearing very cold in the satellite data (that is, they are radiating relatively little energy to space) and low cloud layers radiating nearly as much energy as possible to the surface, at nearly the surface temperature, the greenhouse effect of the atmosphere is nearly at a maximum. The lower (solid) curve was obtained under a single-layer stratus cloud. The middle infrared window is almost but not quite closed. This is because the cloud base is several degrees colder than the surface and because the cloud emissivity is less than one, mean-

ing that the cloud does not contain enough liquid water to emit radiation like a perfect blackbody. A doubling of carbon dioxide in the Earth's atmosphere is expected to increase the flux of infrared radiation at the surface by 3–4 W/m^2. The enhancements in surface infrared radiation related to changing cloud liquid water content and emissivity are on the order of tens of watts per square meter.

The FTIR cloud emission spectra can be used to estimate the effective radius of the cloud droplet size distribution (Lubin 1994), which in turn can indicate whether or not continental air masses are influencing cloud microphysics. Radiative transfer analysis of the AOS-94 cloudy sky emission spectra suggest that 30% of the stratiform clouds sampled have effective droplet radii of 7 μm or smaller, in which case they are probably influenced by continental air masses and aerosol concentrations. By showing this type of microphysical phenomenon, along with the large variability in cloud optical depth that can occur (0–50), this program has illustrated that the summer atmosphere in the high Arctic is as dynamically and radiatively complex as that over any other continent or ocean.

Reference

Lubin, D. (1994) Infrared radiative properties of the maritime Antarctic atmosphere. *Journal of Climate,* **7:** 121–140.

Aerosols

John D. Grovenstein, Richard Leaitch and Fred Hopper

Aerosols, especially those that influence cloud microphysics (droplet size spectra), are important in atmospheric research because they influence climate directly by backscattering and absorption of incoming solar radiation and indirectly by affecting cloud albedo. Wigley (1989) suggested that the latter effect could be the reason that the planet has not exhibited heating as predicted by global climate models of the "greenhouse effect." Generally climate models are poorly parameterized for aerosol and cloud microphysics, especially in the remote Arctic. Therefore, it is necessary to measure these parameters to provide data sets for modelers and to diagnose future environmental change.

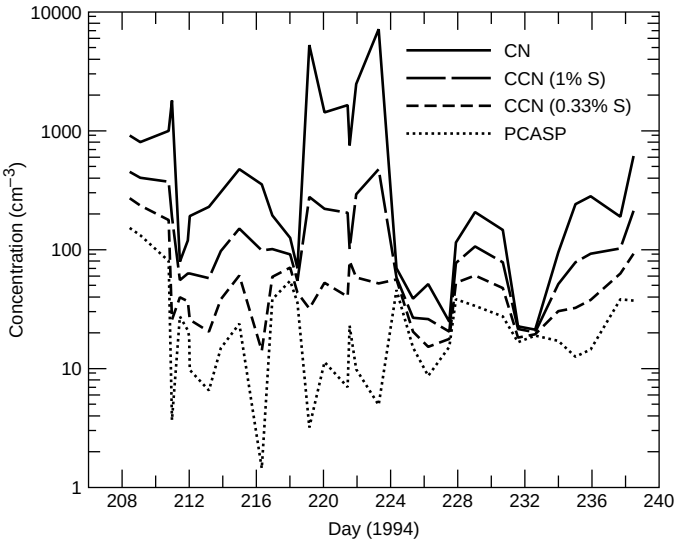

Time series of aerosol concentration for the AOS-94 expedition.

The figure at the left is a time series of aerosol concentration from AOS-94. The uppermost dotted line is the condensation nuclei (CN) concentration measured by TSI models 3025 and 3022 condensation nuclei counters. This number represents the concentration of the finest nuclei (nucleation mode) with a radius of 0.003 μm to the larger aerosols up to a radius of 3 μm. The uppermost solid line is the cloud condensation nuclei (CCN) concentration active at 1% supersaturation. These measurements were taken with an instantaneous CCN spectrometer introduced by Fukuta and Saxena (1979). For this study the spectrometer was operated at a range of 0.2–1.3% supersaturation. The spectrometer makes one spectral sweep every 15 s. The middle dotted line is the CCN concentration active at 0.33% supersaturation measured by the DH Associates cloud con-

John Grovenstein is with the Department of Marine, Earth and Atmospheric Sciences at North Carolina State University in Raleigh, North Carolina, U.S.A. Richard Leaitch and Fred Hopper are with the Atmospheric Environment Service, Downsview, Ontario, Canada.

densation nuclei counter. This instrument records the number of CCN active at a single supersaturation (set at 0.33% for this study). The lowermost dotted line is the large aerosol concentration (0.3–1.0 μm) measured with a Particle Measuring Systems passive cavity aerosol spectrometer probe (PCASP-100X). The instrument provides a histogram of aerosol concentration in 15 size ranges. The concentration from each size range is totaled to provide the concentration reported in the figure.

Sampling began on day 208 with instruments running on a continuous basis. The concentration of aerosols measured by all instruments decreased sharply upon entering the ice. The concentration of CN, CCN (active at 1% supersaturation) and CCN (active at 0.33% supersaturation) "track" each other through the time series, with the PCASP-100X showing this trend but not as dramatically as the other measurements. Generally CCN concentrations in maritime air masses rarely exceed 100 cm^{-3}; however, concentrations above 100 cm^{-3} were measured over a time of days in the remote Arctic Ocean (days 218–224 and days 228–232). These large CCN concentrations also accompanied large CN concentrations, which in one instance (day 224) exceeded 7000 cm^{-3}.

The concentrations of the larger aerosols, measured by the PCASP-100X and the CCN active at 0.33% supersaturation, never exceeded 100 cm^{-3} while we were sampling in the ice. The observations of the largest CN and CCN (active at 1% supersaturation) concentrations correspond to the lowest observed concentrations of the large aerosol with the PCASP-100X. This suggests that the elevated CN concentrations may be due to a local production mechanism. The reduction of the largest aerosol removes a significant surface area for the condensation of precursor gases. The concentration of these gases increases until, by the process of gas-to-particle conversion, they are converted into fine aerosol particles. Between days 218 and 224 the concentration of the finest aerosols are out of phase with the concentrations of the largest aerosols; the peaks in concentration of one corresponds to the minimums of the other. Although this scenario may not be the cause of the observed concentrations, the high concentrations of the precursor gases necessary have been recorded in the Arctic. The figure above shows the relationship between ice coverage and CCN concentration, illustrating the possible production of CCN from precursor gases. When the gas supply is limited by ice cover, CCN concentration decreases. Regardless of the source, the particles are present and are modifying the climate of the remote Arctic.

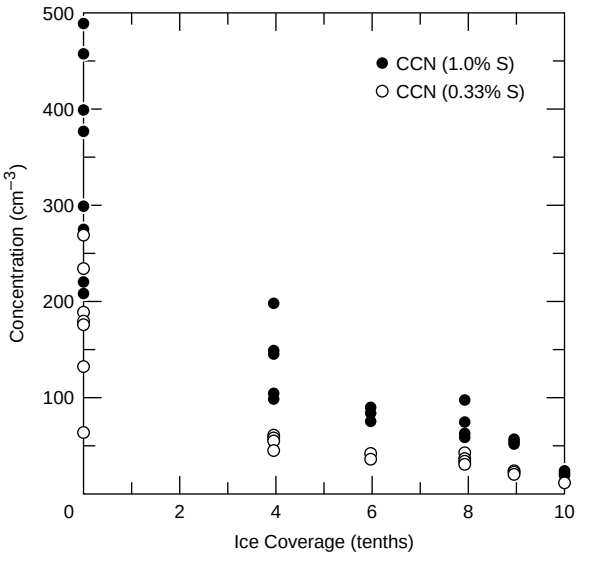

CCN concentration at two supersaturations plotted against ice coverage.

References

Fukuta, N., and V.K. Saxena (1979) A horizontal thermal gradient cloud condensation nuclei spectrometer. *Journal of Applied Meteorology,* **18,** 1352–1362.

Saxena, V.K., and J.D. Grovenstein (1994) The role of clouds in the enhancement of cloud condensation nuclei concentrations. *Atmospheric Research,* **31,** 71–89.

Twomey, S. (1977) The influence of pollution on the shortwave albedo of clouds. *Journal of Atmospheric Science,* **34,** 1149–1152.

Wigley, T.L.M. (1989) Possible climate change due to SO_2 derived cloud condensation nuclei. *Nature,* **339,** 365-376.

— Sea Ice —

Sea Ice Characteristics across the Arctic Ocean

Walter Tucker, Anthony Gow, Hazen Bosworth, Erk Reimnitz and Debra Meese

The Arctic ice cover separates the ocean from the atmosphere, so it is a key component in the exchange of heat, mass and momentum between the two. The properties of the ice cover in summer are especially important, as this is the period of maximum solar radiation. During summer the ice properties become extremely variable, having changed from a highly compact, reflective snow-covered surface during winter and spring to a mottled surface consisting of melt ponds, bare ice and deteriorating snow with many open leads. Major changes occur in the overall surface albedo, the ice cover warms accompanied by draining brine and melting ice, and incorporated sediment and contaminants can be released. The amount of light penetrating into the ocean stimulates biological activity, because a major part of the Arctic Ocean food chain is within a few meters of the ice.

The ice characterization component of AOS-94 consisted of surface albedo measurements, melt pond characterization, snow depth surveys, aerial photography surveys, ice-borne sediment sampling and ice coring. Ice cores were used for thickness, salinity, temperature, chemistry and structural analyses, and samples were provided to associates for stable isotope measurements.

Visual observations and satellite imagery obtained on the section indicated that the concentration of ice increased rapidly from 50–70% south of 72°N to 90–100% for the remainder of the section until the marginal ice zone in the Eurasian Arctic was reached. Ice thickness also increased with northward progress from about 1 m in the first-year ice of the southern Chukchi Sea to about 2.7 m at the North Pole, as verified from visual observations and ice core measurements. With the exception of three ice cores obtained in the Chukchi Sea, all cores on the section were collected from second-year or multiyear ice. The cores revealed thermally degraded ice near the surface above the water level and extremely well drained ice below. Temperatures of the ice were consistently near zero at the surface, increasing linearly to about –1.5°C at the ice–water interface. Salinities were also consistent with previous measurements of summer sea ice (Tucker et al. 1987, Eicken et al. 1995), being zero at the

Walter Tucker, Anthony Gow, Hazen Bosworth and Debra Meese are with the U.S. Army Cold Regions Research and Engineering Laboratory in Hanover, New Hampshire, U.S.A. Erk Reimnitz is with the U.S. Geological Survey in Menlo Park, California, U.S.A.

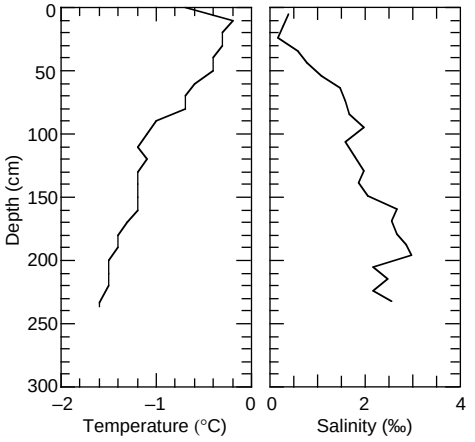

Temperature and salinity profiles for the same core from the North Pole.

surface and increasing to 3–4‰ at depth. In general, the thicker ice had greater salinities near the bottom.

Examination of the crystalline structure revealed that 89% of the total ice sampled consisted of columnar ice. Of the remainder, 9% consisted of granular or frazil ice, and 2% contained platey ice, large platelet-type ice that may have been associated with freezing of under-ice melt ponds as suggested by Jeffries et al. (1995). Much of the granular ice was associated with previously deformed ice, identified by inclined columnar crystals in adjacent sections typical of tilted blocks.

Surveys of snow depth were obtained at all ice sampling stations. South of 80° in the western Arctic, the ice appeared to be snow covered, with very few bare ice spots visible. Close inspection of the snow cover characteristics revealed very large grains, close to 1 cm in diameter. We believe this indicates thermally deteriorated ice, rather than snow. Survey measurements showed mean depths of 6–13 cm of the deteriorated ice. Between 80° and 82°N metamorphosed corn snow was evident. In this region, mean depths ranged from 10 to 15 cm. From 83° to 86°N depths of the old corn snow decreased to 6–8 cm. North of 86° and into the eastern Arctic, new snow was present, generally covering the old coarse snow, and the combined depths were 6–15 cm. At all sites north of 80°, snow depths were variable, usually 0–5 cm on flat thin ice and up to 46 cm on the flanks of pressure ridges. North of 85° it appeared that the melt season was complete, and the depth of the aged snow may represent the minimum for the 1994 ablation season.

Ice core thickness and mean snow depth versus latitude during AOS-94. The straight line is the best-fit linear regression.

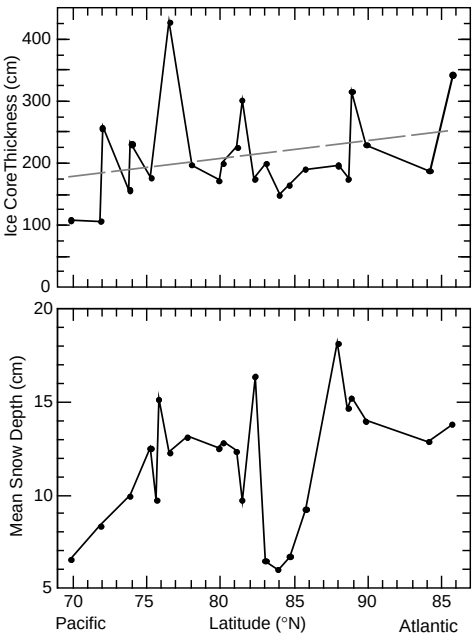

Melt ponds in the Chukchi and southern Beaufort Seas were numerous, but farther north the ponds began to freeze and eventually became snow covered. Image analysis of aerial photographs obtained from helicopter surveys allowed quantitative estimates of the melt pond fraction. On 31 July at 76°N the total pond fraction was 12% and the lead fraction was 6%. On 13 August at 86°N the open pond fraction was 3%, yet 10% consisted of identifiable frozen ponds with a 2- to 5-cm ice cover. The lead fraction had increased to 11%. At 88°N on 18 August no open ponds were identified in the photographs, but an areal fraction of 3% frozen ponds was evident. The open water fraction remained at 11%. Measured melt pond depths ranged from 20 to 60 cm. Six of the 19 ponds sampled were saline and highly stratified, with near zero salinity at the surface to 30‰ at the bottom of the ponds. Saline ponds, though ap-

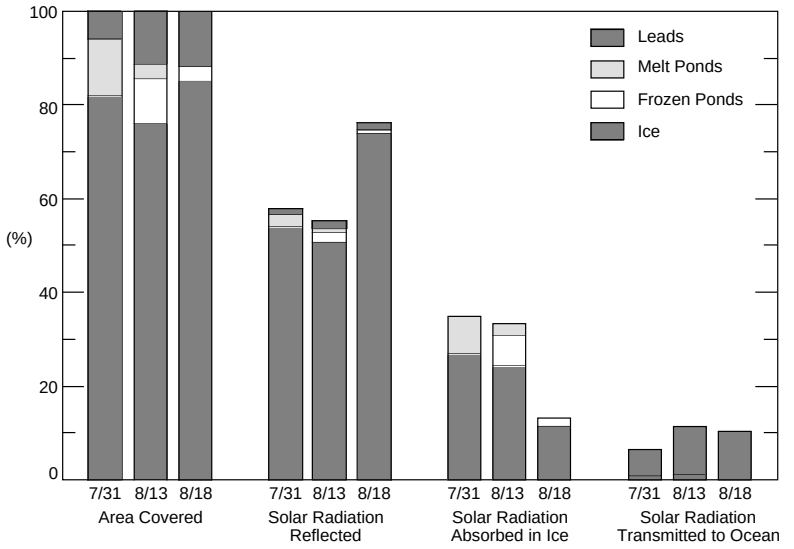

Relative areas of ice and partitioning of incident solar radiation for 31 July, 13 August and 18 August 1994. The contribution from different surface conditions to the disposition of the solar radiation is also show

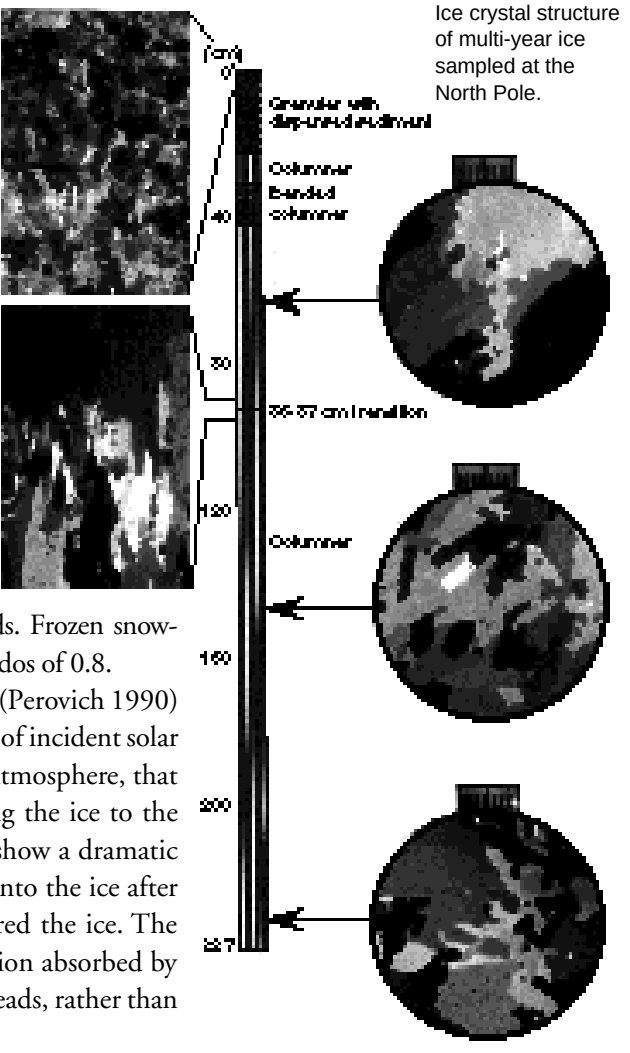

Ice crystal structure of multi-year ice sampled at the North Pole.

pearing to have solid bottoms, obviously had an established hydraulic link with the ocean below. Cores through the bottom ice verified this, showing rotten ice with interconnecting channels. Colors of the ponds varied from very light blue to deep dark green. The color depended on the pond depth, the condition of the bottom ice and biological activity. Chlorophyll *a* concentrations were found to be substantially larger in green freshwater ponds than in the light-blue ponds. The albedos of the ponds also depended on depth and color. Deep ponds with rotten bottom ice had albedos of 0.09; albedos were as high as 0.3 for shallow light-blue ponds. Frozen snow-covered ponds farther north exhibited albedos of 0.8.

A two-stream radiative transfer model (Perovich 1990) has been used to estimate the partitioning of incident solar radiation into that reflected back to the atmosphere, that absorbed by the ice, and that penetrating the ice to the ocean or directly into leads. The results show a dramatic decrease in the solar radiation absorbed into the ice after 18 August, when fresh, light snow covered the ice. The model points out that most of the radiation absorbed by the ocean comes from the absorption by leads, rather than through the ice.

Tony Gow, Erk Reimnitz, Bill Bosworth and Terry Tucker taking cores of dirty ice.

Sediment was observed in and on the ice from the ice edge in the Chukchi Sea to the North Pole. Near the ice edge, sediment covered an estimated 10–15% of the surface of the ice. Farther north it covered less than 1% of the surface and was extremely "patchy" in occurrence. Sediment was notably absent in the Eurasian Arctic, where it has been frequently observed on other expeditions.

Bulk samples of sediment were collected for analysis, and in many locations ice cores were obtained through the dirty ice. Sediment entrained within the ice was invariably associated with granular (frazil) ice formation. Frazil ice is normally associated with turbulent growth conditions. Analyses of the particle sizes found primarily silt- and clay-sized particles; only 5.3% of the total sediment collected was sand, while the proportions of silt and clay were 32.7% and 62.0%, respectively. The few pelecipodes, ostracodes and foraminifera found in the sediment indicate the shallow circum-Arctic shelves as the source of the entrained sediment. The combined evidence indicates that sediment is likely entrained into the ice by ice crystals scavenging suspended sediment during stormy conditions on the continental shelves. Diffraction analysis of the clay fine portion showed it to be composed of primarily illite and chlorite, with smaller amounts of kaolinite and smectite. The smectite proportion increased from near zero in the south to 10–15% in the more northerly samples.

Reverse trajectories calculated for the ice parcels from velocity fields produced by the International Arctic Buoy Program indicate that the shelf source areas from the southernmost samples were the Canadian and Alaskan shelves, while the East Siberian Sea appears to be the source of the more northerly samples. Comparisons of organic carbon between the ice-borne sediment and benthic sediments showed that three times more organic carbon (2.6%) was present in the ice sediments than in the benthos (0.8%). It is likely that the larger amounts in ice are due to biological activity. Conversely the benthic sediments had ten times more carbonate than the ice sediments (10.3 vs. 0.9%,

respectively), probably due to higher concentrations of foraminifera on the sea floor. The visual estimates of sediment on the ice surface would indicate that the amount of sediment being transported by the ice is small, yet because it was observed across most of the Arctic Ocean, it is capable of transporting and redistributing shelf sediments across the entire Arctic Basin.

A primary objective of the detailed ice-sediment study was to determine if radiocesium was present within the ice-entrained sediment. In the ice-borne sediments, ^{137}Cs activities ranged from 4.9 to 73 Bq/kg (dry weight). Many of the samples had ^{137}Cs activities exceeding those found in benthic sediments in the deep basins or the shelves of the Beaufort, Chukchi or Bering Seas, though the levels are far too low to be of concern to health. The highest value (73 Bq/kg), found north of the Chukchi Sea, is comparable to levels present in the sediments of the Yenesey and Ob River estuaries and the Kara Sea. However, the three-year reverse trajectory indicated that the source area for this parcel of ice was the offshore Banks Island region. Since there is no known source in the Banks Island area, either the ice parcel was far older than three years and had been incorporated elsewhere in the Beaufort Gyre or the trajectory calculation neglected the possibility of easterly transport along the Siberian shelf. Another remote possibility may be that radiocesium levels are enhanced during the process of sediment entrainment into ice.

References

Eicken, H., M. Lensu, M. Lepparanta, W.B. Tucker III, A.J. Gow and O. Salmela (1995) Thickness, structure, and properties of level summer multiyear ice in the Eurasian sector of the Arctic Ocean. *Journal of Geophysical Research,* **100:** 22,697–22,710.

Jeffries, M.O., K. Schwartz, K. Morris, A.D. Veazey, H.R. Krouse and S. Cushing (1995) Evidence for platelet ice accretion in Arctic sea ice development. *Journal of Geophysical Research,* **100:** 10,905–10,914.

Perovich, D.K. (1990) Theoretical estimates of light reflection and transmission by spatially complex and temporally varying sea ice covers. *Journal of Geophysical Research,* **95:** 9,557–9,567.

Tucker, W.B. III, A.J. Gow and W.F. Weeks (1987) Physical properties of summer sea ice in the Fram Strait. *Journal of Geophysical Research,* **92:** 6,787–6,803.

Measurements of Ice Mechanical Properties

F. Mary Williams

During AOS-94, ice mechanical properties were measured by the Institute for Marine Dynamics. Williams (1994) gives details on the methods and results. The program was supported by Ship Safety, Canadian Coast Guard, as part of a broad ship technology program.

Under the ship technology program, ice loads at three locations on the hull of the *Louis S. St-Laurent* were monitored throughout the voyage, and significant events were recorded. Ship performance was documented by continuous recording of propulsion system parameters, as well as ship speed and position. The ice properties that influence hull loads and ship performance are the thickness, strength and density of the ice and the quality of the snow cover.

Ice temperature and salinity were measured at 10-cm intervals, and ice density was measured at selected depths in vertical ice cores. Two cores were taken at every science station in the ice using the Rapid-Core, a crane-deployed coring device operated from the deck of the ship. Additional cores at sites distant from the ship were taken using a hand corer. Often, average ice temperatures were –2°C, and average salinities were around 2‰. The ice contained large brine channels, and brine in the upper layers had drained out.

Measurements of ice density from core samples are difficult at these temperatures. The result depends strongly on the amount of brine trapped in the sample, which in turn depends on both the structure of the ice in the core and sample handling. Most of the local density values were between 0.82 and 0.92 Mg/m^3.

The inertial and buoyant forces of ice on the ship depend on the global, in-situ ice density. This quantity, determined from freeboard measurements and adjusted for the snow burden, was consistently between 0.92 and 0.93 Mg/m^3.

A beam test is a direct measure of the flexural strength of the ice. When logistics permitted, beam tests, in a standard size and configuration (Williams and Parsons 1994), were carried out on the ice immediately after cutting the samples. A typical result is a series of eight beams of columnar-grained ice at –1.8°C, with an average flexural strength of 499 kPa. Some beam samples were cold soaked and tested in the coldroom onboard the ship.

F. Mary Williams is with the Institute for Marine Dynamics in St. John's, Newfoundland, Canada.

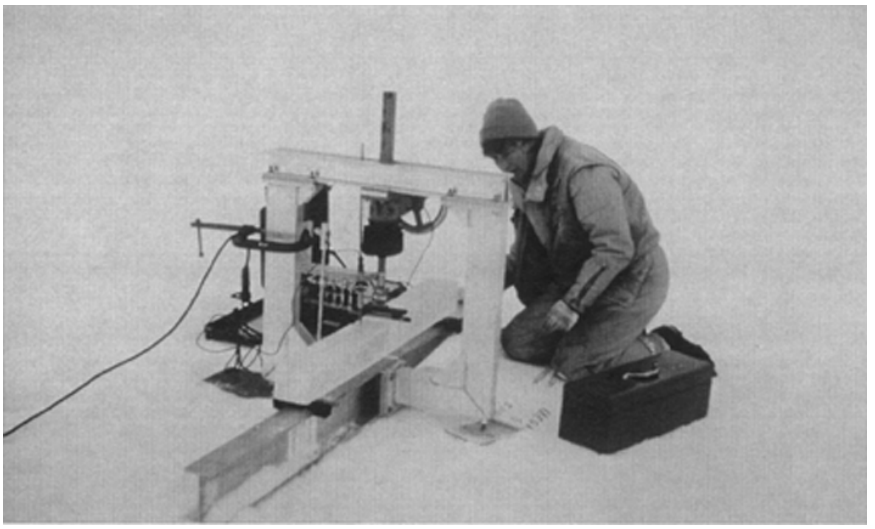

Mary Williams measuring the flexural strength of ice beams.

When ice fails against the ship hull, the relationship between the average ice pressure and the loaded area depends, in part, on the maximum pressure sustained over actual contact areas, or hot spots. In materials that deform plastically, this pressure, called the hardness, may be considered a material property. Hardness was measured using a 136° pyramid Vickers Indenter. Hardness decreased as contact area increased, from maxima near 60 MPa over 10^{-5} m^2 to values near 15 MPa over 10^{-4} m^2. The effects of temperature and of work done on the ice are being investigated.

Since ice thickness varies with date and location, a ship-based measurement is not representative of the entire Arctic. However, such a measurement is appropriate in an analysis of ship performance and hull loads. A video camera aimed at the ice surface near the starboard shoulder of the ship ran continuously throughout the trip. A computer-generated scale, calibrated at the ice surface, overlaid the image on the video record and measured the thickness and length of ice pieces turned up by the ship. Statistical results will not be available until these data have been carefully analyzed.

To determine the ice crystal structure, rough thin sections of ice from some of the cores and all of the beams were prepared in the coldroom and photographed through crossed polaroid filters. Most of the photos show highly metamorphosed, unoriented, largely granular ice in a range of grain sizes. One surprise was an ice sample with zero salinity and very large grains (>8 cm in diameter) inadvertently taken from a concealed, refrozen melt pond.

Snow reduces ship performance through the inertial, buoyant and friction forces it exerts on a moving ship. The water content and grain size of snow affect imagery collected by satellite-borne microwave sensors by changing the apparent brightness temperature of the ice surface. Thus, snow density and type are key links between remotely sensed ice imagery and actual ship performance. Global snow density was measured in small full-thickness samples,

Ice properties in four navigation zones during AOS-94. The maximum ice strength is an index of maximum hull loads, and the mean ice strength is an index of ship performance.

Latitude (°N)	Ice cover (10ths)	Floe size (km)	Max strength (kPa)	Mean strength (kPa)
70–80	8 to 9+	0.5	470	250
80–88	9+ to 10	3.0	250	250
88–90	10	1.0	500	500
85–81	8 to 9+	0.5	600	300

and the type was recorded qualitatively. Typical global snow densities were 0.42 Mg/m^3 for large-grained, wet snow and 0.25 Mg/m^3 for fine, new snow.

For evaluating the ship's performance, and also for interpreting the ice forces on the hull of the ship, the ice and snow mechanical properties data were separated into four navigation zones. Up to latitude 80°N, there was considerable surface melt and brine drainage. The ice was porous and contained many flaws, allowing relatively easy ship passage. However, mean ice temperatures indicate that layers of intact, relatively cold ice were present in some floes, with a risk of significant hull loads.

North of 80°, where air temperatures were lower, mean ice temperatures were slightly higher than in the first zone. This apparent paradox is due to melt surfaces advancing more rapidly than conduction isotherms and is recognized in icebergs (Diemand 1984). The ice was close to its melting point and presented low strengths throughout the thickness.

The heavy ice at the highest latitudes, 88°N and beyond, was composed of extensively damaged, worked and reconsolidated ice features. For this fairly homogeneous ice, a higher ice strength applies to both ship performance and load risk.

The transit was rapid and the sampling sparse from 90°N south to 85°N. Hence, it is not certain where to place the boundary between zone 3 and zone 4. However, south of 85°N the ice was clearly thinner, less complex and of lower concentration. The drained, low-salinity ice had begun to refreeze. The completely frozen freshwater melt pond at Station 37 was an illustration. Because of extensive flaws due to melting, the mean ice strength was low, but the presence of solid, low-salinity ice pushed up load risk levels.

References

Diemand, D. (1984) Iceberg temperatures in the North Atlantic—Theoretical and measured. *Cold Regions Science and Technology,* **9(2):** 171–178.

Williams, F.M. (1994) The Canada/U.S. 1994 Arctic Ocean Section—Ice mechanical properties measurements. Institute for Marine Dynamics: TR-1994-29.

Williams, F.M., and B.L. Parsons (1994) Size effect in the flexural strength of ice. 13th International Conference on Offshore Mechanics and Arctic Engineering, Houston, Vol. IV, p. 15–22.

— *Geology and Paleoceanography* —

Sources of Ice-Rafted Detritus and Iceberg Tracks in the Arctic Ocean

Dennis A. Darby and Jens F. Bischof

The sources of ice-rafted detritus (dropstones) were determined by matching the elemental composition of iron oxide grains and percentages of grain types in Arctic Ocean deep-sea sediment cores to potential sources around the Arctic Ocean. This "fingerprinting" technique required prior characterization of source areas in the Arctic providing debris that could be rafted into the central Arctic Ocean by icebergs or sea ice. Eleven statistically unique source areas were defined by grain type percentages and microprobe chemical analyses of thousands of individual iron oxide grains (Darby and Bischof 1996).

Erk Reimnitz collecting sediment from the ice.

For the first time the sources of ice-rafted grains in the Arctic Ocean were traced with a high level of statistical probability. This allowed us to reconstruct the ice drift tracks and the ocean surface currents in the past and to get a better understanding of the nature and history of Arctic glaciations. Finally the potential of pollutants being spread throughout the Arctic Ocean from point sources on the Russian shelves can be assessed.

The major sources of detritus in 17 of the deep-sea cores thus far analyzed (4 of 18 cores from the AOS-94 cruise and 13 from previous expeditions) are the Banks and Victoria Island area and the Sverdrup Basin area around Ellef Ringnes Island and northern Melville Island. The Mackenzie River basin con-

Dennis Darby and Jens Bischof are with the Department of Geological Sciences at Old Dominion University in Norfolk, Virginia, U.S.A.

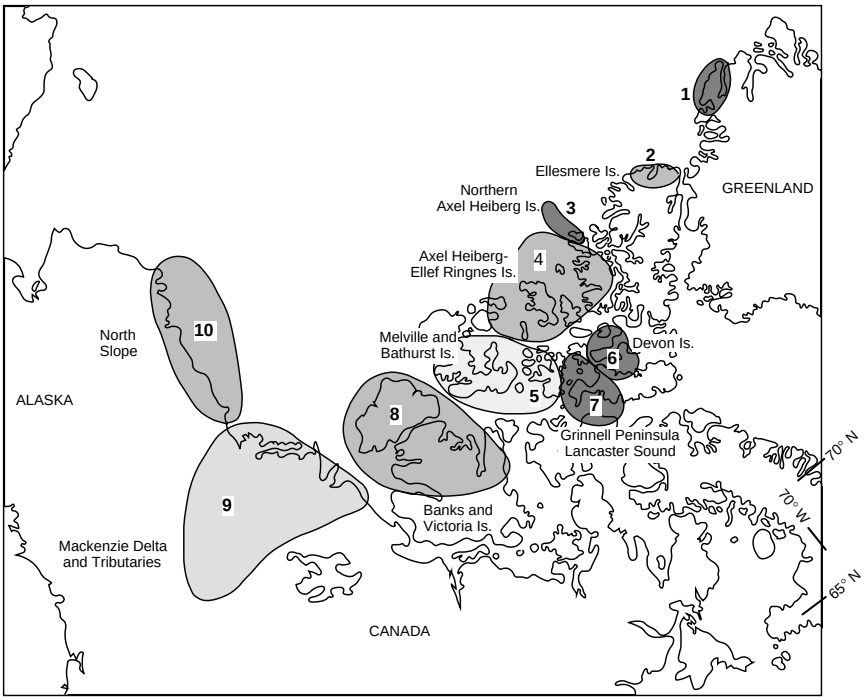

Source areas for Arctic ice-rafted debris based on statistically unique grain-type content and chemistry of iron oxide grains. Not shown is another area in the Kara Sea and the 102 till and glacio-marine sediment sample locations used to define these areas.

tributes on average less than 10% to the ice-rafted detritus in the cores analyzed. Areas of existing ice caps such as Ellesmere Island, Axel Heiberg Island and Greenland contribute even less to the western Arctic Ocean. About 25% of the iron oxide grains in the studied Arctic Ocean core samples were from unknown source areas. All glacial sources except those of the Barents Shelf and adjacent land masses were sampled to varying degrees of thoroughness. We suspect that many of the iron oxide grains from presently unknown sources (the average from 17 cores is 26%) may have been rafted by sea ice from the Russian shelves. This has serious implications because of the modern pollution from radioactive dumps and other pollutants attached to sediment in parts of this shelf area.

Down-core changes in source area contributions show that cyclic surging of ice sheets and ice caps has occurred at least throughout the last 780,000 years in the Arctic. The cyclicity is less than about 30,000 years and probably less than 10,000 years during glacial intervals, but because of the lack of a more detailed chronostratigraphy in the Arctic cores, the frequency cannot be resolved further. Pulses of ice rafting from different sources in ^{14}C-dated Holocene sediments (<10,000 years old) of the central Arctic Ocean lasted less than 2,000 years.

The Laurentide ice sheet that calved into the Arctic Ocean from Melville or Banks Island to the Mackenzie Delta area coexisted with several small ice caps or possibly a larger ice sheet over the Queen Elizabeth Islands. This is based on the discovery of detritus from both ice masses in the same 0.5- to 1-cm-thick core samples.

The last glaciation in the Queen Elizabeth Islands transported little ma-

terial from the interior areas, inland from the Arctic Ocean, such as the Precambrian Shield. Grain-type percentages in glacial deposits on and around these islands closely match rock types of local formations. Heavy mineral and iron oxide grains show less-clear affinities to local rock types but generally corroborate the local nature of tills and glaciomarine sediments in the Queen Elizabeth Islands.

Today's Beaufort Gyre circulation in the western Arctic Ocean, a clockwise ice drift, cannot explain the observed compositional differences between widely spaced core locations. The data obtained thus far suggest that the surface circulation in the western Arctic was toward Fram Strait, even along the Canadian Arctic coast during glacial intervals. This means that surface currents were opposite or perpendicular to the southwestward currents today within a couple of hundred kilometers of the Canadian Arctic coast. Thus large numbers of icebergs moved northeastward near the coast and into the North Atlantic during glacial maxima, while a thick floating ice cap blocked or greatly inhibited icebergs from reaching the central and western parts of the Arctic Ocean. This is further supported by the slower sedimentation rates in these central areas.

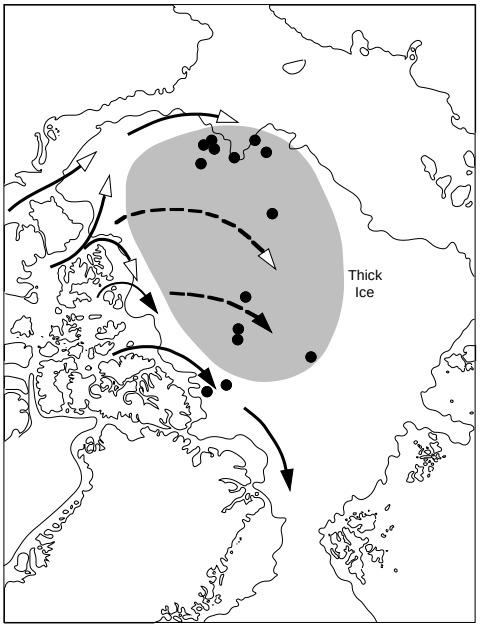

Iceberg drift tracks and surface currents for earlier glacial maxima in the western Arctic Ocean based on dropstones and iron oxide grains. The zone of thick ice inhibits iceberg drift and causes low sedimentation rates. Arrows depict iceberg drift from the Laurentide Ice Sheet (open arrows) and glaciers from the Queen Elizabeth Islands (solid arrows). Core locations used for this reconstruction are shown as black dots.

Unusual magnetite spherules (40–60 μm) with about 6–18% zinc oxide and 18% nickel oxide were found at over 30 sites in the Queen Elizabeth Islands and in several Arctic Ocean cores in sediment as old as 780,000 years. Iron meteorites lack zinc because of its volatility at temperatures of atmospheric entry, so an impact event in zinc-bearing limestones such as the Haughton Astrobleme (~22 million years ago) is still considered to be a likely explanation for such spherules. However, a detailed search for these spherules in ejecta from the Haughton Astrobleme on Devon Island was negative. Thus, if these spherules were formed by such an event, it is yet to be discovered in the Queen Elizabeth Islands.

Reference

Darby, D.A. and J.F. Bischof (1996) A statistical approach to source determination of lithic and Fe oxide grains: An example from the Alpha Ridge, Arctic Ocean. *Journal of Sedimentary Research*, **66:** 599–607.

Late Quaternary Paleoceanography of the Canada Basin, Central Arctic Ocean

William M. Briggs and Thomas M. Cronin

This project is based on quantitative analysis of the ostracodes present in seafloor boxcores and piston cores collected during AOS-94. Ostracodes are small, bivalved crustaceans whose shells, or valves, are made up of calcium carbonate in the form of the mineral calcite, which also contains trace amounts of magnesium.

Seafloor sediments of the central Arctic Ocean (CAO) contain two types of deep-sea ostracodes: cladocopids and podocopids. Cladocopid ostracodes are extremely abundant in the CAO, where they are represented by about 13 species of the genus *Polycope*. Cladocopids are part of the epifaunal bottom community, and they can swim for short distances just a few centimeters above the sea bottom. The podocopid ostracodes of Arctic Ocean sediments, with one exception, are bottom-dwelling species, some living at the sediment–seawater interface (epifaunal) and others living in the substrate just below the interface (infaunal).

The exception is the genus *Acetabulastoma*, which has a lifestyle of commensalism on at least two species of gammarid amphipods that are part of the under-ice community in Arctic marine environments. Whether due to the death of the host amphipod species or the release of ostracode shells from the host species by accidental detachment, death or molting, the shells of *Acetabulastoma* eventually sink through the water column and come to rest on the seafloor, where they become part of the ostracode bottom fauna. Their shells are therefore not indicative of the ostracode assemblages used to characterize certain water masses. The presence or absence of *Acetabulastoma* in downcore ostracode assemblages can be used as a proxy indicator of the magnitude and extent of ice cover in the CAO. This has important implications for CAO ice-cover history and its linkages to paleoceanography, paleoclimatology and global change.

Many ostracodes in the marine realm live within narrowly defined environmental tolerance limits, and their distribution on the seafloor is governed by variables such as the temperature, salinity, oxygen concentration and nutrients in the overlying water column and the type of sediments on the seafloor.

William Briggs is with the Institute of Arctic and Alpine Research at the University of Colorado at Boulder, Colorado, U.S.A. Thomas Cronin is with the U.S. Geological Survey at Reston, Virginia, U.S.A.

Liz Osborne processing seafloor cores in the *Polar Sea* core laboratory.

Studies of ostracodes in surface sediments from piston core and boxcore tops, collected mainly from the Eurasia Basin of the Arctic Ocean and analyzed using multivariate quantitative and clustering techniques, have shown that many ostracode species that form assemblages in the Arctic Ocean have distinct bathymetric ranges that are related to the depth-stratified water masses of the present-day water column. Thus, we are able to recognize assemblages of ostracodes that are diagnostic of:

- Polar surface water (0–100 m), below which lies a 100-m-thick halocline layer;
- Arctic intermediate water (Atlantic water) (200–800 m); and
- Arctic Ocean deep water (to 4000 m or more).

These water masses are in themselves easily differentiated from one another because each has a characteristic temperature–salinity signature, which is related to water density, which in turn, determines their position in the stratified water column. We, therefore, are able to recognize and "calibrate" these modern analog ostracode assemblages with what is known of the physicochemical properties of each water mass or subdivisions of the water mass into upper and lower parts. Thus, "depth-related" ostracode assemblages in modern-day Arctic seafloor sediments are proxy indicators of water mass type. Moreover, downcore changes in ostracode assemblages, when compared to the modern analog coretop assemblages by a quantitative method called the modern analog technique (MAT), will result in a proxy record of the water-mass history over a basin, abyssal plain, ridge, rise or plateau in the deeper (≥4 km) to shallower (~1 km) parts of the Arctic Ocean during late Quaternary time.

We have found:

- Well-preserved ostracodes and good biostratigraphies downcore in boxcores from the Mendeleyev and Lomonosov Ridges and slopes;
- Ostracodes in 18 boxcore tops; and
- Well-preserved adult specimens of the deep-sea ostracode genus *Krithe* to be used in shell-chemistry studies.

The longest of the 18 boxcores is 46 cm long. On average, sedimentation rates are on the order of 1–2 cm per 1000 radiocarbon years (1 kyr) in the CAO for the Holocene (the last 10,000 kyr). Sedimentation rates during the last glaciation have been variously estimated at 0.1–0.2 cm/kyr up to 0.5 cm/kyr, based on accelerator mass spectrometry (AMS) ^{14}C dating. Thus, the ages of the pre-Holocene sections of the boxcores in all likelihood span all of the last glaciation, which dates from approximately 70–10 kyr ago, and may be older. All of the boxcores, then, must record the time of the last glacial maximum (approximately 18 kyr ago) through to the present.

Our objective is to study the ostracodes in boxcore sections from the last glacial maximum through Termination 1a and 1b to the present. Termination 1a marks the beginning of the last deglaciation, dated at 15.7 kyr ago (16,650 calendar years B.C.), and Termination 1b marks the end of the last glacial–deglacial transition, dated at 7.2 kyr ago (6,000 calendar years B.C.). Modern surface and deep-sea circulation patterns and seasonal ice-free conditions are believed to have been established in the northern North Atlantic and Arctic Oceans following Termination 1b. These changes are in direct response to the drawdown and final collapse of the great Northern Hemisphere ice sheets (the Laurentide and the Fennoscandian). Quantitative analysis of the downcore ostracode assemblages by the MAT will record upslope and downslope migrations of ostracode assemblages in response to changing oceanographic conditions due to changes in circulation following the decay and collapse of these ice sheets.

To date, we have sampled five of the eighteen boxcores from sites on the Mendeleyev Ridge and slope, the Lomonosov Ridge and slope, and the Pole Abyssal Plain. All of these cores have well-preserved ostracodes, except for the one from the Pole Abyssal Plain, which has poorly preserved ostracodes in the top few centimeters downcore and no calcareous faunas of any type farther downcore. The well-preserved downcore ostracodes will greatly aid in the paleoceanographic history of the Mendeleyev and Lomonosov Ridges and other ridge areas of the Arctic Ocean. High-resolution downcore AMS ^{14}C and oxygen isotope records, which will be made available by Glenn Jones and William Curry of the Woods Hole Oceanographic Institution, will be indispensable to the project. These records, when augmented by the ostracode biostratigraphy, will allow us to pinpoint the timing of paleoceanographic events in the Arctic Ocean over the last few centuries and millennia, and these data will help predict future change. We are separating out adult specimens of two species of the deep-sea ostracode genus *Krithe* for use in downcore single-valve geochemical analyses by Paul Baker and Gary Dwyer of Duke University, who, in collaboration with Thomas M. Cronin, are developing geochemical proxy tools to determine paleotemperatures and other physicochemical variables in the deep ocean based on the shell chemistry of *Krithe*. New distribution records of the ostracodes in coretop samples will allow us to fine tune the Arctic Ocean Database, and these data will greatly enhance the resolution of the MAT. We will also examine selected piston cores for much older paleoceanographic and paleoclimatic records when samples from these cores become available.

Elemental and Isotope Geochemistry of Sediment from the Arctic Ocean

Bryce L. Winter, David L. Clark and Clark M. Johnson

Elemental and radiogenic isotope studies of marine silicate sediment have greatly increased our understanding of the lower-latitude and southern oceans. However, no comprehensive study had been conducted in the Arctic Ocean. Elemental and radiogenic isotope compositions of marine silicate sediment are powerful tools for understanding the sediment source region, including its location, general lithologic composition, age and crustal depth of exposure. Upon identifying the source location and using sediment compositional variations to establish distribution patterns, it may be possible to reconstruct sediment transport pathways and infer transport mechanisms. This may provide independent information concerning paleoceanographic or paleoatmospheric circulation patterns and contribute to better paleoclimate reconstructions.

Surface sediments collected along the AOS-94 track (Mendeleyev Ridge, Makarov Basin, Lomonosov Ridge, Amundsen Basin and Nansen Basin) have been analyzed for major and trace elements via instrumental neutron activation and x-ray fluorescence. We are completing Rb–Sr, Nd and Pb isotope analyses via thermal ionization mass spectrometry. We have analyzed the major and trace element compositions for 20 other deep-ocean sediments (Canada Basin, Northwind Ridge and Alpha Ridge), 3 sea ice samples and 19 samples of sediment from rivers and shelf areas that are potential source regions (Queen Elizabeth Islands, northern Canada, Kara Sea, Ob River, Yenisey River and Pechora Sea).

Initial examination of the elemental data shows that all deep ocean sediment, except that from the Canada Basin, has much higher concentrations of transition elements, such as Co and Ni, than does sea ice sediment and the sediment samples from potential source regions. Transition elements are concentrated in hydrogenous oxide coatings, which accumulate on sediment particles at the sediment–water interface in marine settings. Sediment from the Canada Basin is deposited by turbidity currents at much higher sedimentation rates than other areas of the central Arctic Ocean; hence, there is less accumulation of hydrogenous oxide coatings on sediment from the Canada Basin.

Sediment from the Ob and Yenisey Rivers and the Kara Sea have much higher concentrations of compatible elements (such as Cr and Sc) than all the

Bryce Winter, David Clark and Clark Johnson are with the Department of Geology and Geophysics at the University of Wisconsin-Madison in Madison, Wisconsin, U.S.A.

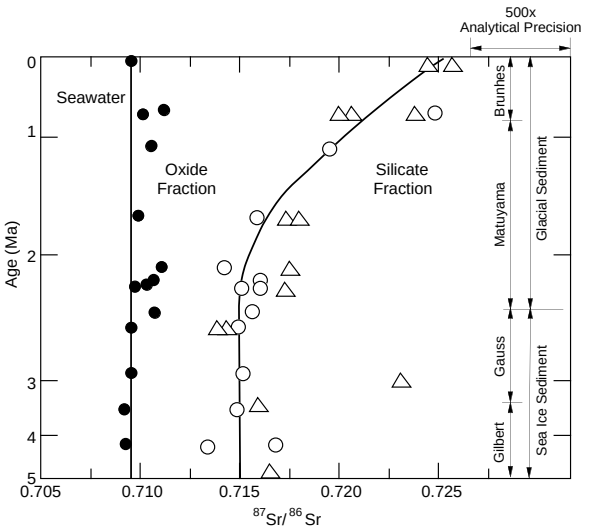

Sr isotope variations of components of Late Cenozoic sediment from the Alpha Ridge, central Arctic Ocean. The components that were analyzed include the oxide fraction of ferromanganese micronodules (solid circles), the silicate fraction of ferromanganese micronodules (open circles) and bulk silicate sediment (open triangles).

other sediments that have been analyzed. This is consistent with the high concentrations of smectite in this region and indicates that the extensive Mesozoic basalt complexes of the adjacent continental land mass are important sources of sediment to this shelf region. However, these rivers and the Kara Sea shelf in general cannot be important sources of sediment for the central Arctic Ocean.

Late Cenozoic sediments on the Alpha Ridge in the central Arctic Ocean (~5 m thick) were deposited at very low sedimentation rates (~1 mm/ky) and can be separated into two distinct sedimentary packages based on lithology. The lower package (~5–2.4 Ma) is composed of silty lutites that are interpreted to have been deposited by sea ice. The upper sedimentary package (~2.4–0 Ma) is composed of alternating sandy and silty lutites and has glacial dropstones occurring throughout the sequence. The younger cyclic sequence is interpreted to have been deposited by glacial ice; the coarse layers were deposited during glacial maxima and deglaciation, whereas the fine intervals were deposited during interglacial periods. We have analyzed detrital silicate material, planktonic foraminifera and the diagenetic (oxide) fraction of ferromanganese micronodule (50–300 μm) separates throughout a composite Late Cenozoic sedimentary sequence for variations in Nd, Sr and Pb isotopes and rare earth elements. The oxide fractions of Fe–Mn micronodule separates were isolated using a chemical reductant. The foraminifera and the diagenetic fractions record the isotope variations of Arctic seawater.

The Sr, Nd and Pb isotope compositions of the siliciclastic fraction are homogeneous during the time of sea ice sedimentation (~5–2.4 Ma), whereas $^{87}Sr/^{86}Sr$ and $^{206}Pb/^{204}Pb$ ratios progressively increase and $^{143}Nd/^{144}Nd$ ratios decrease during the time of glacial sedimentation. We interpret these isotope variations to indicate a progressive change in the source of sediments to the central Arctic Ocean beginning at the time of initiation of continental glaciation (~2.4 Ma). All the isotope systems are remarkably consistent and indicate that the sediment source region during glacial sedimentation (~2.4–0 Ma) had a greater supracrustal component and/or an older average age relative to the source that supplied sediment during the time of sea ice sedimentation (~5–2.4 Ma). The isotope data are consistent with derivation of the older (~5–2.4 Ma) sediment entirely from the Siberian shelf, whereas the Canadian Island region became a progressively more important source of sediment since ~2.4 Ma. The general increase in the amount of coarse sediment since ~2.4 Ma is consistent with this hypothesis. We intend to further refine and substantiate sediment source regions by analyzing circum-Arctic river and shelf sediments for isotope variations.

— *Ship Technology* —

Real-Time Remote Sensing for Ice Navigation

Caren Garrity, Dan Lubin and Réné O. Ramseier

AOS-94 explored areas never before studied by surface ships. An investigation of historical ice conditions indicated that we could expect an average of 83 ±11% ice concentration along the planned route to the North Pole. A major advantage of this expedition was the installation onboard the *Polar Sea* of a TeraScan receiver and processing system developed by SeaSpace Corporation. The system was capable of real-time reception and processing of imagery from the advanced very high resolution radiometer (AVHRR) on NOAA satellites as well as the special sensor microwave imager (SSM/I) data from the Defense Meteorological Satellite Program (DMSP) satellites.

The AVHRR imagery is in the visible and infrared wavelengths, and these sensors are useful for real-time weather information. Their usefulness for monitoring ice motion on this voyage was extremely limited due to the nearly constant cloud cover and considerable fog. During AOS-94, 5.3% of the transit days to the North Pole were nearly cloud free, and 17 days were free from fog. To be useful for ice navigation, a satellite sensor needs to "see" through clouds and fog. Sensors using the microwave frequency range such as the SSM/I have this capability.

Three SSM/I algorithms were used to map sea ice during AOS-94: NASA Team (NASA, U.S.), AES (Canadian Atmospheric Environment Service) and 85 GHz (Scripps, U.S.). The former two algorithms provide coarser-resolution ice maps by combining the lower-frequency channels of the satellite sensor (19 and 37 GHz). Previous comparisons of these are summarized, including an error analysis, in Steffen et al. (1992). The 85-GHz ice concentration maps have twice the resolution (12.5 km), and the new 85-GHz algorithm is summarized in Lomax et al. (1995). The reported error for derived total ice concentrations during the winter is approximately 9% for the NASA Team and AES algorithms. This error is due to signature uncertainty and the uncertainty in atmospheric parameters, including instrument noise effects. As a result of this experiment the 85-GHz algorithm has been evaluated (Lubin et al. 1996)

While AOS-94 was useful for comparing the ice concentrations derived from the three algorithms, it is difficult to "validate" the sea ice algorithms, since observing ice from the bridge of a ship is somewhat qualitative and the visibility is limited to a small area. The visibility was estimated to be from 0.05 to

Caren Garrity and Réné Ramseier are with the Microwave Group–Ottawa River, Inc., in Dunrobin, Ontario, Canada. Dan Lubin is with the California Space Institute at the University of California–San Diego in La Jolla, California, U.S.A.

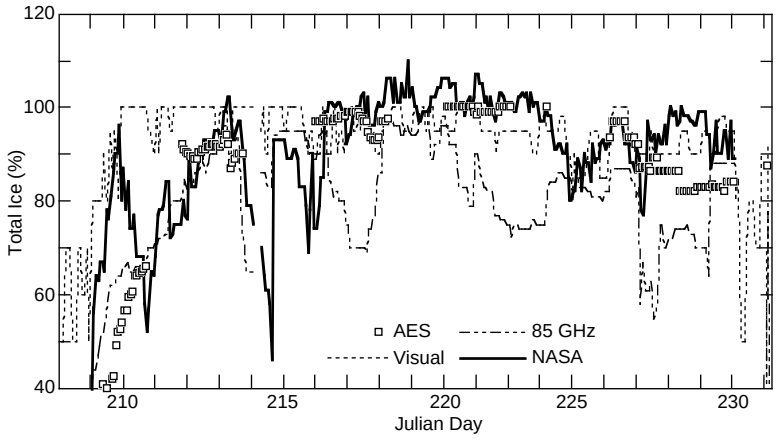

Ice concentration along the *Polar Sea*'s track to the North Pole.

10 nautical miles during the transect. Often the ice concentrations were overestimated, since the farther one looks towards the horizon, the less open water can be seen. When the ship is progressing slowly through a vast old ice floe, for example, from the ship the ice concentration could appear to be 100%.

The total ice concentration along the ship's track was derived from each of the algorithms and estimated from visual ice observations. The average visually estimated ice concentration was 93% along the total ship's track (A.R. Engineering, and Science and Technology Corporation 1994). The AES and 85-GHz algorithms show an average of 88% and 84%, respectively; the NASA team algorithm, which appears to underestimate the ice concentration, averaged 78%.

The microwave sensors are influenced by cloud liquid water content and snow wetness, which cause an increase in the brightness temperature detected by the sensors. The NASA Team and AES algorithms, using the lower frequencies, are less sensitive to atmospheric moisture than the 85-GHz algorithm. The derived ice concentrations are significantly affected by the snow wetness, however (Garrity 1991, 1992). For example, the 85-GHz derived ice concentrations can be as large as 110%. When using the 85-GHz algorithm over regions of lower ice concentration, the reference polarizations in a given image must be chosen with care because there the polarization-based algorithm is more sensitive to cloud opacity and can easily and substantially underestimate the ice concentration (Lubin et al. 1996). However, near the ice edge, the 85-GHz derived ice concentrations were closer to visual observations than the conventional algorithms were, most likely due to better resolution. Comparison of 85-GHz brightness temperatures measured from space with both the lower-frequency measurements and with the shipboard observations shows that much of the information about surface properties, including snow wetness and volume scattering in multiyear ice, is contained in the 85-GHz signal, despite the higher atmospheric opacity.

Using the 85-GHz algorithm, ice concentrations greater than 100% are reduced to 100% and a colored ice map is produced for operational use. The influences of the atmosphere and snow wetness on derived ice concentrations are less than 10% for the high ice concentrations encountered during AOS-94, so this is not a critical problem. For determining total ice concentration during summer in the high Arctic, the new 85-GHz algorithm is as good as the conventional lower-frequency algorithms, if not better because of the doubled resolution.

The 85-GHz SSM/I ice product aided navigation and planning of scientific station stops on a daily basis. For example, the ship was rerouted to the west of 180° because of the 100% total ice concentration to the east. The 100% ice concentration areas were consistent during the experiment, and the consistency was confirmed using the three algorithms and helicopter surveys. The SSM/I ice maps provided an overview, which aided the process of deciding how to proceed from the North Pole. The SSM/I and AVHRR data provided ice and weather information during AOS-94 and met the criteria for being operational, that is, timeliness, coverage and interpretation. It was clearly demonstrated that the ships could easily reach their goal by having a mini-ice center in the high Arctic, where communication is difficult and expensive.

Caren Garrity measuring snow wetness.

References

A.R. Engineering, and Science and Technology Corporation (1994) Hull/ice interaction loads measurements on-board the *Louis S. St-Laurent* during the 1994 trans-Arctic voyage: Trip report and data summary. Submitted to Fleet Systems, Canadian Coast Guard, by A.R. Engineering, Calgary, Alberta, Canada, and Science and Technology Corporation, Columbia, MD, U.S.A.

Garrity, C. (1991) Passive microwave remote sensing of snow covered floating ice during spring conditions in the Arctic and Antarctic. Doctor of Philosophy, Graduate Programme in Earth and Space Science, York University, North York, Ontario, Canada.

Garrity, C. (1992) Characterization of snow on floating ice and case studies of brightness temperature changes during the onset of melt. In *Microwave Remote Sensing of Sea Ice.* Geophysical Monograph 68, p. 313–326.

Lomax, A.S., D. Lubin and R.H. Whritner (1995) The potential for interpreting total and multiyear ice concentrations in SSM/I 85.5 GHz imagery. *Remote Sensing of Environment,* **54:** 13–26.

Lubin, D., C. Garrity, R.O. Ramseier and R.H. Whritner (1996) Evaluation of the special sensor microwave imager 85.5 GHz channels for total sea ice concentration retrieval during the 1994 Arctic Ocean Section. Submitted to *Remote Sensing of the Environment.*

Steffen et al. (1992) The estimation of geophysical parameters using passive microwave algorithms. In *Microwave Remote Sensing of Sea Ice.* Geophysical Monograph 68, p. 201–231.

Ship Technology Program

Larry Schultz and Rubin Sheinberg

The AOS-94 ship technology program consisted of two parts. One part was concerned with measuring the icebreaking capability of the two icebreakers, the USCGC *Polar Sea* and the CCGS *Louis S. St-Laurent*, while transiting high-Arctic ice conditions. The other part involved measuring the loads imposed on the hull of the *Louis S. St-Laurent* due to impact with the ice.

Icebreaking performance data typically define the power required for an icebreaker to break a given thickness of uniform ice at a given speed. Plans were made to perform dedicated performance tests in a range of uniform conditions if such were encountered. No uniform ice conditions suitable for performance testing were encountered, however, in the entire expedition.

Polar Sea breaking ice.

In contrast, trafficability data provide information on the ability of an icebreaker to transit from point to point in a given geographic area in a real-world mix of ice conditions. Ice trafficability data were recorded hourly during the entire time the ships operated in ice, resulting in about 500 hours of data on ship propulsion, environmental conditions and ice conditions. The data on ice conditions included the classification of the ice as first year, second year or multiyear; the lead width; the average and maximum floe size; the concentration of the ice cover broken down in increments of thickness; the average and maximum thickness; the pressure ridge encounter rate; and the average and maximum sail height of the pressure ridges. The environmental data included the snow depth and type, a characterization of the ice pressure, and the diameter and concentration of melt ponds. Data on open-water performance and seakeeping were collected during the open-water transit legs of the expedition.

Larry Schultz is with Advanced Marine Enterprises, Inc., in Arlington, Virginia, U.S.A. (He was formerly with Science and Technology Corporation in Columbia, Maryland.) Rubin Sheinberg is with the U.S. Coast Guard in Baltimore, Maryland, U.S.A.

Finally, the performance study also included an analysis of the shipboard science spaces and equipment onboard both ships, based on observations and interviews with the scientists. The trafficability and performance data will contribute to the knowledge base available for the design of future icebreakers in terms of ship resistance and powering and in terms of a realistic mix of ice conditions and operating modes for high-Arctic transit. Since the expedition completed a full transect of the Arctic Ocean from the Pacific to the Atlantic via the North Pole, the data recorded on ice conditions and environmental conditions will be extremely valuable in planning future high-Arctic icebreaker expeditions.

The ice impact loads portion of the program is part of an ongoing joint effort between the Canadian and U.S. Coast Guards to improve ice load impact criteria for ice-going ships. Collaborative work between the two governments to measure the pressure distribution on the hull of an icebreaker during ice impact incidents started in 1982 with a bow measurement panel on the *Polar Sea*. Since then data have been collected and analyzed from five deployments of the *Polar Sea* in both the Arctic and the Antarctic, one extended deployment of the Swedish icebreaker *Oden* to the Arctic Ocean, and one deployment of the *Nathaniel B. Palmer* to the Weddell Sea in Antarctica in winter. The measurements have provided the first insight into the magnitudes of local ice impact pressures and how they vary with time, contact areas and ice conditions. The data collected on the *Louis S. St-Laurent* during AOS-94 focused on the relative magnitude of forces and pressures on three areas of the hull structure: the bow, the shoulders and the bottom. Additionally, vessel maneuvering and powering data were collected for characterizing the vessel operations during the recorded hull–ice impact events. Data were also gathered on the environmental and ice conditions during the events.

Data for 3217 impact events were recorded on the data acquisition system. The system was configured such that an impact on any single measurement area could trigger an event. In some cases, simultaneous impacts were recorded on two or all three of the measurement areas. The greatest number of impacts were recorded at the bow, as would be expected. Side impacts were the next most frequent, followed by bottom impacts. If the multiple-impact cases are taken into account, the total number of recorded impacts is 4037. Preliminary analysis has shown that the magnitude of the forces and pressures is consistent with previous measurements in multiyear ice. Ongoing data analysis will determine data trends and correlate impacts with ship operating and ice conditions. Extreme load profiles will then be developed and relationships established for the frequency, magnitude and pattern of the loads on the three instrumented hull areas. The relationships will then be compared with those specified in the Revised Canadian Hull Construction standards, and recommendations will be made as appropriate.

Hull–Ice Interaction Load Measurements on the CCGS *Louis S. St-Laurent*

David Stocks

A strategic objective of the Canadian Coast Guard Northern Operations Programme is to support the scientific community in their requirements for platforms to conduct investigations in the Canadian Arctic. A further departmental objective, with respect to ensuring safety and environmental protection in the Canadian Arctic, requires that regulations be developed for ships operating in these regions.

The U.S. and Canadian Coast Guards have, over the last decade, cooperatively executed an extensive program of ice–ship hull interaction investigations on ice-strengthened ships. This initiative was stimulated by the joint need to develop structural standards for the design of ice-strengthened ships and has, for the most part, focused on the most highly loaded area of the ships' hull, the bow. Several ships have been instrumented for dedicated ice trials of their bow areas, including the CCGS *Louis S. St-Laurent* and the USCGC *Polar Star*. More recently the USCG and CCG combined their resources to conduct experiments on the Swedish icebreaker *Oden* during its 1991 North Pole voyage and the American icebreaker the *Nathaniel B. Palmer* during its 1992 voyage to the Antarctic.

The objective of this component of AOS-94 was to enhance the body of knowledge with respect to the structural response of ice-strengthened ships, specifically in areas of the ship's hull never before examined, such as the ship's side aft of the bow and bottom forward, and in areas of Arctic ice never before encountered by Western vessels. The benefits of this work are two-fold; first, to aid in the development and verification of the Arctic Shipping Pollution Prevention Regulations (structural standards), and second, to demonstrate and prove the capability of the platform to support the scientific missions.

The project was jointly sponsored by the CCG and USCG, and contracts were let to A.R. Engineering Ltd., Calgary, Alberta, Canada, and Science and Technology Corporation, Columbia, Maryland, U.S.A. Three phases were contracted:

- The installation of instrumentation onboard the ship;
- The acquisition of data during the voyage; and
- The synthesis and analysis of data after the voyage.

David Stocks is with the Canadian Coast Guard in Ottawa, Ontario, Canada.

The Canadian contractor was primarily responsible for the first phase, the second phase was a joint responsibility, and the third phase is being completed, primarily by the U.S. contractor.

A hull loads data acquisition system was installed on the CCGS *Louis S. St-Laurent* to acquire strain gauge data from three locations on the hull: the bow (24 strain gauges), the shoulder (28 strain gauges) and the bottom (11 strain gauges). To support the load measurements a ship navigation data acquisition and video monitoring system was also installed.

The data acquisition system was designed to trigger the data recorder to record significant impact events when a predetermined load was exceeded. It simultaneously recorded the speed, power and direction of the ship, as well as ice thickness and strength, for later correlation to ice condition and vessel operations.

Louis S. St-Laurent breaking ice.

The data acquisition system was operational from when the ship entered the ice on 26 July (70.08°N, 168.38°W) until it exited on 31 August. A total of 4037 separate events were recorded during that period. Ice observations were made continuously from the bridge of the *Polar Sea*. The forward-looking video system recorded the encountered ice, and the after-looking video system recorded the interaction of broken ice at the location of the strain gauges. Physical ice data were collected on an opportunity basis by ice science partners from the Institute of Marine Dynamics, St. John's, Newfoundland, to establish the thickness and strength of the encountered ice. The average ice thickness varied from 1.0 m (3.2 ft) on entry to 2.0 m (6.7 ft) at the Pole. The maximum ice thickness (excluding ridges) was 3.54 m (11 ft).

The data set derived from this voyage is the largest ever collected on a single deployment and doubles the quantity of information collected on previous collaborative USCG–CCG projects. The ongoing analysis will reduce the strain data to pressure loads and assess the trends in data versus ice and ship operating conditions, compute extreme value statistics and compare results between other areas of this ship and other ship experiments.

— Communications and Data Management —

Special Communications Solutions

Michael Powers

The unique environment of the deep Arctic requires special communications solutions, especially with an expedition of the complexity of AOS-94. Two of the special communications systems developed for and used on AOS-94 were the Internet e-mail system and the inter-ship communications system.

Providing Internet e-mail service on polar expeditions poses special problems as the ship proceeds north of the range of standard geosynchronous communications satellites. Members of the *Polar Sea*'s communications team explored a number of options in preparation for the expedition. The solution chosen was to use the Lincoln Experimental Satellites (LES) to link with the University of Miami ATS Satellite Control Facility at Malabar, Florida.

The two Lincoln Experimental Satellites, LES-8 and LES-9, were developed by MIT's Lincoln Labs for the Air Force and operate on the military UHF band (225–400 MHz). Both LESs follow inclined geosynchronous orbits, moving 17.8° north and south of the equator each 24 hours. The *Polar Sea* used LES-9 while it was north of the equator, which provided at least four hours of access each day.

Using the installed Navy Satellite Communications System equipment, the *Polar Sea* used data packet technology to send and receive information with a minicomputer at University of Miami's site in Malabar, Florida. The minicomputer provided Internet access for e-mail and file transfer, using the standard Internet file transfer protocol (ftp).

Aboard the *Polar Sea*, scientists and crew members prepared outgoing e-mail as text files on floppy diskettes. E-mail from scientists on the *Louis S. St-Laurent* was initially delivered on floppies by helicopter and later by the inter-ship communications system described below. Incoming e-mail was printed and delivered to the recipients.

The Internet e-mail connection allowed scientists to communicate with colleagues ashore throughout the expedition. In one case the ability to communicate by e-mail allowed the scientists and technicians aboard the *Polar Sea* to successfully troubleshoot a problem with their equipment. This meant that they were able to conduct their tests without interruption.

The connection was also used to download ice imagery from the National

---

Cdr. Michael Powers was Executive Officer of the USCGC Polar Sea.

Ice Center. While the *Polar Sea*'s installed TeraScan system provided real-time ice imagery, the capability of accessing National Ice Center information provided an option had there been a problem with TeraScan.

For inter-ship communications a VHF-FM line-of-sight link between the *Polar Sea* and the *Louis S. St-Laurent* was installed by Coast Guard technicians while the expedition was transiting from Victoria, British Columbia, to Nome, Alaska. This link was tied into each ship's telephone system, allowing one to pick up the phone on the *Polar Sea* and call someone on the *Louis S. St-Laurent.* This communications link proved invaluable in allowing the senior leaders of the expedition on both ships to consult and plan for each day's operation.

In addition, the link allowed scientists on the *Louis S. St-Laurent* to send and receive their e-mail electronically, which was much more reliable than waiting for the next helicopter flight between the two ships.

Data Management

Claire S. Hanson and David L. McGinnis

Data from AOS-94 are valuable national and international scientific resources and must be preserved for analysis by both current and future generations of scientists. To ensure preservation, data management coordination for AOS-94 will be provided by the National Snow and Ice Data Center (NSIDC), University of Colorado at Boulder. NSIDC is funded by the National Science Foundation's Office of Polar Programs as the Data Coordination Center for the Arctic System Science (ARCSS) Program; the AOS-94 data will be integrated into the ARCSS data management project.

A data archiving plan is being developed in collaboration with the AOS-94 project leaders to ensure that AOS-94 data sets and data products, along with complete documentation, will be archived at NSIDC and accessible through discipline-appropriate data centers. Examples of these centers with which NSIDC has close working relationships include the NOAA National Geophysical Data Center's Marine Geology and Geophysics Division and its Paleoclimate Group, the NOAA National Oceanographic Data Center, the NOAA National Climatic Data Center, and the Department of Energy's Carbon Dioxide Information and Analysis Center. Copies of the marine core data, bathymetric data, physical oceanography and primary productivity data, and atmospheric chemistry and related data from AOS-94 will be sent to these centers for incorporation into their databases. In cases such as biology and contaminants where there is currently no national center having responsibility for a particular discipline, NSIDC will maintain that AOS-94 data and provide access services until a discipline center is developed or designated.

NSIDC's ARCSS Data Coordination Center emphasizes ease of access, comprehensive documentation, and a researcher-centered philosophy. Our goal is to make the migration of valuable data as easy as possible. For adding data to the archive we develop a plan with each investigator. When an investigator and the NSIDC ARCSS staff agree that the data are ready, data sets are transferred to NSIDC and made available via electronic means such as anonymous ftp and/or the World Wide Web. When logical groupings of data are identified, and the volume is sufficient to warrant it, a CD-ROM is considered as an

Claire Hanson and David McGinnis are with the National Snow and Ice Data Center at the Cooperative Institute for Research in Environmental Sciences at the University of Colorado in Boulder, Colorado, U.S.A.

additional data delivery medium. The ARCSS data management effort is a two-way street; we work with investigators to archive their data while making these same data readily available for other investigators.

Data sets and products from AOS-94 will be listed in the on-line and hard-copy versions of the ARCSS Data Catalog, as well as in the Global Change Master Directory, the Arctic Environmental Data Directory and the International Arctic Environmental Data Directory. These on-line information services provide a means of notifying the international science community of these data sets, with up-to-date contact information to order the data. In addition, NSIDC maintains an ARCSS Web site (http://arcss.colorado.edu) that will explicitly list AOS-94 data with ordering information and/or links to download the data from within a Web browser. News of ARCSS data issues and activities is available in the quarterly newsletter *NSIDC Notes*, obtainable by free subscription and on the NSIDC Web site.

The AOS-94 data archiving plan will stipulate a period of exclusive use by the investigators, perhaps two years from the end of the cruise, after which the data should be moved into the archive and released for general distribution. The time period of exclusive use has not yet been negotiated with the project leaders or the individual investigators.

— Appendices —

— *AOS-94 Participants* —

USCGC Polar Sea

Kent Berger-North, Biology
Axys
Sidney, British Columbia

Hazen W. Bosworth, Sea ice
U.S. Army Cold Regions Research and Engineering Laboratory
Hanover, New Hampshire

Peter C. Brickell, Atmospheric and upper ocean chemistry
Air Quality Measurements and Analysis Research Division
Atmospheric Environment Service
Downsview, Ontario

John P. Christensen, Seafloor geochemistry
Bigelow Laboratory for Ocean Sciences
West Boothbay Harbor, Maine

Lisa Clough, Biology
Department of Biology
East Carolina University
Greenville, North Carolina

Charles Geen, Atmospheric and upper ocean chemistry
Bovar-Concord Environmental
Toronto, Ontario

Michel Gosselin, Biology
Department of Oceanography
University of Quebec at Rimouski
Rimouski, Quebec

Anthony J. Gow, Sea ice
U.S. Army Cold Regions Research and Engineering Laboratory
Hanover, New Hampshire

Arthur Grantz, Marine geology
U.S. Geological Survey
Menlo Park, California

John D. Grovenstein, Atmospheric and upper ocean chemistry
Department of Marine, Earth and Atmospheric Sciences
North Carolina State University
Raleigh, North Carolina

Patrick Hart, Marine geology
U.S. Geological Survey
Menlo Park, California

Daniel Lubin, Atmospheric radiation and climate
California Space Institute
University of California, San Diego
La Jolla, California

Bonnie J. Mace, Biology
Lamont-Doherty Earth Observatory
Palisades, New York

Steven May, Marine geology
U.S. Geological Survey
Prescott, Washington

Sandy Moore, Biology
College of Oceanic and Atmospheric Sciences
Oregon State University
Corvallis, Oregon

Michael Mullen, Marine geology
U.S. Geological Survey
Menlo Park, California

Mary O'Brien, Biology
Institute of Ocean Sciences
Sidney, British Columbia

Walter Olson, Marine geology
U.S. Geological Survey
Menlo Park, Californi

Elizabeth Osborne, Marine geology
McLean Laboratory
Woods Hole Oceanographic Institution
Woods Hole, Massachusetts

Kevin O'Toole, Marine geology
U.S. Geological Survey
Menlo Park, California

Fred Payne, Marine geology
U.S. Geological Survey
Menlo Park, California

Larry Phillips, Marine geology
U.S. Geological Survey
Menlo Park, California

Erk Reimnitz, Sea ice
U.S. Geological Survey
Menlo Park, California

James Rich, Biology
Graduate College of Marine Studies
University of Delaware
Lewes, Delaware

William Robinson, Marine geology
U.S. Geological Survey
Menlo Park, California

Larry Schultz, Ship technology
Advanced Marine Enterprises
Arlington, Virginia

Rubin Sheinberg, Ship technology
Naval Engineering Division
U.S. Coast Guard
Baltimore, Maryland

Evelyn Sherr, Biology
College of Oceanic and Atmospheric Sciences
Oregon State University
Corvallis, Oregon

Nathalie Simard, Biology
Department of Oceanography
University of Quebec at Rimouski
Rimouski, Quebec

Delphine Thibault, Biology
Department of Oceanography
University of Quebec at Rimouski
Rimouski, Quebec

Walter Tucker, Sea ice
U.S. Army Cold Regions Research and Engineering Laboratory
Hanover, New Hampshire

Patricia Wheeler, Biology
College of Oceanic and Atmospheric Sciences
Oregon State University
Corvallis, Oregon

Robert A. Whritner, Atmospheric radiation and climate
Arctic and Antarctic Research Center
Scripps Institution of Oceanography
University of California, San Diego
La Jolla, California

Louis S. St-Laurent

Knut Aagaard, Oceanography
Applied Physics Laboratory
University of Washington
Seattle, Washington

Louise Adamson, Contaminants
Institute of Ocean Sciences
Sidney, British Columbia

Ikaksak Amagoalik, Oceanography
Institute of Ocean Sciences
Sidney, British Columbia

Ken Asmus, Sea ice and remote sensing
Ice Services Branch
Atmospheric Environment Service
Ottawa, Ontario

Janet E. Barwell-Clarke, Oceanography
Institute of Ocean Sciences
Sidney, British Columbia

Eddy Carmack, Oceanography
Institute of Ocean Sciences
Sidney, British Columbia

Sylvester Drabitt, Documentation
Institute of Ocean Sciences
Sidney, British Columbia

Brenda Ekwurzel, Oceanography
Lamont-Dougherty Earth Observatory
Palisades, New York

James A. Elliott, Oceanography
Bedford Institute of Oceanography
Dartmouth, Nova Scotia

Katherine Ellis, Contaminants
Bedford Institute of Oceanography
Dartmouth, Nova Scotia

Sean Farley, Marine mammals
Department of Zoology
Washington State University
Pullman, Washington

Caren Garrity, Sea ice and remote sensing
Microwave Group-Ottawa River
Dunrobin, Ontario

Wayne Grady, Documentation
Macfarlane, Walter and Ross
Toronto, Ontario

Michael Hingston, Oceanography
BDR Research Ltd
Bedford Institute of Oceanography
Dartmouth, Nova Scotia

Oolateetah Iqaluk, Oceanography
Institute of Ocean Sciences
Sidney, British Columbia

Liisa M. Jantunen, Contaminants
Atmospheric Environment Service
Downsview, Ontario

E. Peter Jones, Oceanography
Bedford Institute of Oceanography
Dartmouth, Nova Scotia

Robie Macdonald, Contaminants
Institute of Ocean Sciences
Sidney, British Columbia

Fiona McLaughlin, Oceanography/contaminants
Institute of Ocean Sciences
Sidney, British Columbia

Christopher Measures, Oceanography
Department of Oceanography
University of Hawaii
Honolulu, Hawaii

David A. Muus, Oceanography
Scripps Institution of Oceanography
University of California, San Diego
La Jolla, California

Richard Nelson, Contaminants
Bedford Institute of Oceanography
Dartmouth, Nova Scotia

Stefan Nitoslawski, Documentation
Galafilm, Inc.
Montreal, Quebec

David Paton, Contaminants
Institute of Ocean Sciences
Sidney, British Columbia

Rick Pearson, Oceanography
Institute of Ocean Sciences
Sidney, British Columbia

Ron Perkin, Oceanography
Institute of Ocean Sciences
Sidney, British Columbia

Malcolm Ramsay, Marine mammals
Department of Biology
University of Saskatchewan
Saskatoon, Saskatchewan

Ron Ritch, Ship technology
A.R. Engineering
Calgary, Alberta

James A. Schmitt, Oceanography
Scripps Institution of Oceanography
University of California, San Diego
La Jolla, California

Douglas Sieberg, Oceanography
Institute of Ocean Sciences
Sidney, British Columbia

James St. John, Ship technology
Science and Technology Engineering Corporation
Columbia, Maryland

James H. Swift, Oceanography
Scripps Institution of Oceanography
University of California, San Diego
La Jolla, California

Darren Tuele, Contaminants
Institute of Ocean Sciences
Sidney, British Columbia

Christopher Walker, Documentation
Institute of Ocean Sciences
Sidney, British Columbia

Robert T. Williams, Oceanography
Scripps Institution of Oceanography
University of California, San Diego
La Jolla, California

F. Mary Williams, Sea ice
NRC Institute for Marine Dynamics
St. John's, Newfoundland

Frank Zemlyak, Oceanography
Bedford Institute of Oceanography
Dartmouth, Nova Scotia

CCGS *Louis S. St-Laurent* Crew

Commanding Officer	Philip Grandy	Chief Engineer	Mark Cusack
Chief Officer	Michael Hemeon	Sr Electrical Officer	Phillip Seaboyer
First Officer	William Turner	Jr Electrical Officer	William Falconer
Second Officer	Stephen Baxter	Senior Engineer	Nigel Hawksworth
Third Officer	Thomas Lafford	First Engineer	Mark Frogley
Bosun	Abraham Welcher	Second Engineer	Matthew Turner
Carpenter	Phillip Walker	Third Engineer	David Baker
Leading Seaman	Dale Hiltz	Supernumery Engineer	Darrin Arkerman
Leading Seaman	Leslie Drake	Electrician	Chris Wood
Leading Seaman	Kenneth Baker	Electrician	Edward Ginter
Seaman	Rico Amamio	Engineroom Supervisor	David Baur
Seaman	Alfred Jarvis	Engineroom Technician	Wayne Ryan
Seaman	Albert Sears	Engineroom Technician	Kenneth Pettipas
Seaman	Karl Gouthro	Engineroom Technician	Stephen Baxter
Seaman	William Wallace	Engineroom Technician	William Fagan
Seaman	Arthur Larkin	Oiler	Phil Macpherson
		Oiler	Robert Boucher
Logistics Officer	James Purdy	Oiler	Greg Engler
Logistics Officer	Elizabeth Campbell	Oiler	Thomas Hann
Chief Cook	Randy Turner	Oiler	Stephen Gagnon
Senior Storekeeper	David Wallingham	Oiler	Winston Langille
Storekeeper	Rick Strickland	Oiler	Alexander Myers
Clerk	Angela Macdonald		
Cook	Stephen Oliver	Radio Operator	Gordon Stoodley
Cook	Daneil Jones	Electronics Technician	Robert Brown
Steward	Graham Weldon	Ice Observer	Alfred Kooz
Steward	Graham Ritchie	Helicopter Pilot	Yvan Giroux
Steward	Graeme Garrett	Helicopter Pilot	Ralph Hemphill
Steward	Jacqueline Bourdon	Helicopter Engineer	Percy Gammon
Steward	Leo Higgins	Nurse	Cylethia Lee
Steward	Ralph Bowley		
Steward	Mark Lewis		
Steward	Robert Schoots		
Steward	Thomas Beaver		

USCGC *Polar Sea* Crew

Officers

CAPT Lawson W. Brigham	Commanding Officer
CDR Michael N. Powers	Executive Officer
LCDR Daniel K. Oliver	Engineering Officer
LCDR Robert L. Kaylor	Senior Aviation Officer
LCDR Stephen M. Wheeler	Deck Watch Officer/Ice Pilot
LCDR Steven G. Sawhill	Operations Officer
LT Edward J. Hansen	Aviation Engineering Officer
LT Kevin M. Balderson	Aviation Operations Officer
LT Theodore R. Salmon	Aviation Administration Officer
LT April A. Brown	Deck Watch Officer/Marine Science Officer
LTJG Karen Arnold	Deck Watch Officer/Exchange Officer
LTJG Lawrence C. Goerss	Damage Control Assistant/Morale Officer
LTJG Edward J. Lane III	Deck Watch Officer/Communications Officer
LTJG John D. Reeves	Assistant Engineering Officer
ENS Vincent J. Skwarek	Student Engineer

ENS Sean M. Carroll	Deck Watch Officer/Administrative Officer
CW04 Charles R. Steele, Jr.	Supply Officer
CW04 James J. Levesque	Engineering Watch/Electronics Officer
CW03 Donald A. Knesebeck	Deck Watch Officer/First Lieutenant
CW02 Harry J. Poland	Medical Officer
CW02 James E. Carlin	Engineering Watch/Main Propulsion Asst.

Enlisted Personnel

EMCM Warren E. Booth	DCC Michael W. Andreucci
EMC Jann H. Millard	DC2 Michael J. McAndrews
EMC Carl D. Pieplow	DC2 Ronald C. Plowman
EM2 Robert T. Nietering	DC3 David C. Garner
EM2 Gerard A. Hebert Jr.	
EM2 Charles G. McPhee	
EM3 Terry L. Maurer Jr.	MKCM Jeffery J. Andrie
EM3 Oscar O. Beck	MKC Glenn J. West
EM3 Clinton S. Thurlow	MKC Troy T. Luna
	MK1 Daniel L. Lenz
ETCS Peter W. Churchill	MK1 Garry D. Bennett
ETC Robert J. Reiter	MK1 Donald S. Nothem
ET1 Johnny N. Allen	MK1 Marvin L. Heeter Jr.
ET3 Randall C. Kibler	MK2 Thomas L. Dammann
ET3 Cary D. Biss	MK2 James E. Hale II
ET3 Todd A. Grant	MK3 Eric C. Alfred
ET3 Stuart D. Robertson II	MK3 Juan C. Juarez
	MK3 Raymond A. Morris III
TT2 James E. Riley	MK3 Jeffrey R. Siron
	MK3 Jason T. Watkins
FN Barbara C. Bennett	FN Richard E. Russell
FN Larry W. Bishop	FN Patrick J. Vincler
FN Eric F. Cheigh	FA Louis E. Frattarelli Jr.
FN Patrick J. Corso	FA Sean P. McSweeney
FN Daniel R. Ferguson	FA Jeffrey P. Pierce
FN John R. Hays	FA Maurice Ponce
FN Stephen L. McVay	FA Thomas J. Scheidemantel
QMCM Gary A. Thurston	YNC Terrence J. Brennan
QM2 Gil A. Contreras	YN1 Langston D. Brooks
QM3 Jennifer M. Hogge	YN2 Brian P. McClure
QM3 Peter J. Kanavas	
QM3 Laura L. Knehr	SKC Dana V. Hanberg
	SK2 Robert T. King
BMCS Charles D. Buckley	SK1 Bryan D. Petersen
BM1 Christopher R. Buell	SK3 Michael B. Sanicharra
BM2 Anthony D. Whiting	SN Joseph A. Bergman
BM3 Hans Esteves	
	HSC Mark L. Stocks
GM1 Vincent L. Demeyer	HS2 Jeffrey W. Ongemach
SN Mitchel H. Barker	SN Robert J. Odaniel
SN Jason M. Crandall	SN Andy R. Stafford
SN Derrick L. Cross	SN Jason A. Stouffer
SN Adam P. High	SN Bradley R. Tull
SN Loren D. Huggins	SA Jakobb N. Baldwin
SN Peter M. Jagel	SA Lura D. Etchison

SN Sean M. Johannsen
SN Justin R. Jolley
SN Matthew M. Kenny
SN Cobran D. Lappin
SN Wesley McMillan III
SN James A. McMurphy

MST1 Corey A. Bennett
MST2 John T. Pierce
MST3 Noell A. Bolleurs
MST3 Elisa M. Fusco

SSCS Alan R. Walsh
SS1 Michael T. Lapolla
SS1 Michael R. Sieg
SS1 Joseph Grant
SS2 Nathaniel Hightower
SS3 Douglas A. Van Kampen
SS3 Jonathan R. Carton
SS3 Jimmie L. Patterson
SS3 Ruston C. Johnson
SNSS Kenneth J. Bennett

SA David B. Gore
SA Matthew E. Kor
SA Jason T. Lopez
SA Collin A. Maas
SA Aaron S. Schmude
SA Jeffrey E. Williams

RM1 Steven M. Schofield
RM2 Matthew J. Dini
RM2 Paul J. Gladding
RM2 Jeffrey D. Spears
RM3 Scott D. Haywood
RM3 Rod E. Koepp

ADC Robert C. Fawcett
AD1 William D. Anderson
AE1 Mark R. Mobley
AT1 Scott W. Thiel
AD2 Michael B. Kellams
AT2 Henry C. Parker
AE2 William J. Shaw
AM3 J. Guillermo Verde

— Science Stations —

Polar Sea

No.	*Date*	*N Lat.*	*Long.*	*Depth (m)*	*Sampling program**
1	25 Jul	67°59′	168°50′W	49	Bc
2	26 Jul	70°00′	168°45′W	40	P, B, Bc (5), I
3	27 Jul	72°00′	168°51′W	55	P, B, I
4	28 Jul	74°01′	168°50′W	120	P, B, I
5	30 Jul	75°25′	170°44′W	900	P, B, I
6	30 Jul	75°21′	170°30′W	525	B, Bc (2)
7	1 Aug	76°39′	173°20′W	2250	P, B, Bc (2), I
7b	2 Aug	77°49′	176°21′W		I
8	3 Aug	78°08′	176°48′W	1047	P, B, Bc (2), Pc, I
8a	3 Aug	78°09′	176°02′W	1426	Pc
9	4 Aug	78°08′	176°41′W	1035	Pc
10	4 Aug	78°09′	174°38′W	1673	Pc
11	4 Aug	78°58′	175°48′W	1050	B
12	5 Aug	79°59′	174°17′W	1638	B, Bc, Pc (2), I
13	6 Aug	80°09′	173°17′W	2654	P, B, Pc
13a	6 Aug	80°09′	173°22′W	2556	Bc, I
14	7 Aug	80°13′	172°46′W	3098	Pc
15	7 Aug	80°12′	173°19′W	2726	Pc
16	8 Aug	80°20′	178°43′W	1568	B, Bc (3), Pc, I
17	9 Aug	81°15′	179°00′E	2255	P, B, Bc (2), I
18	10 Aug	81°34′	176°58′E		I
19	11 Aug	82°26′	175°50′E	2414	P, B, Bc (2), I
20	12 Aug	83°10′	174°06′E	3145	Bc, Pc, I
21	13 Aug	84°06′	174°59′E	3205	P, B, Bc, Pc, I
22	14 Aug	84°50′	170°42′E		I
23	15 Aug	85°54′	166°50′E	3535	P, B, Bc (2), I
24	16 Aug	87°09′	160°32′E	4020	P, B, Bc, Pc
25	18 Aug	88°04′	147°47′E	2191	P, B, Bc (2), I
26	19 Aug	88°48′	143°29′E	1034	B, Bc (2)
27	19 Aug	88°52′	141°55′E	1634	Pc
28	19 Aug	88°52′	140°31′E	2015	Bc, Pc, I
29	20 Aug	88°56′	138°55′E	3047	Bc, Pc
30	20 Aug	89°01′	137°41′E	4064	Bc, I
31	22 Aug	89°59′	031°45′E	4290	P (2), B (2), Bc, Pc, I
32	25 Aug	85°43′	037°50′E	3585	P, B, Bc (2), I
33	26 Aug	84°16′	034°37′E	4052	P, B, Bc, I

*P-production, B-biomass, Bc-box core, Pc-piston core, I-ice.

Combined P and B stations include CTD, nutrients, pCO_2, halocarbons, organics, DMSP, DOC, DON, POC, PON, zooplankton, chlorophyll, phytoplankton, heterotrophic protists, bacteria, primary production, nutrient uptake, bacterial production, protistan herbivory, bactivory, zooplankton excretion, and zooplankton herbivory.

B stations include CTD, nutrients, halocarbons, and chlorophyll.

Box cores (Bc) were variously sampled depending on whether they served the geological or biological programs.

I stations include ice cores, albedo, sediments, and ice contaminants.

Depths are uncorrected.

In addition, over 1300 nautical miles of video and still photography ice morphology survey lines were flown to measure floe and melt pond size distributions.

Atmospheric chemistry and physics measurements were made throughout the voyage, either continuously or through flask sampling or intermittent pumping. These observations include volatile organics, dimethyl sulfide, ozone, carbon monoxide and dioxide, organohalides, sulfur dioxide and acid gases, major ions and stable isotopes, aerosols and condensation nuclei. Measurements of halomethanes in water, snow and ice were made while on station.

Radiation measurements were also made throughout the voyage. These were done with a Fourier transform IR spectroradiometer (mid-IR), an experimental near-IR detector, a total IR pyrgeometer, a solar pyranometer, a near-IR pyranometer and a UV radiometer.

Louis S. St-Laurent

No.	*Date*	*N Lat.*	*Long.*	*Depth (m)*	*Sampling program **
1	25 Jul	67°47′	168°47′W	50	O, C
2	27 Jul	72°08′	168°50′W	53	O, C, I
3	28 Jul	73°00′	168°49′W	66	O, C, I
4	28 Jul	73°30′	168°51′W	116	O, C, I
5	28 Jul	73°59′	168°44′W	184	O, C, I
6	29 Jul	74°30′	168°50′W	195	O, C, I
7	29 Jul	75°00′	169°59′W	261	O, C, I
8	29 Jul	75°27′	170°35′W	887	O, C, I
9	30 Jul	75°45′	171°14′W	1679	O, C, I
10	30 Jul	75°57′	171°40′W	1886	O, I
11	1 Aug	76°38′	173°19′W	2227	O, C, I
12	2 Aug	77°20′	175°02′W	1852	O, I
13	2 Aug	77°48′	176°18′W	1217	O, C, I
14	3 Aug	78°09′	176°54′W	956	O, C, I
15	4 Aug	78°08′	174°18′W	1853	O, I
16	4 Aug	78°59′	175°49′W	1062	O, C, I
17	5 Aug	79°59′	174°19′W	1670	O, C, I
18	6 Aug	80°09′	173°15′W	2655	O, C, I
19	7 Aug	80°09′	176°46′W	2115	O, C, I
20	8 Aug	80°20′	178°38′W	1436	O, C, I
21	8 Aug	80°43′	179°59′W	1640	O, C, I
22	9 Aug	81°15′	179°01′E	2208	O, C, I
23	9 Aug	81°35′	176°52′E	2524	O, C, I
24	10 Aug	82°28′	175°40′E	2430	O, C, I
25	11 Aug	83°10′	173°56′E	3088	O, C, I
26	12 Aug	84°04′	175°04′E	3135	O, C, I
27	13 Aug	84°51′	170°42′E	3323	O, C, I
28	15 Aug	85°54′	166°42′E	3456	O, C, I
29	16 Aug	87°09′	160°42′E	3939	O, C, I
30	18 Aug	88°04′	147°50′E	2130	O, C, I
31	19 Aug	88°47′	142°44′E	1029	O, C, I
32	19 Aug	88°52′	140°00′E	1983	O, C, I
33	20 Aug	88°57′	139°12′E	2938	O, C, I
34	20 Aug	89°01′	137°09′E	4080	O, C, I
35	22 Aug	90°00′		4215	O, C, I
36	25 Aug	85°44′	37°45′E	3471	O, C, I
37	26 Aug	84°15′	35°05′E	3979	O, C, I
38	27 Aug	83°51′	35°41′E	3954	O
39	31 Aug	75°00′	6°03′W	3448	O, C

*O-oceanography, C-contaminants, I-ice.

O stations include CTD, oxygen, nutrients, carbonate and alkalinity, CFCs (including $CC1_4$, helium-tritium, ^{18}O, ^{14}C and trace metals.

C stations include hydrocarbons, HCHs, other organics (e.g., toxophenes), radionuclides and trace metals, using both large-volume bottle sampling and submerged and surface pumps. Contaminant samples were also collected from snow samples, net hauls and box cores.

I stations variously include vertical temperature and salinity profiles in the ice, beam tests, crystallography, and electrical and physical properties of the snow cover. There were also continuous ship-based radiation measurements at 37 GHz, vertically polarized.

Depths are uncorrected.

In addition, 72 CTD stations to 1500 m were occupied using a portable system carried by helicopter and deployed from the ice. Two 48-hr contaminant moorings were also deployed and recovered by helicopter. Finally, the marine mammals program made detailed studies of seven polar bears, again working from helicopters.

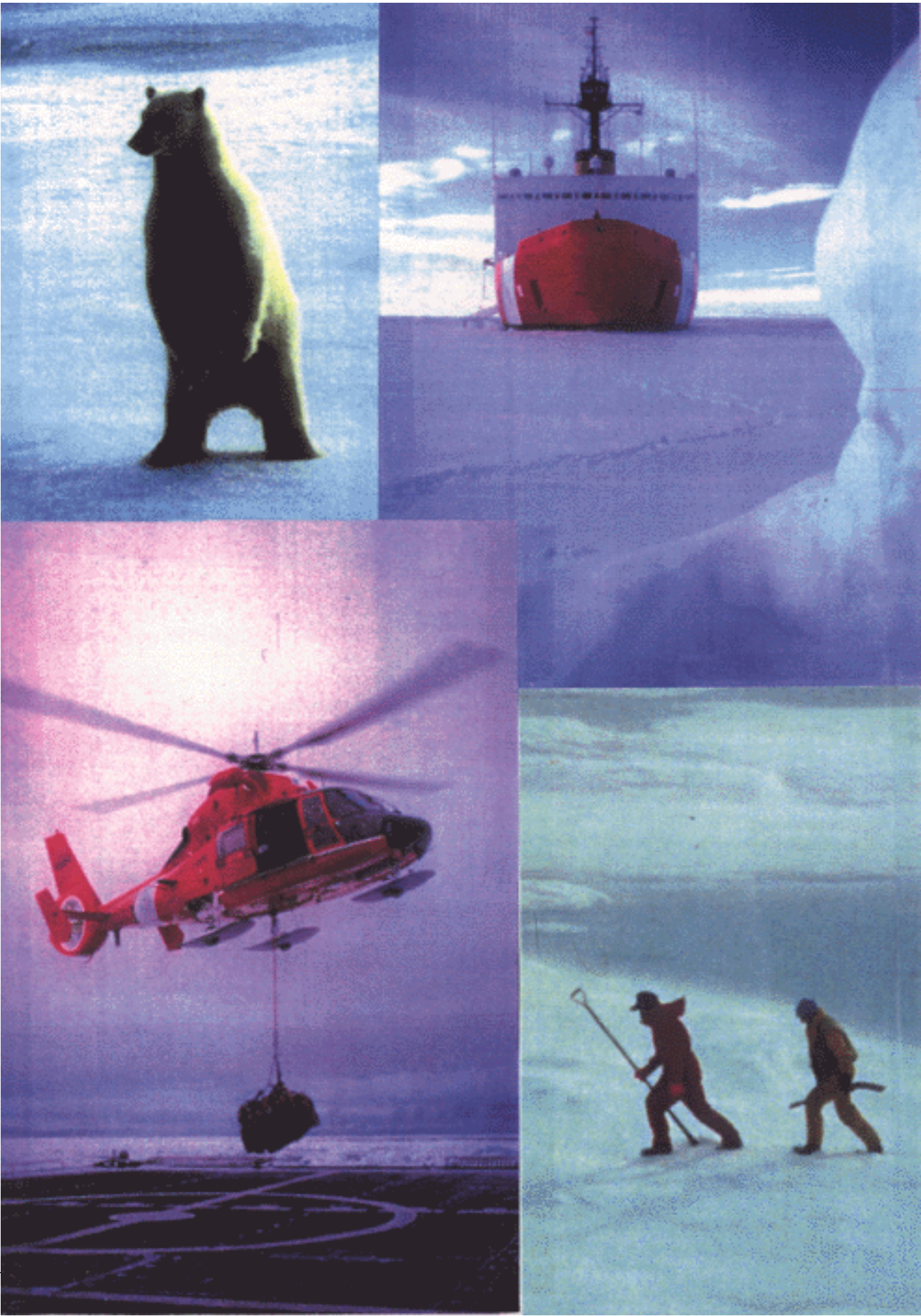

1994 Arctic Ocean Section

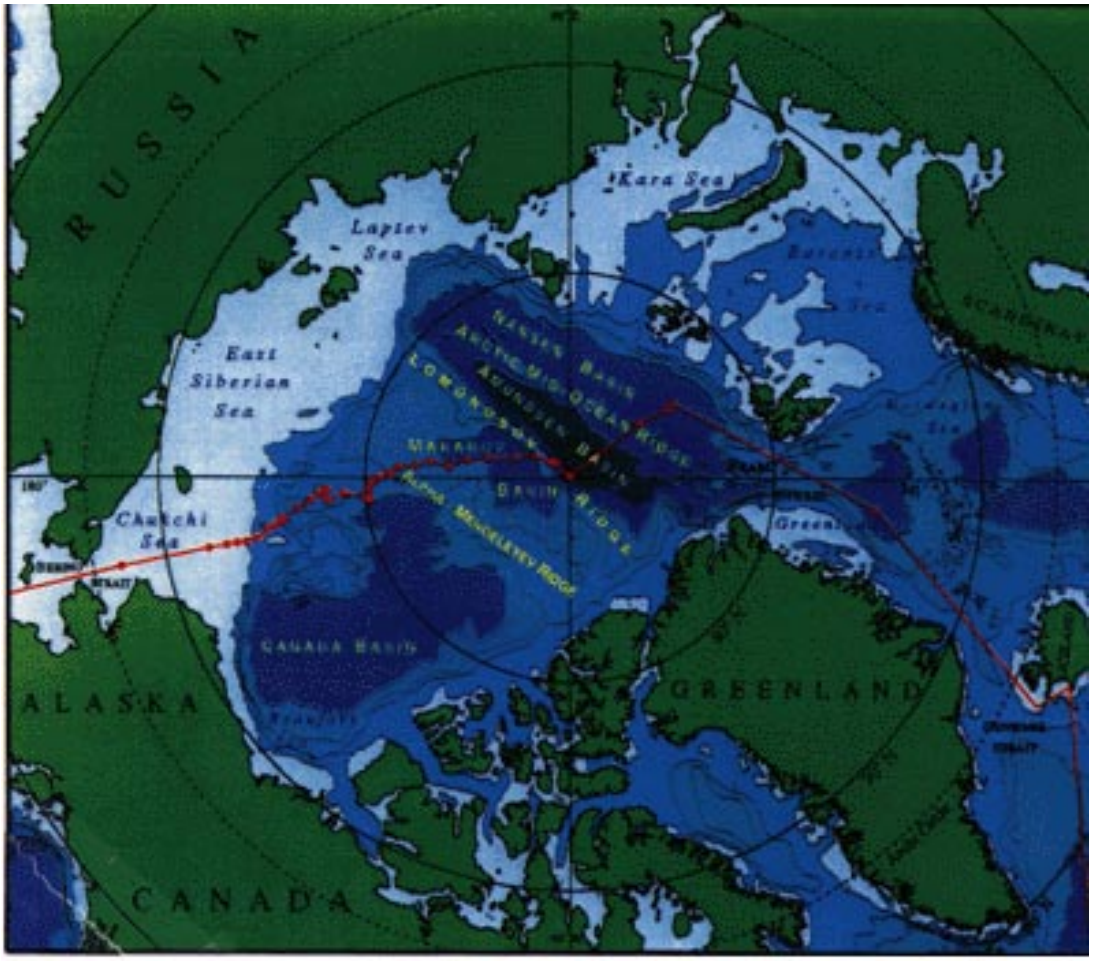

Cruise track of the *Louis S. St-Laurent* and the *Polar Sea* between July 24 and September 3, 1994. The dots represent the science stations. (Map created by Christopher Guay.)

Ship and helicopter photos on previous page by Peter Brickell.

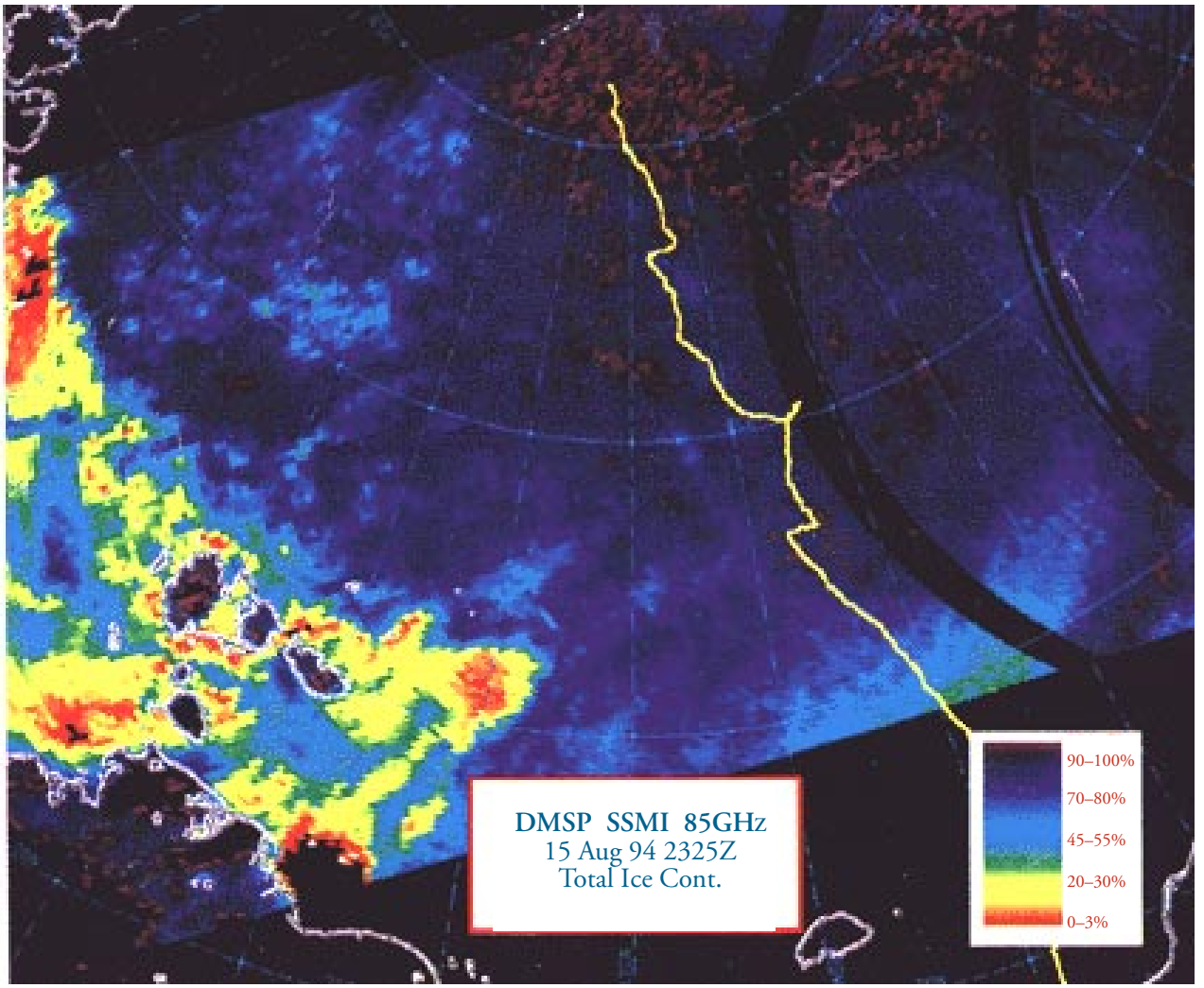

Total ice concentration for August 15, 1994. The track of the *Polar Sea* is shown in white. This Defense Meteorological Satellite Program (DMSP) image was derived using the 85-GHz passive microwave channel of the Special Sensor Microwave Imager (SSM/I). The images were received and processed in near real time by the TeraScan system aboard the *Polar Sea*. For more information about how images such as this were created and used during AOS-94, see p. 97.
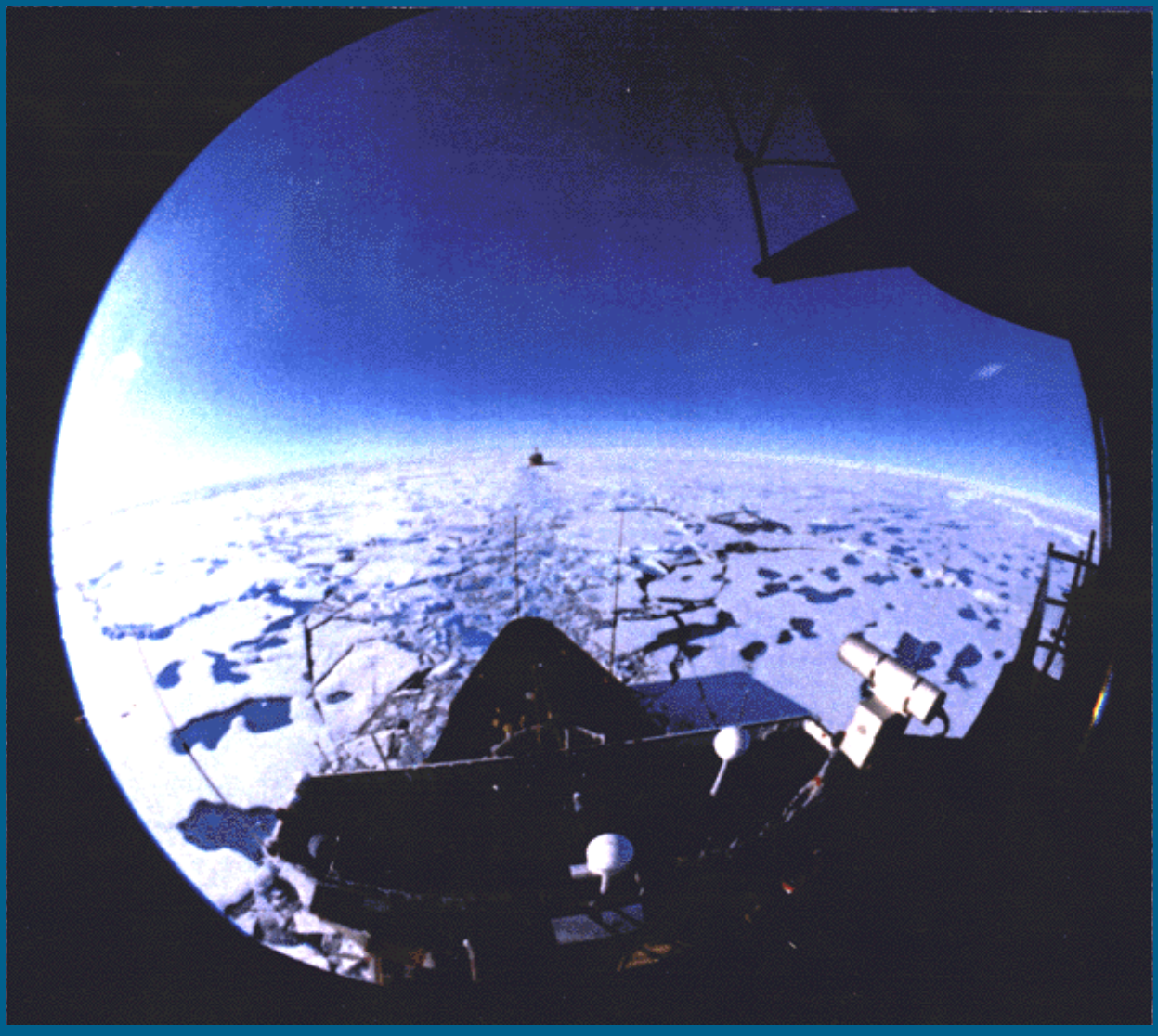
Photo on back cover by Charles Geen